

Sterically rigid bismuth pincer complexes; observation of the growing polymer chain in polar monomer polymerisation.

Zoë R. Turner,* Jamie T. Wilmore, Nicholas H. Rees, and Jean-Charles Buffet*

*Chemistry Research Laboratory, Department of Chemistry, University of Oxford, Mansfield Road,
Oxford OX1 3TA, United Kingdom. Tel: +44(0) 1865 285157;
E-mail: jean-charles.buffet@chem.ox.ac.uk, zoe.turner@chem.ox.ac.uk,*

Table of Contents

I.	General considerations	S3
II.	Representative NMR spectra	S4
III.	Crystallographic data	S18
IV.	Polymerisation data	S44
V.	References	S94

I. General considerations

All manipulations were carried out using standard Schlenk line or drybox techniques under an atmosphere of dinitrogen or argon. Protio solvents were degassed by sparging with dinitrogen, dried by passing through a column of activated sieves (pentane, hexane, toluene, benzene) and stored over potassium mirrors, or distilled from sodium metal (thf) and stored over activated 4 Å molecular sieves, or distilled from sodium-potassium alloy (diethyl ether) and stored over a potassium mirror. Deuterated solvents were dried over potassium (C_6D_6 , C_7D_8) or CaH_2 (C_4D_8O), distilled under reduced pressure and freeze-pump-thaw degassed three times prior to use.

1H NMR spectra were recorded at 298 K, unless otherwise stated, on Bruker AVIIHD 400 nanobay or Bruker AVIII 500 spectrometers and $^{13}C\{^1H\}$ or ^{13}C NMR spectra on the same spectrometers at operating frequencies of 100 and 125 MHz respectively. Two dimensional 1H - 1H and ^{13}C - 1H correlation experiments were used, when necessary, to confirm 1H and ^{13}C assignments. All NMR spectra were referenced internally to residual protio solvent (1H) or solvent (^{13}C) resonances and are reported relative to tetramethylsilane ($\delta = 0$ ppm). Chemical shifts are quoted in δ (ppm) and coupling constants in Hertz. Elemental analyses were carried out at London Metropolitan University. Mass spectrometry was completed by the Mass Spectrometry Research Facility at the University of Oxford. Matrix-assisted laser desorption/ionisation time of flight spectra were collected using a Bruker MALDI Autoflex TOF MS. Samples were run using either a DHB or DCTB matrix. The DHB matrix was prepared by mixing the sample with DHB (10 mg mL $^{-1}$ in 70:30 H_2O :CH $_3CN$) in a 1:1 volume ratio. The DCTB matrix was prepared by mixing 10 μL of sample with 10 μL DCTB (40 mg mL $^{-1}$ in THF) and 2.5 μL KTFA (5 mg mL $^{-1}$ in THF). 1.5 μL of the mixed solutions were spotted on the MALDI plate and dried prior to the run. Polymer molecular weights (M_n , M_w and M_w/M_n) were determined by GPC using an Agilent 1260 Infinity II GPC/SEC instrument equipped with an Agilent PLgel Mixed-D column (300 mm length, 7.5 mm diameter) and a refractive index (RI) detector or on an Shimadzu LC-20AD instrument at 40 °C. Two Mixed Bed PSS SDV linear S columns were used in series. thf was used as an eluent at 35 °C with a flow rate of 1.0 mL min $^{-1}$. Samples were dissolved in thf at a concentration of 1.0 mg mL $^{-1}$ and filtered before injection. Linear polystyrenes were used as primary calibration standards and the appropriate Mark-Houwink corrections were applied to calculate the experimental molecular weights. FTIR measurements were made with a Thermo Scientific Nicolet iS5 FTIR spectrometer by using either KBr pellets or a 0.5 mg mL $^{-1}$ DCM solution housed in a cell with KBr windows and data collected in the transmission mode. DSC samples were run on a DSC3+ (Mettler Toledo, Ltd) using 5 mg of polymer in a sealed aluminium 100 μL crucible. An empty crucible was used as a reference, and the DSC was calibrated using indium. Samples were heated from 25 to 250 °C and cooled back again at a rate of 5 °C per minute, two heating cycles were run with polymer melt temperature values taken from the second heating cycle.

($^{Mes,Ph}L$)BiI(thf) $_2$ and ($^{Mes,Ph}L$)SbI, $^{[1]}$ KO-2,6-R-C $_6$ H $_3$ (R = Me, iPr , tBu) and KOAm, $^{[2]}$ KN" (N" = N(SiMe $_3$) $_2$) $^{[3]}$, KCH $_2$ Ph $^{[4]}$ and lactyl lactates S,S-HOC(H)(Me)C(=O)OC(H)(Me)C(=O)OR (R = Me,

ⁱPr)^[5] were prepared with reference to published procedures. Lactate salts KOC(H)(Me)C(=O)OR (R = Me, ⁱPr, ^tBu) were prepared *in situ* by deprotonation of the appropriate HOC(H)(Me)C(=O)OR (S-configuration for R = Me, ⁱPr, *R*-configuration for R = ^tBu) using KN" at room temperature in thf.

II. Representative NMR spectra

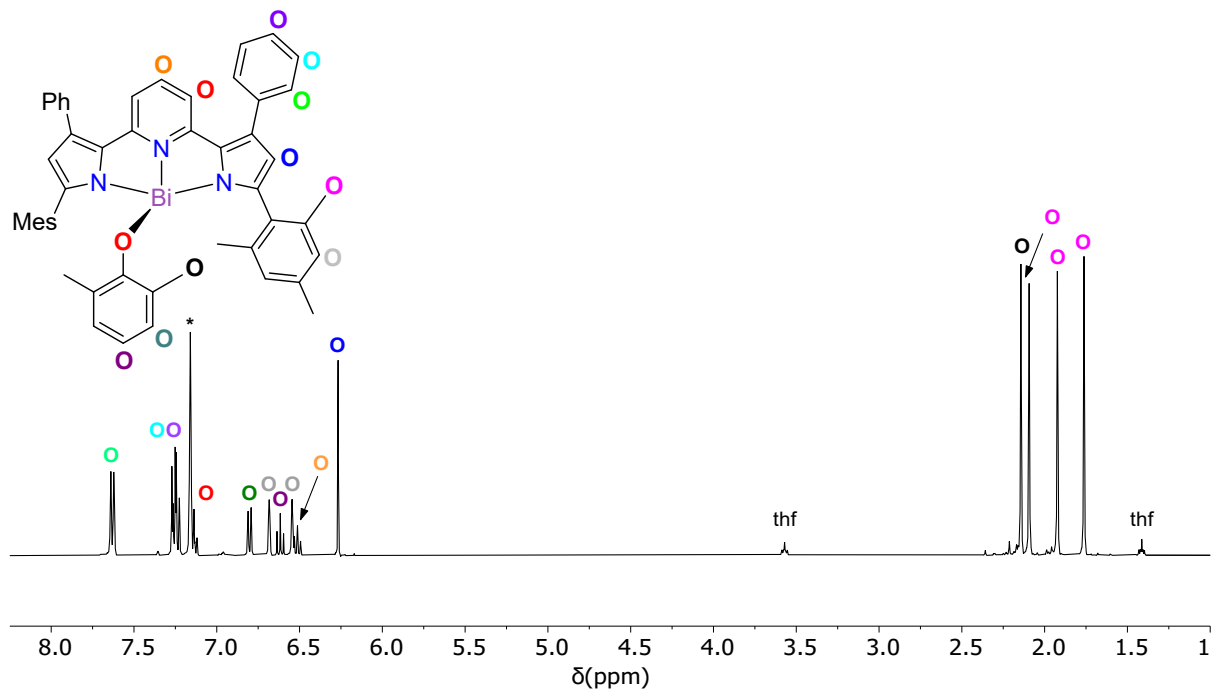


Fig. S1. ^1H NMR spectrum (C_6D_6 , 500 MHz, 298 K) of $(^{\text{Mes},\text{Ph}}\text{L})\text{Bi}(\text{OXyl})$ (**1**). * denotes residual protio solvent fraction of C_6D_6 .

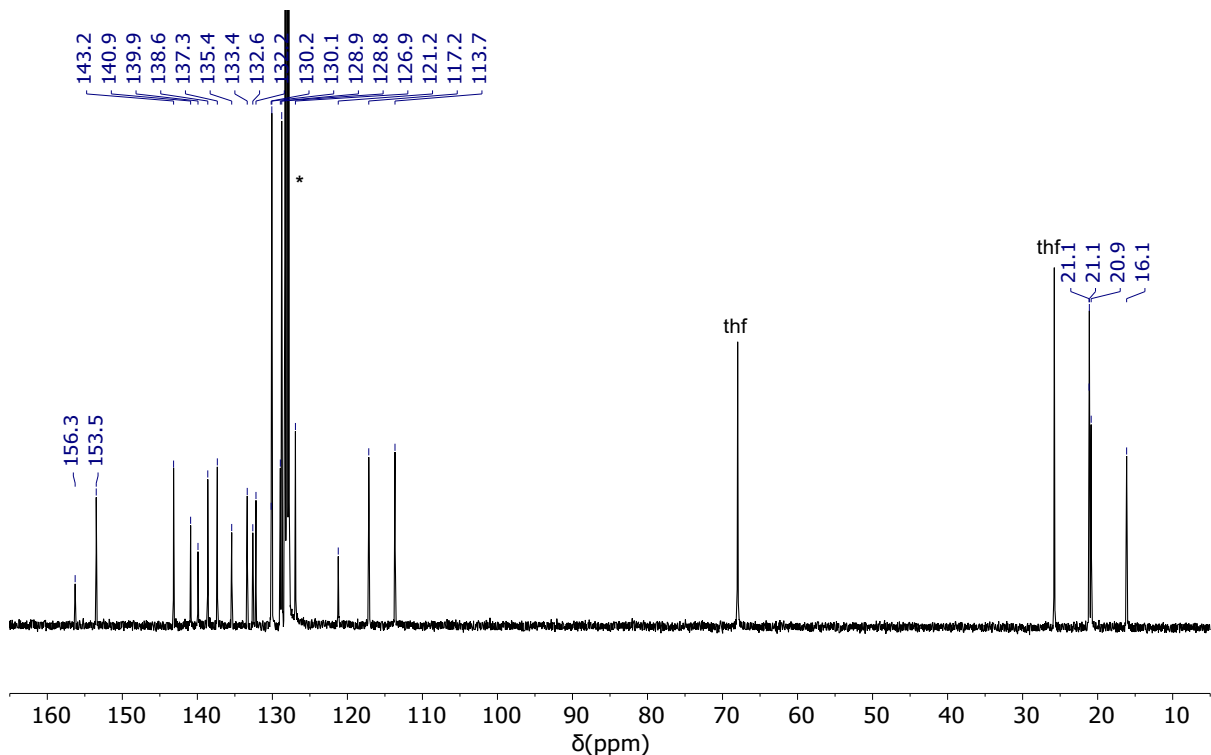


Fig. S2. $^{13}\text{C}\{^1\text{H}\}$ spectrum (C_6D_6 , 125 MHz, 298 K) of $(^{\text{Mes},\text{Ph}}\text{L})\text{Bi}(\text{OXyl})$ (**1**). * denotes residual protio solvent fraction of C_6D_6 .

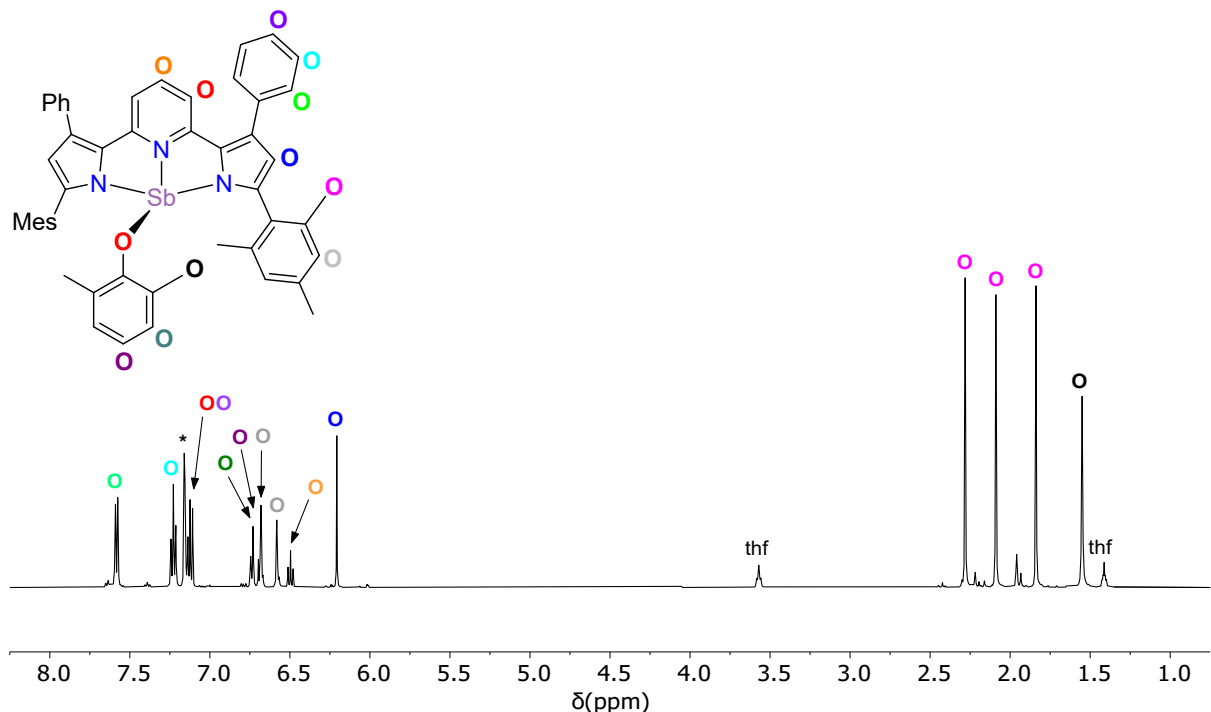


Fig. S3. ^{1}H NMR spectrum (C_6D_6 , 500 MHz, 298 K) of $(^{Mes,Ph}L)Sb(OXyl)$ (2). * denotes residual protio solvent fraction of C_6D_6 .

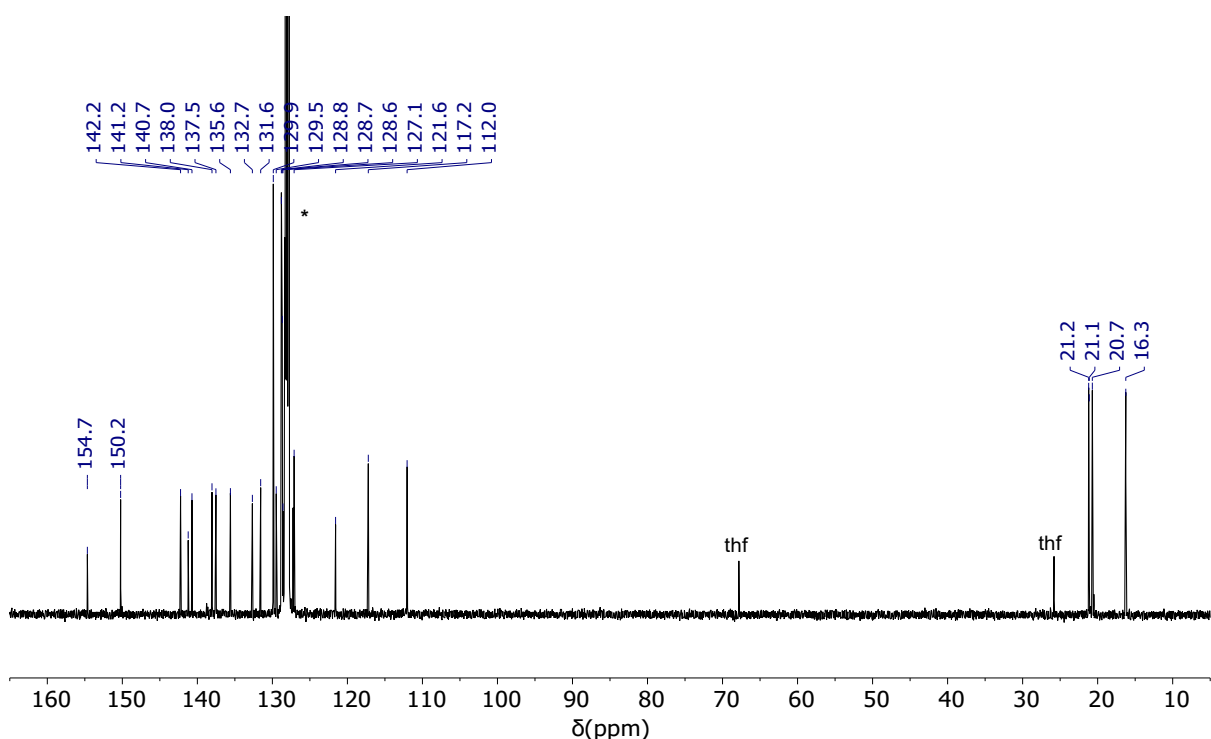


Fig. S4. $^{13}C\{^{1}H\}$ NMR spectrum (C_6D_6 , 125 MHz, 298 K) of $(^{Mes,Ph}L)Sb(OXyl)$ (2). * denotes C_6D_6 .

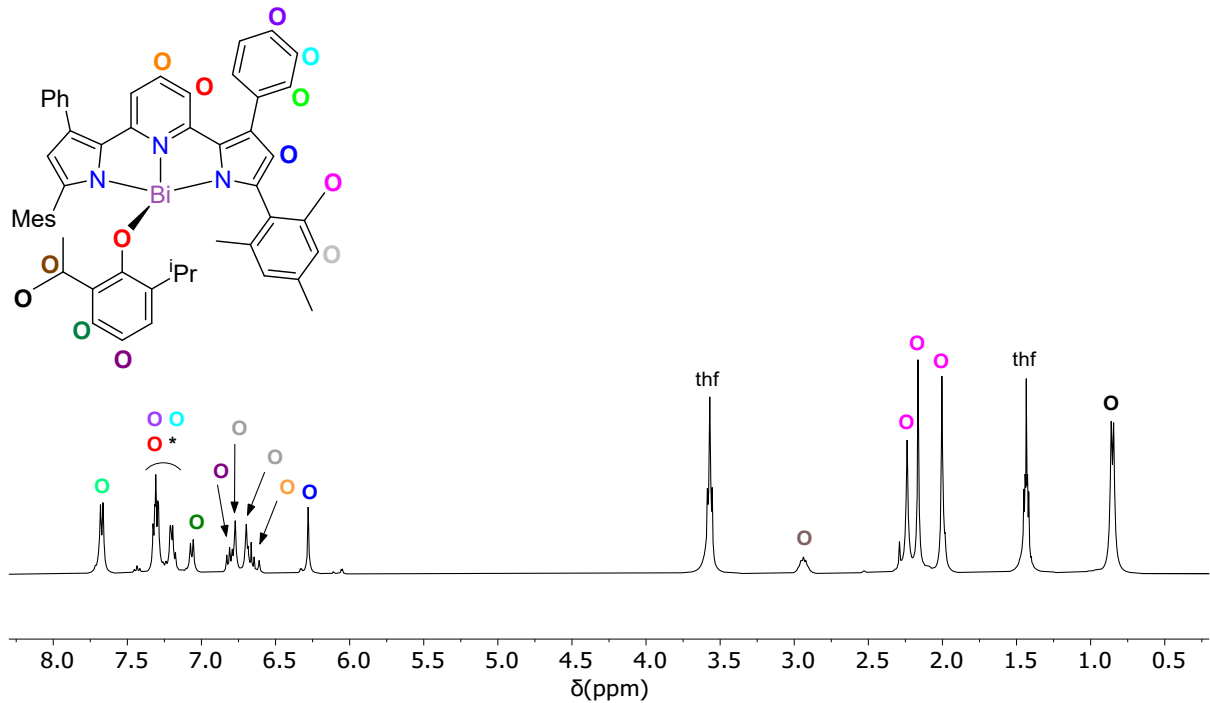


Fig. S5. ^1H NMR spectrum (C_6D_6 , 400 MHz, 298 K) of $(^{\text{Mes},\text{Ph}}\text{L})\text{Bi}(\text{ODipp})$ (3). * denotes residual protio solvent fraction of C_6D_6 .

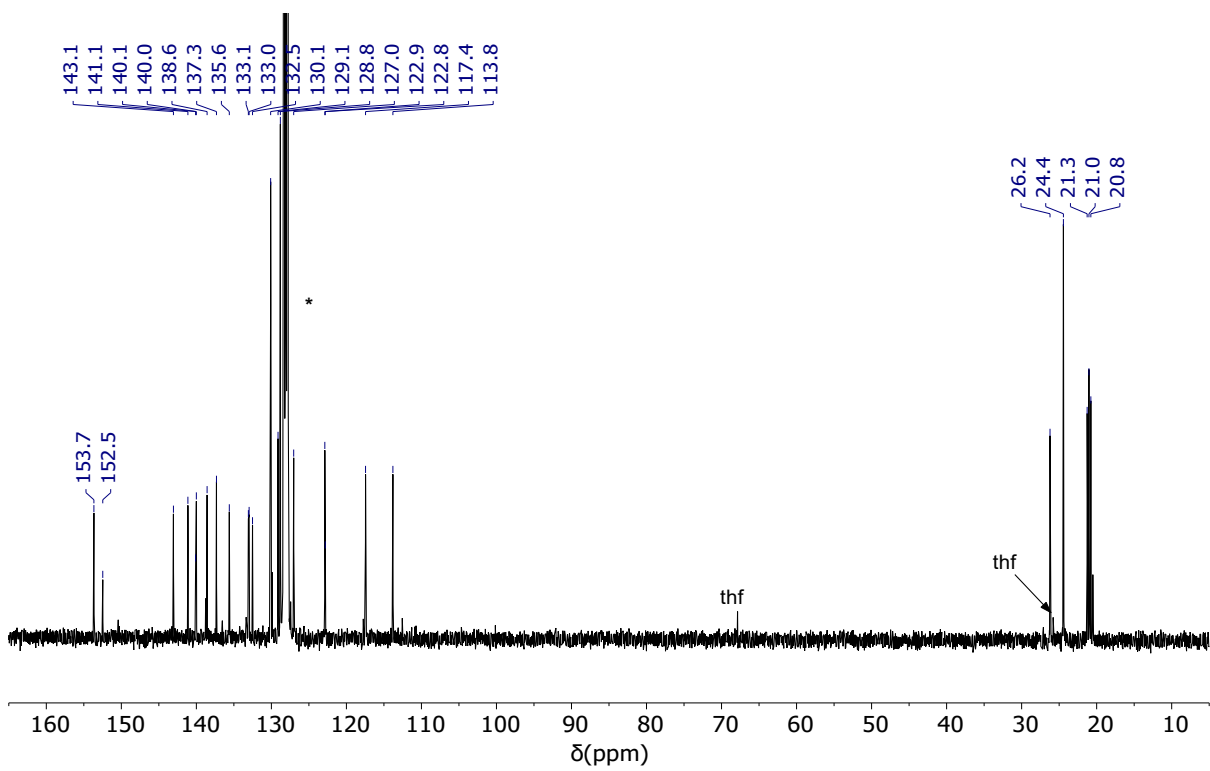


Fig. S6. $^{13}\text{C}\{^1\text{H}\}$ NMR spectrum (C_6D_6 , 100 MHz, 298 K) of $(^{\text{Mes},\text{Ph}}\text{L})\text{Bi}(\text{ODipp})$ (3). * denotes C_6D_6 .

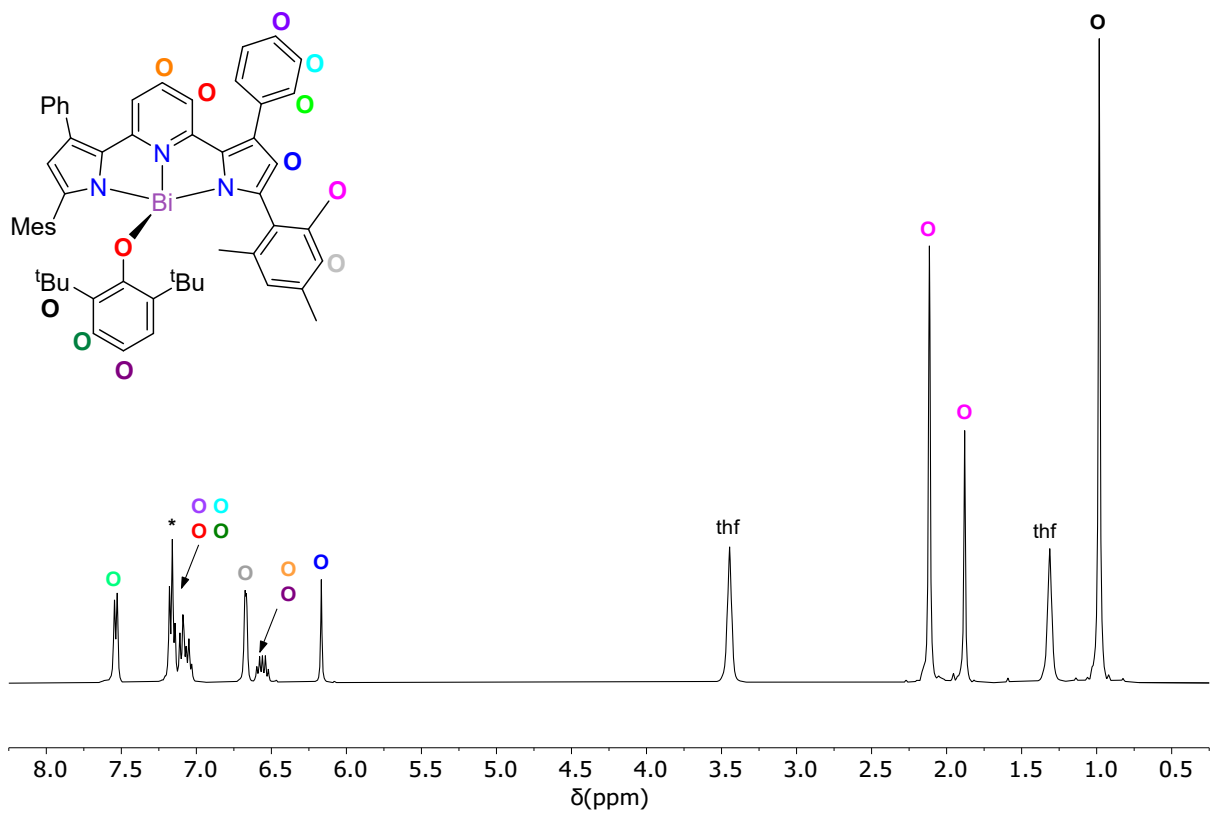


Fig. S7. ^1H NMR spectrum (C_6D_6 , 400 MHz, 298 K) of $(^{\text{Mes},\text{Ph}}\text{L})\text{Bi(OAr}^{\text{t-Bu}})$ (**4**). * denotes residual protio solvent fraction of C_6D_6 .

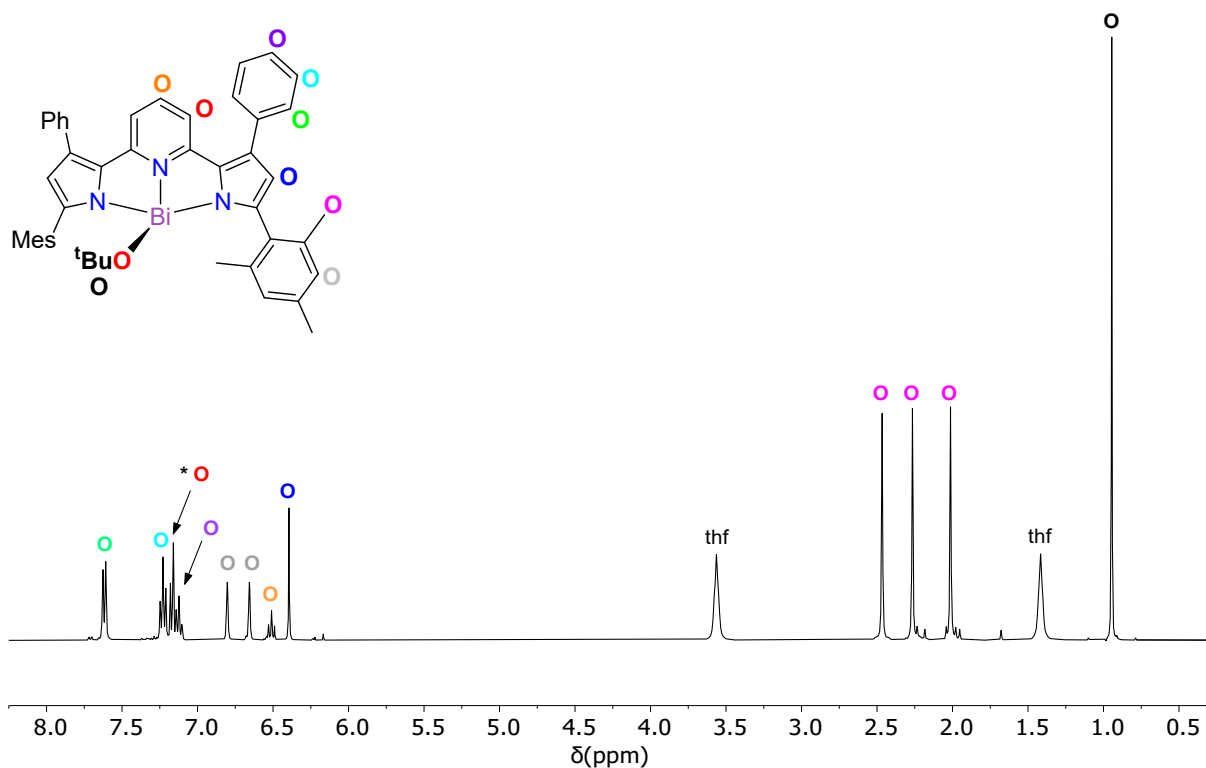


Fig. S8. ^1H NMR spectrum (C_6D_6 , 400 MHz, 298 K) of $(^{Mes,Ph}L)Bi(O^tBu)$ (5). * denotes residual protio solvent fraction of C_6D_6 .

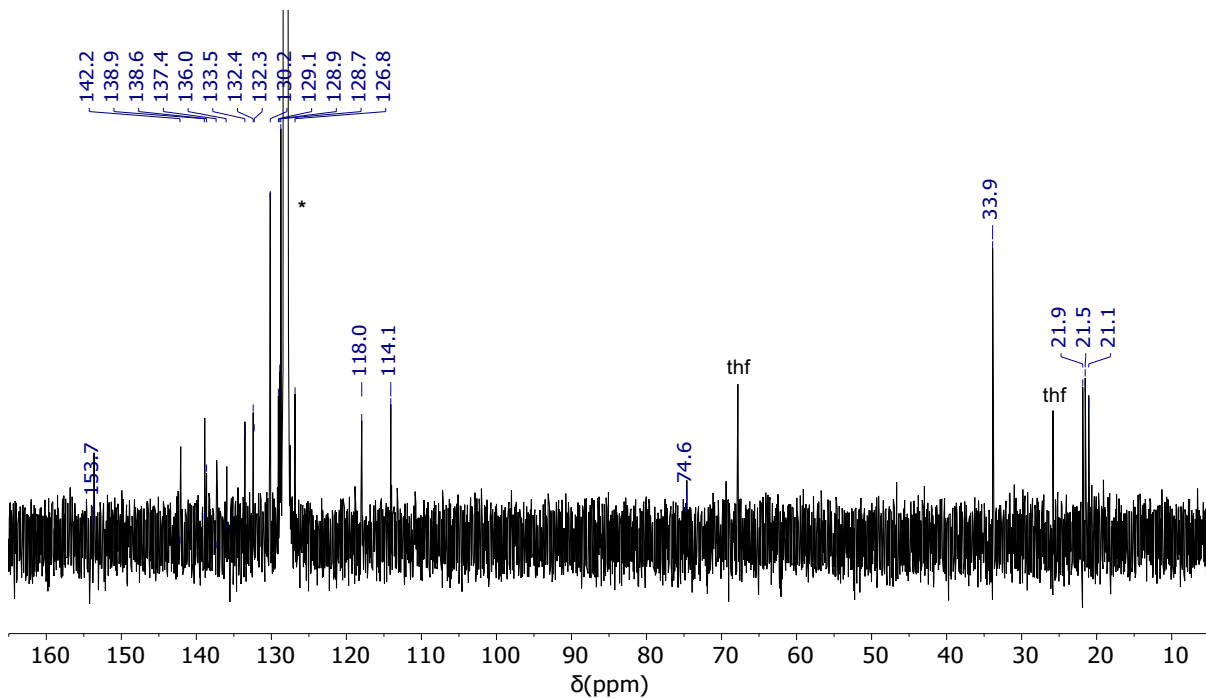


Fig. S9. $^{13}\text{C}\{^1\text{H}\}$ NMR spectrum (C_6D_6 , 100 MHz, 298 K) of $(^{Mes,Ph}L)Bi(O^tBu)$ (5). * denotes C_6D_6 .

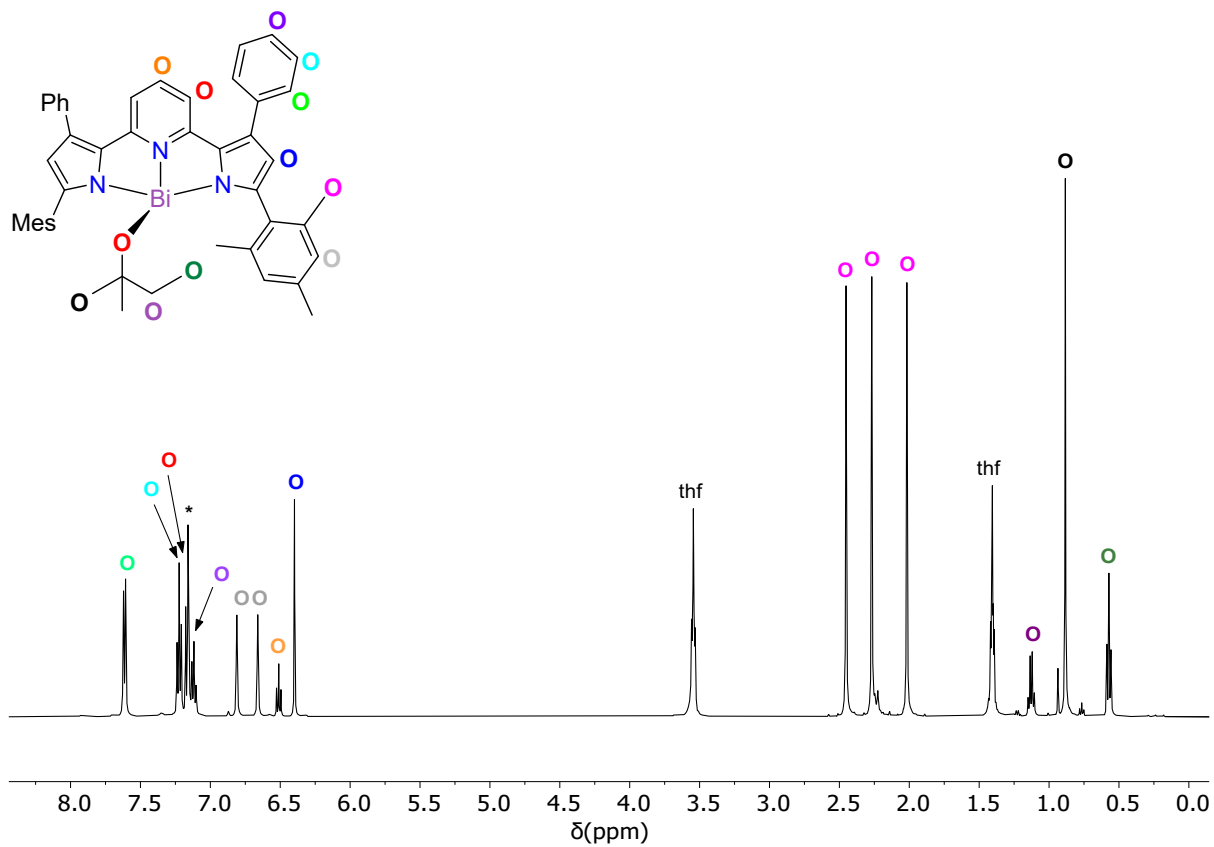


Fig. S10. ^1H NMR spectrum (C_6D_6 , 500 MHz, 298 K) of $(^{\text{Mes},\text{Ph}}\text{L})\text{Bi}(\text{OAm})$ (**6**). * denotes residual protio solvent fraction of C_6D_6 .

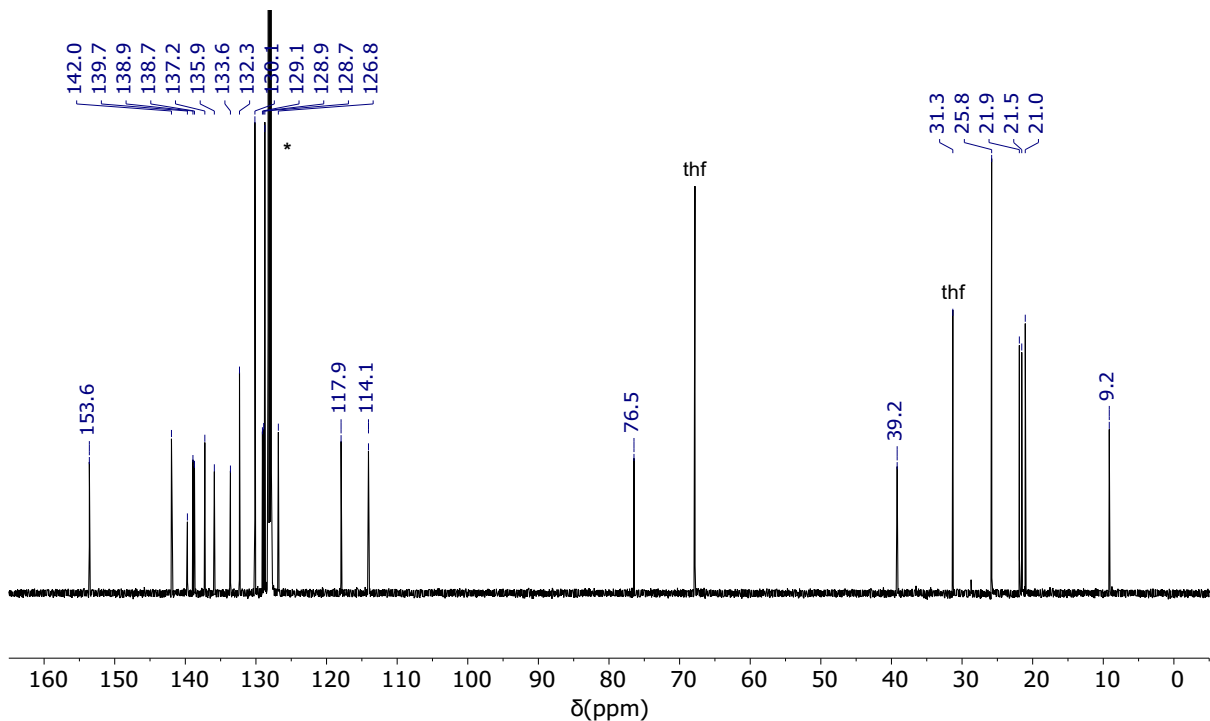


Fig. S11. $^{13}\text{C}\{^1\text{H}\}$ NMR spectrum (C_6D_6 , 125 MHz, 298 K) of $(^{\text{Mes},\text{Ph}}\text{L})\text{Bi}(\text{OAm})$ (**6**). * denotes C_6D_6 .

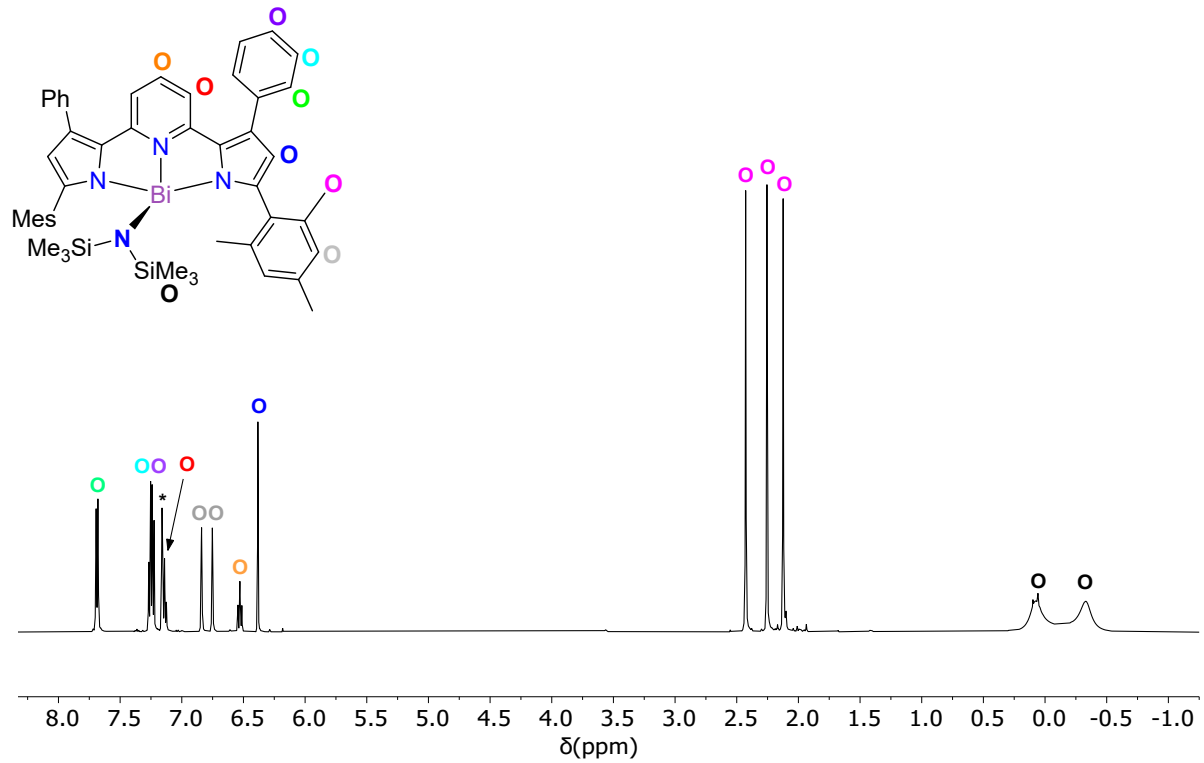


Fig. S12. ^1H NMR spectrum (C_6D_6 , 500 MHz, 298 K) of $(^{\text{Mes},\text{Ph}}\text{L})\text{Bi}(\text{N}''')$ (7). * denotes residual protio solvent fraction of C_6D_6 .

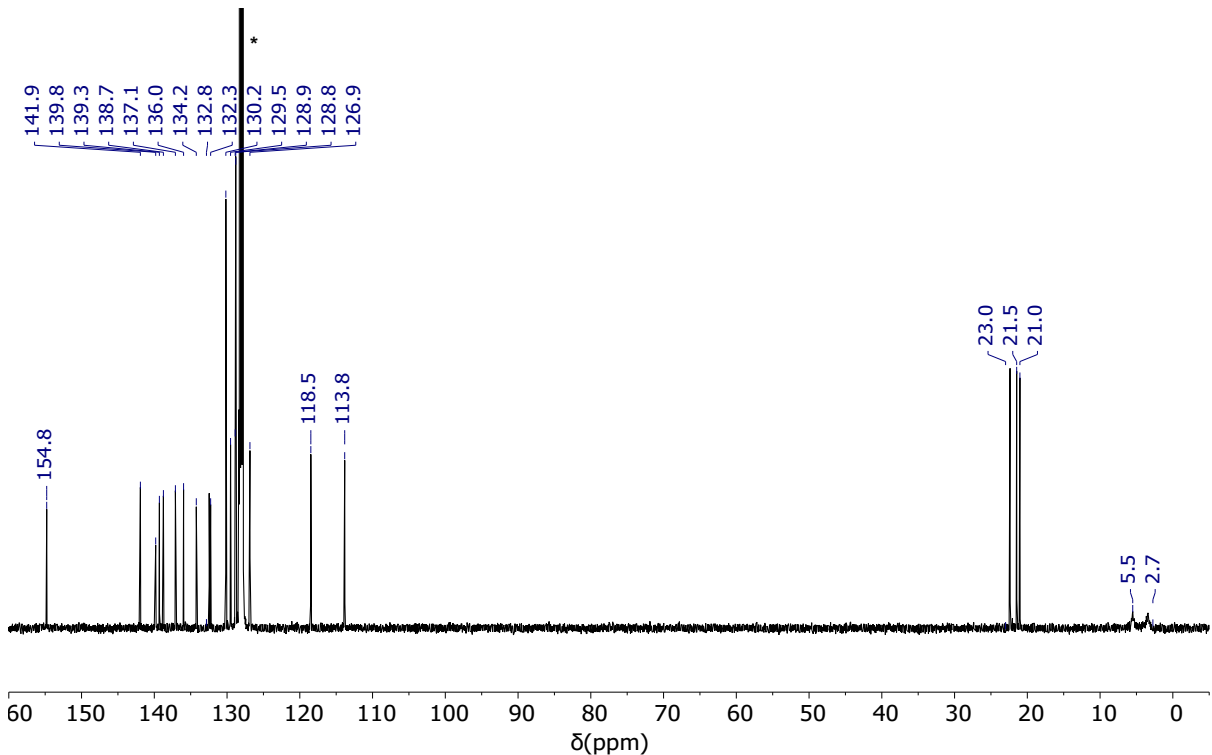


Fig. S13. $^{13}\text{C}\{^1\text{H}\}$ NMR spectrum (C_6D_6 , 125 MHz, 298 K) of $(^{\text{Mes},\text{Ph}}\text{L})\text{Bi}(\text{N}''')$ (7). * denotes C_6D_6 .

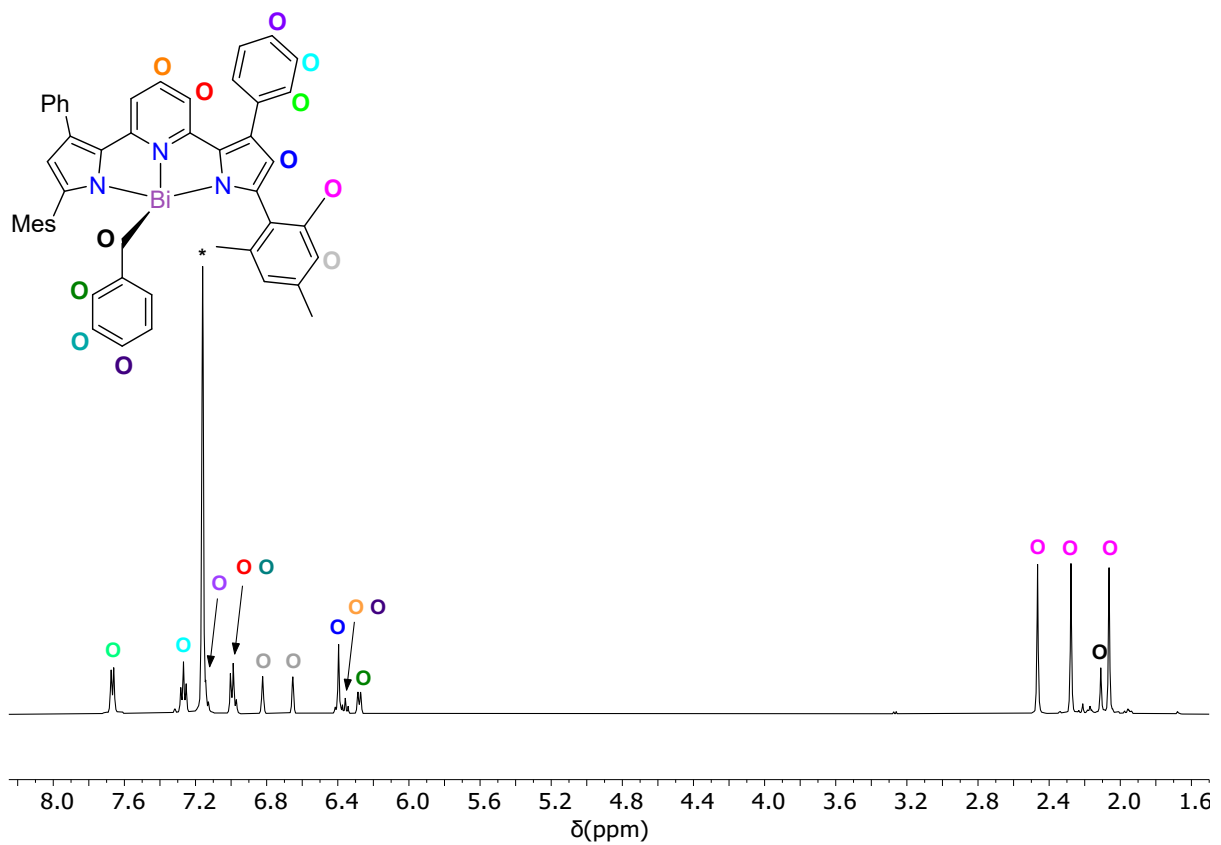


Fig. S14. ^1H NMR spectrum (C_6D_6 , 500 MHz, 298 K) of $(^{\text{Mes},\text{Ph}}\text{L})\text{Bi}(\text{CH}_2\text{Ph})$ (8). * denotes residual protio solvent fraction of C_6D_6 .

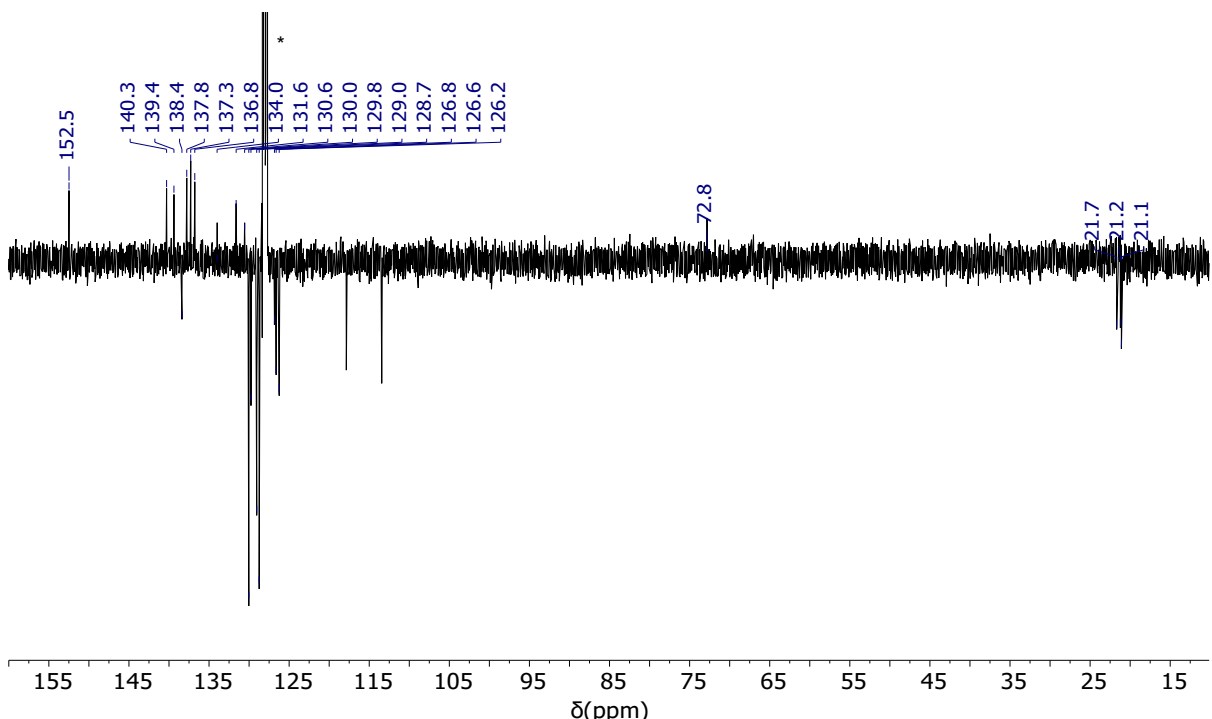


Fig. S15. $^{13}\text{C}\{^1\text{H}\}$ APT (attached proton test) NMR spectrum (C_6D_6 , 125 MHz, 298 K) of $(^{\text{Mes},\text{Ph}}\text{L})\text{Bi}(\text{CH}_2\text{Ph})$ (8). * denotes C_6D_6 .

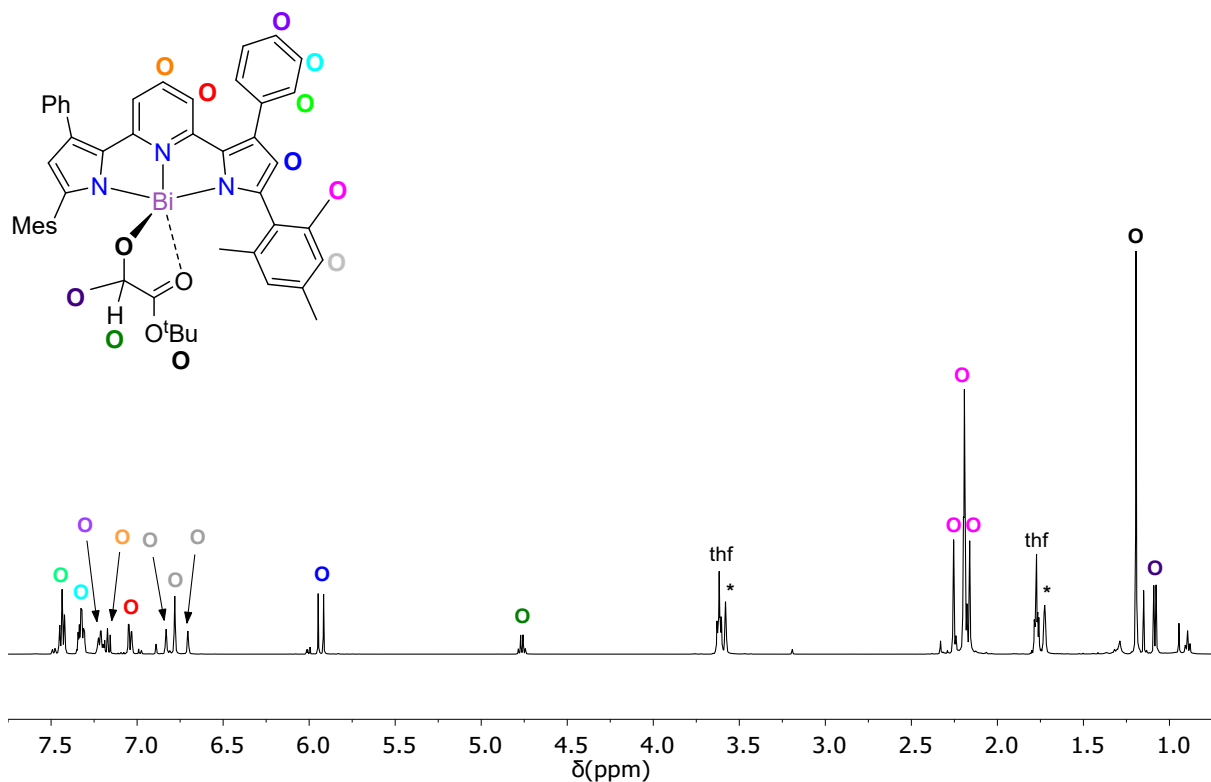


Fig. S16. ^1H NMR spectrum ($\text{C}_4\text{D}_8\text{O}$, 500 MHz, 298 K) of $(^\text{Mes,Ph}\text{L})\text{Bi}\{\text{OC}(\text{H})(\text{Me})\text{C}(=\text{O})\text{O}^\text{t}\text{Bu}\}$ (**9**). * denotes residual protio solvent fraction of $\text{C}_4\text{D}_8\text{O}$.

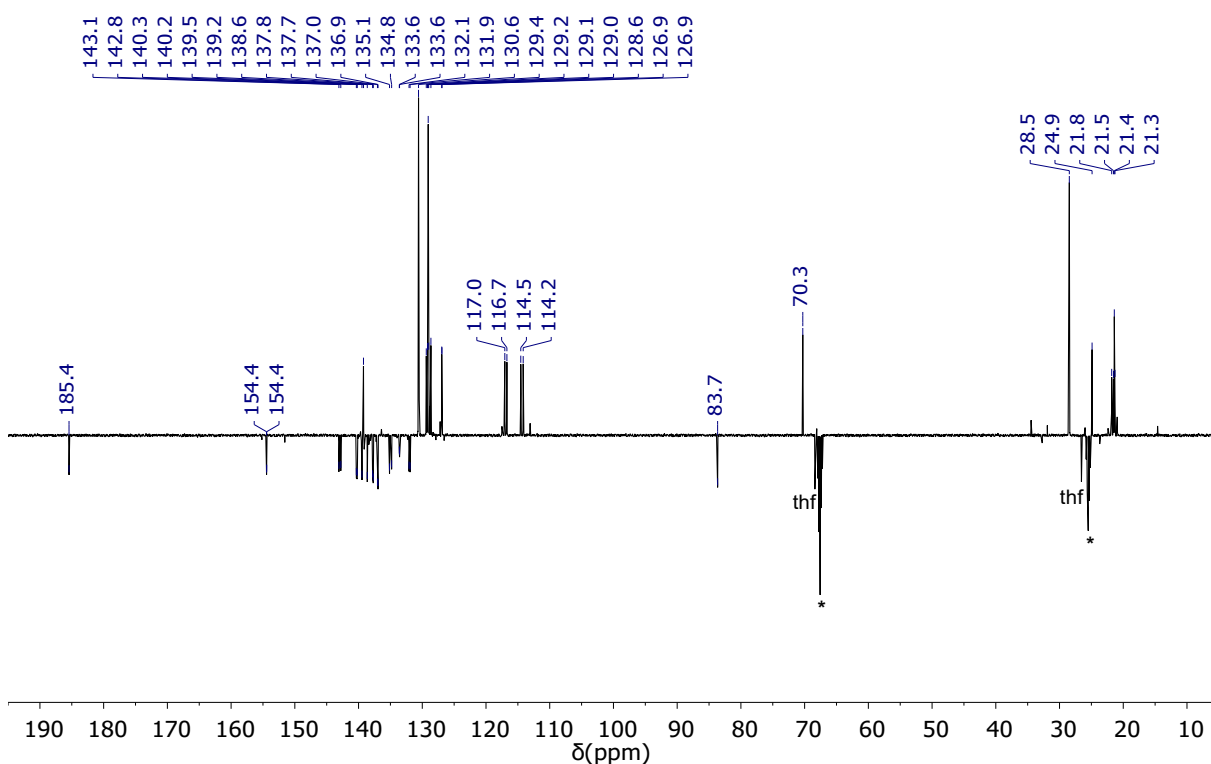


Fig. S17. $^{13}\text{C}\{^1\text{H}\}$ APT NMR spectrum ($\text{C}_4\text{D}_8\text{O}$, 100 MHz, 298 K) of $(^\text{Mes,Ph}\text{L})\text{Bi}\{\text{OC}(\text{H})(\text{Me})\text{C}(=\text{O})\text{O}^\text{t}\text{Bu}\}$ (**9**). * denotes $\text{C}_4\text{D}_8\text{O}$.

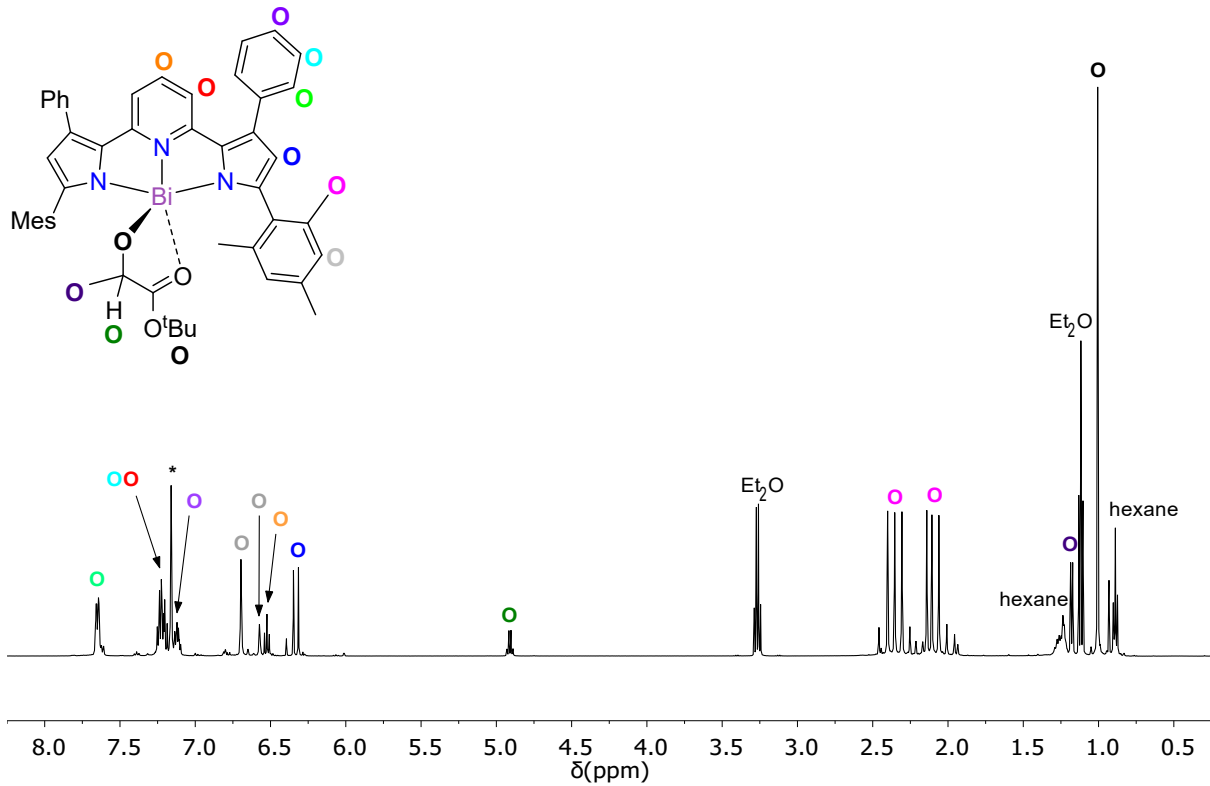


Fig. S18. ^1H NMR spectrum (C_6D_6 , 500 MHz, 298 K) of single crystals of $(^\text{Mes,Ph}\text{L})\text{Bi}\{\text{OC}(\text{H})(\text{Me})\text{C}(=\text{O})\text{O}^\text{t}\text{Bu}\}$ (**9**). * denotes residual protio solvent fraction of C_6D_6 .

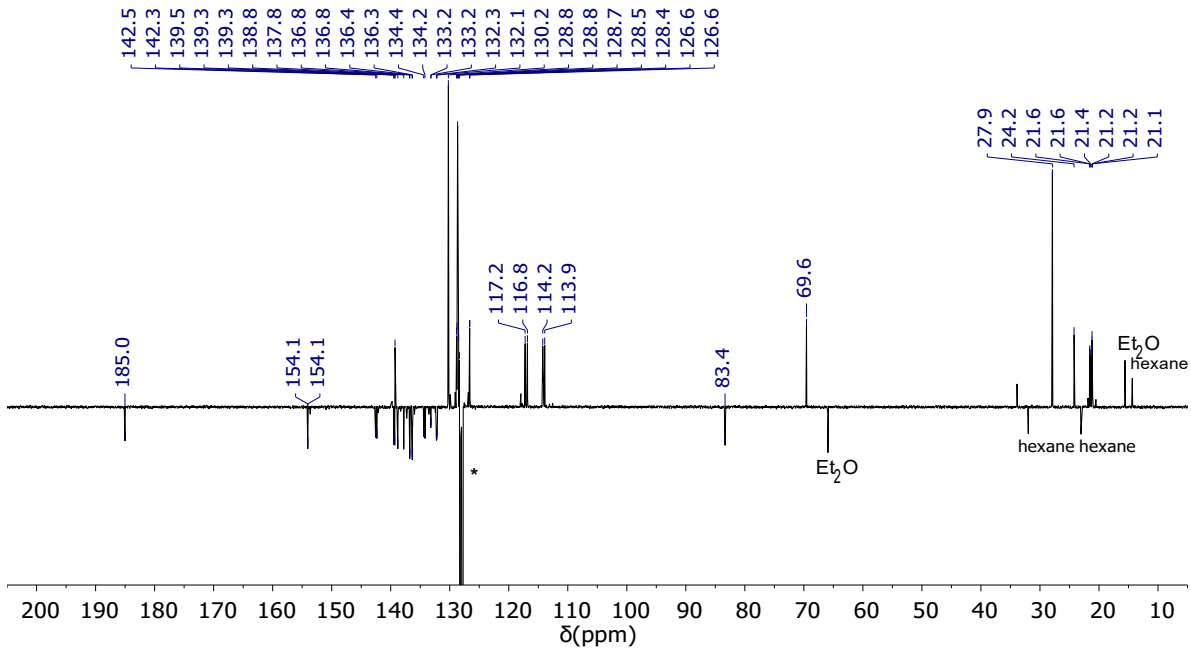


Fig. S19. $^{13}\text{C}\{^1\text{H}\}$ APT NMR spectrum (C_6D_6 , 100 MHz, 298 K) of single crystals of $(^\text{Mes,Ph}\text{L})\text{Bi}\{\text{OC}(\text{H})(\text{Me})\text{C}(=\text{O})\text{O}^\text{t}\text{Bu}\}$ (**9**). * denotes C_6D_6 .

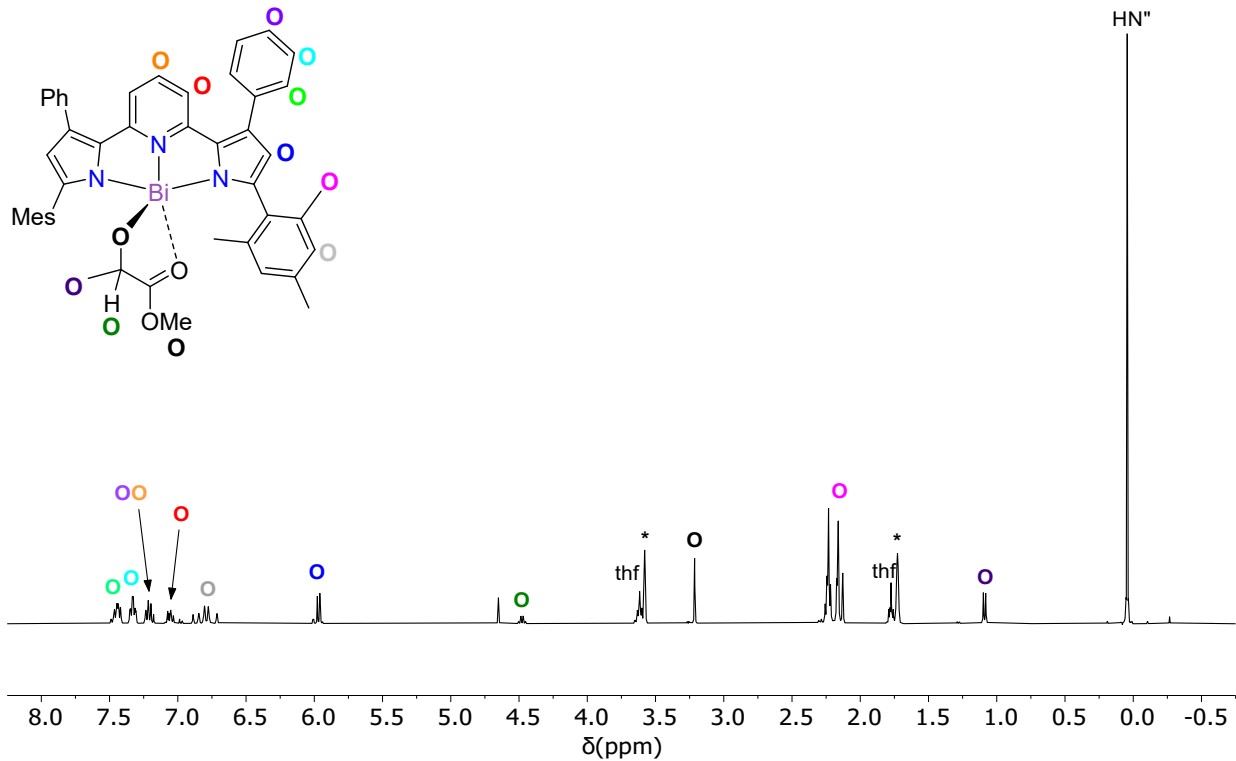


Fig. S20. ^1H NMR spectrum ($\text{C}_4\text{D}_8\text{O}$, 400 MHz, 298 K) of $(^{\text{Mes},\text{Ph}}\text{L})\text{Bi}\{\text{OC(H)(Me)C(=O)}\text{OMe}\}$ generated *in situ* (**10**). * denotes residual protio solvent fraction of $\text{C}_4\text{D}_8\text{O}$.

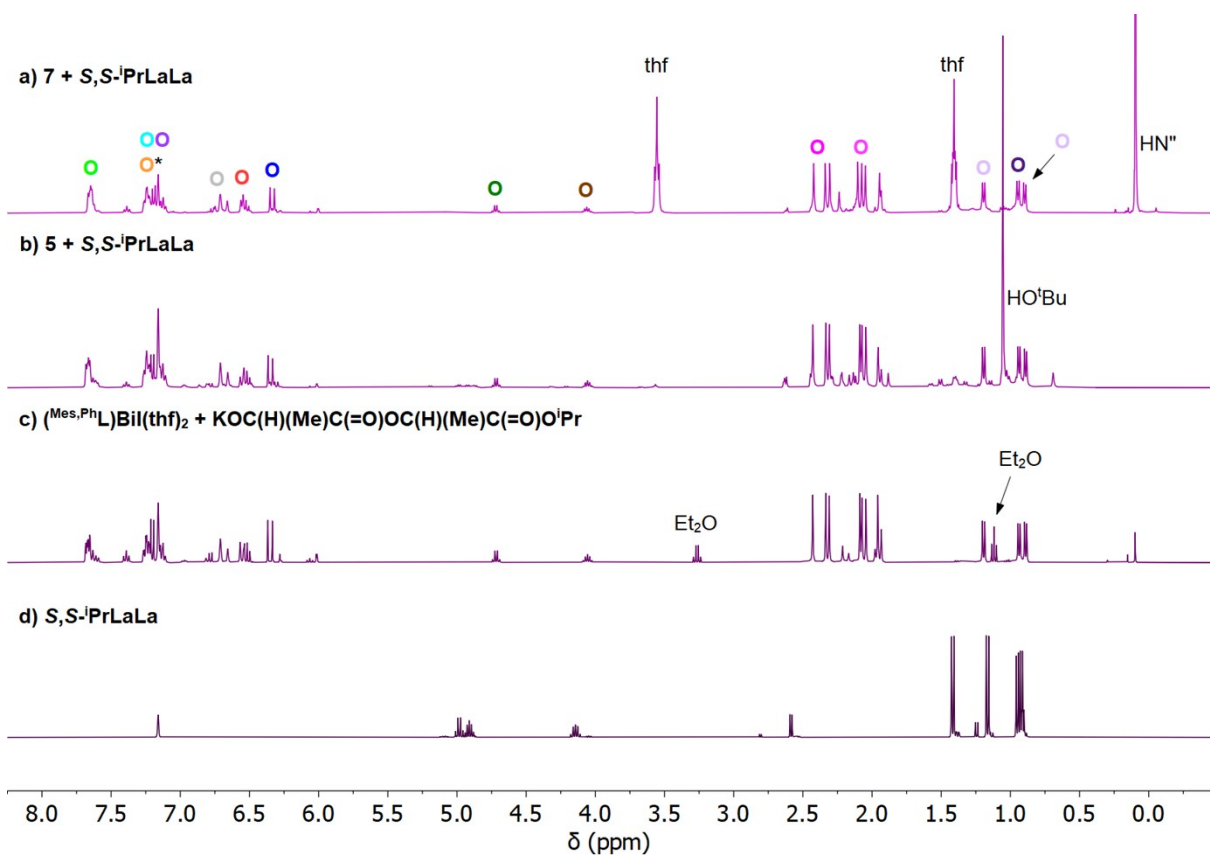
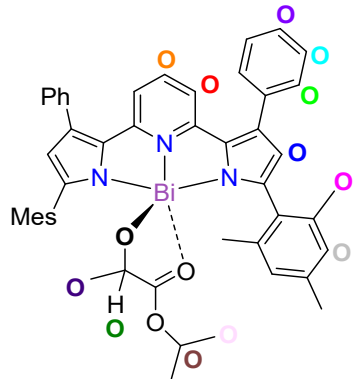


Fig. S21. ^1H NMR spectra (C_6D_6 , 500 MHz, 298 K) of $(^{\text{Mes},\text{Ph}}\text{L})\text{Bi}\{\text{OC}(\text{H})(\text{Me})\text{C}(=\text{O})\text{O}^{\text{i}}\text{Pr}\}$ (**11**) generated by reaction of a) **7** with $S,\text{S-}^{\text{i}}\text{PrLaLa}$, b) **5** with $S,\text{S-}^{\text{i}}\text{PrLaLa}$, c) $(^{\text{Mes},\text{Ph}}\text{L})\text{BiI}(\text{thf})_2$ with $\text{KOC}(\text{H})(\text{Me})\text{C}(=\text{O})\text{OC}(\text{H})(\text{Me})\text{C}(=\text{O})\text{O}^{\text{i}}\text{Pr}$, d) $S,\text{S-}^{\text{i}}\text{PrLaLa}$. * denotes residual protio solvent fraction of C_6D_6 . $S,\text{S-}^{\text{i}}\text{PrLaLa} = \text{HO}(\text{H})(\text{Me})\text{C}(=\text{O})\text{OC}(\text{H})(\text{Me})\text{C}(=\text{O})\text{O}^{\text{i}}\text{Pr}$.

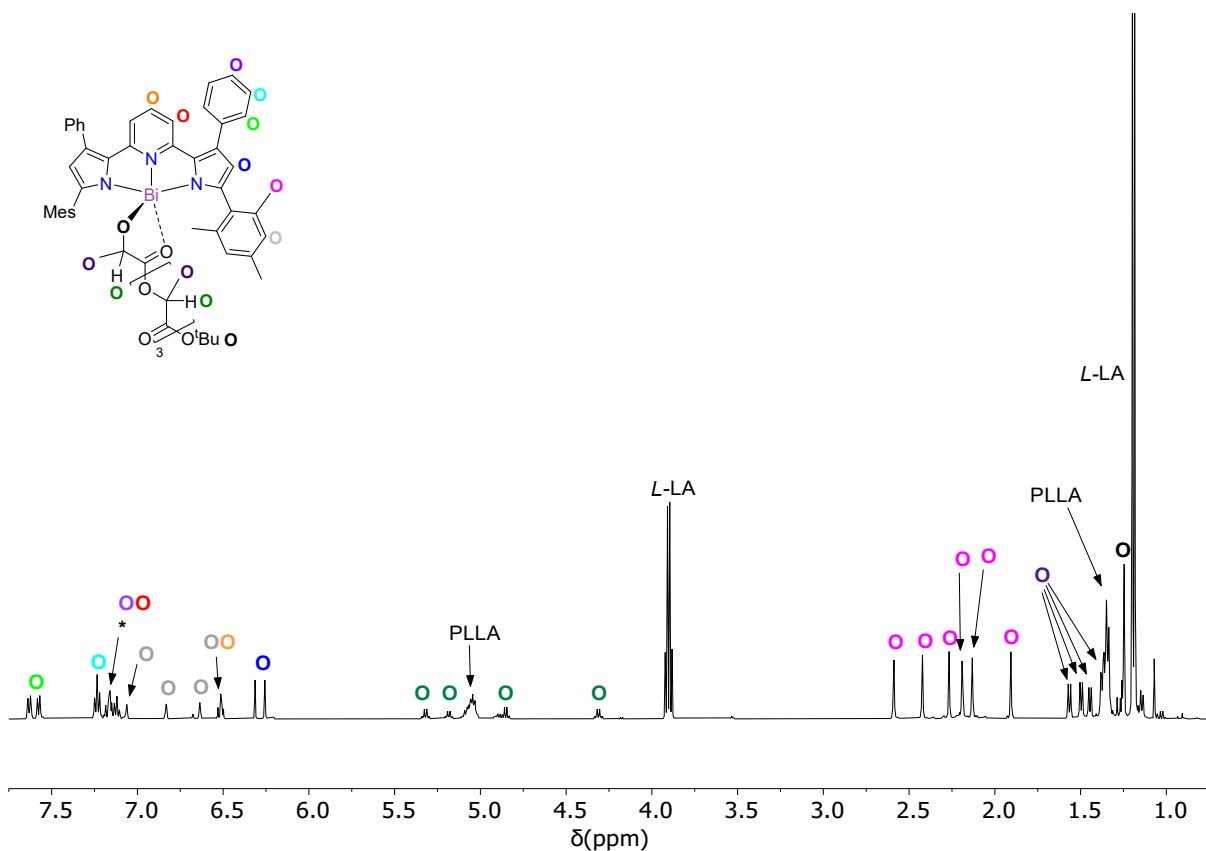


Fig. S22. ¹H NMR spectrum (C_6D_6 , 500 MHz, 298 K) of $(^{Mes,Ph}L)\text{Bi}\{\text{OC(H)(Me)C(=O)}\}_4\text{O}^t\text{Bu}$ (**12-O^tBu**), formed from the reaction between $(^{Mes,Ph}L)\text{Bi(O}^t\text{Bu})$ (**5**) and 10 eq. of *L*-LA at 80 °C for 48 h. * denotes residual protio solvent fraction of C_6D_6 .

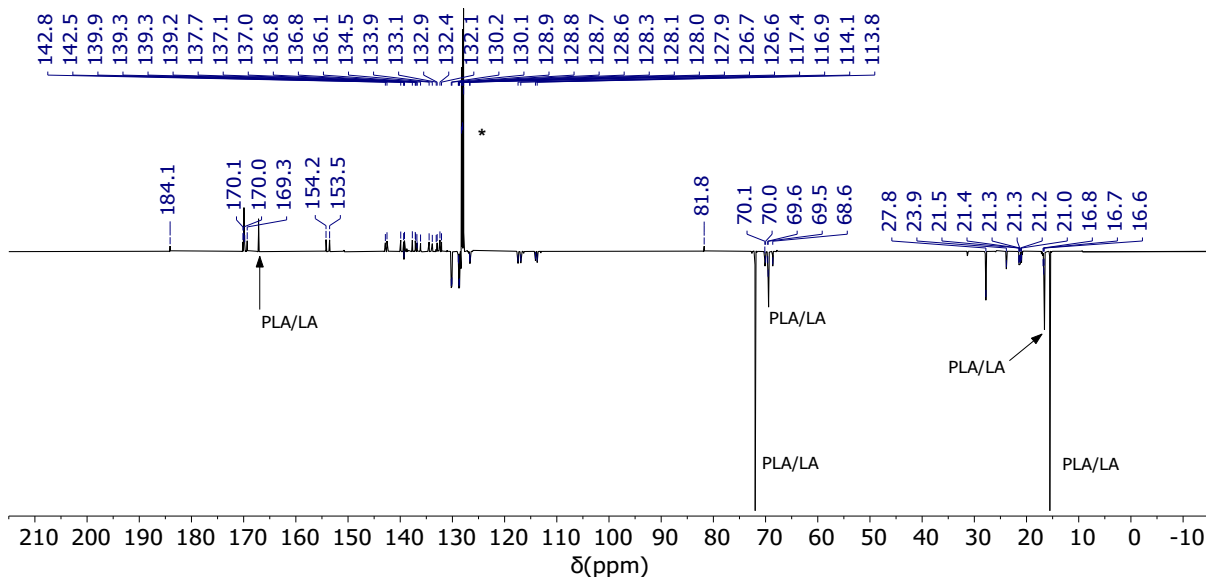


Fig. S23. ¹³C APT NMR spectrum (C_6D_6 , 500 MHz, 298 K) of $(^{Mes,Ph}L)\text{Bi}\{\text{OC(H)(Me)C(=O)}\}_4\text{O}^t\text{Bu}$ (**12-O^tBu**). * denotes C_6D_6 .

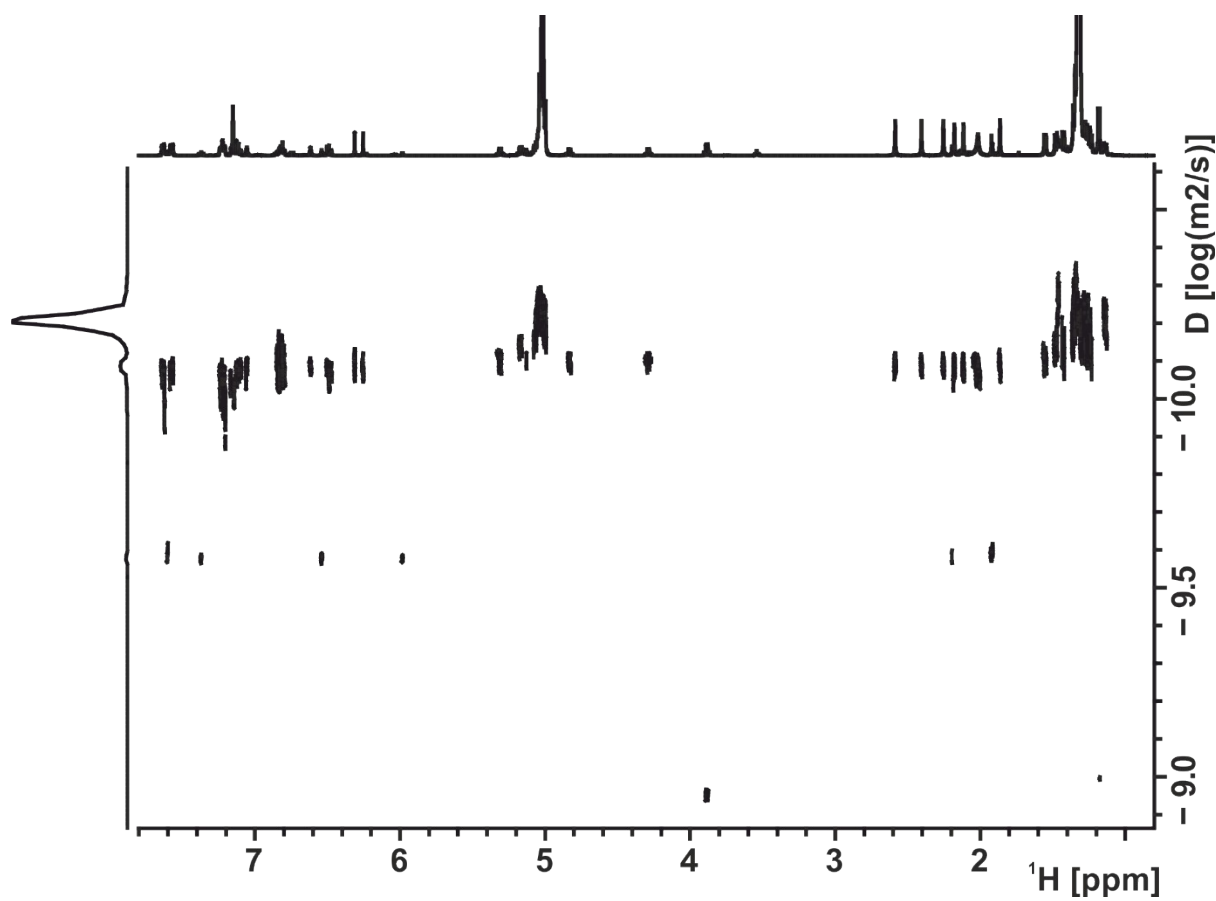


Fig. S24. ¹H-detected DOSY NMR spectrum (C_6D_6 , 500 MHz, 298 K) of the product between $(^{\text{Mes},\text{Ph}}\text{L})\text{Bi(OXyl)}$ and 10 eq. of *L*-LA (**12-OXyl**).

III. Crystallographic data

Crystals were mounted on MiTeGen MicroMounts using perfluoropolyether oil and rapidly transferred to a goniometer head on a diffractometer fitted with an Oxford Cryosystems Cryostream open-flow nitrogen cooling device.^[6] Data collections were carried out at 150 K using an Oxford Diffraction Supernova diffractometer using mirror-monochromated Cu $K\alpha$ radiation ($\lambda = 1.54178 \text{ \AA}$) and data were processed using CrysAlisPro^[7] The structures were solved using direct methods (SIR-92)^[8] or a charge flipping algorithm (SUPERFLIP)^[9] and refined by full-matrix least-squares procedures using the Win-GX software suite.^[10]

Computer programs: *CrysAlis PRO* 1.171.39.46 (Rigaku Oxford Diffraction, 2018) *CrysAlis PRO*, Agilent Technologies, Version 1.171.35.21 (release 20-01-2012 CrysAlis171 .NET) (compiled Jan 23 2012, 18:06:46); SUPERFLIP. Palatinus, L.; Chapuis, G. *J. Appl. Cryst.* 2007, 40, 786-790, : Sir-92. Altomare, A.; Cascarano, G.; Giacovazzo, C.; Guagliardi, A. *J. Appl. Cryst.* 1994, 27, 435., SIR92 Altomare, A.; Cascarano, G.; Giacovazzo, C.; Guagliardi, A. *J. Appl. Cryst.* 1994, 27, 435, *SHELXL2014* (Sheldrick, 2014), *ORTEP-3 for Windows*. Farrugia, L. *J. J. Appl. Cryst.* 1997, 30, 565.

Table S1. Selected experimental crystallographic data.

Complex	$(^{Mes,Ph}L)Bi(OXyl).(^{Mes,Ph}L)Bi(OXyl)(Et_2O)$ (1.1·Et ₂ O)	$(^{Mes,Ph}L)Bi(ODipp)$ (3)	$(^{Mes,Ph}L)Bi(OAr^{tBu})(Et_2O)$ (4·Et ₂ O)
Crystal data			
Chemical formula	C ₅₁ H ₄₆ BiN ₃ O·2(C ₅₁ H ₄₆ BiN ₃ O·C ₄ H ₁₀ O) 2925.89	C ₅₅ H ₅₄ BiN ₃ O 981.99	C ₅₇ H ₅₈ BiN ₃ O·C ₄ H ₁₀ O 1084.16
M _r			
Crystal system, space group	Triclinic, $P\bar{1}$	Triclinic, $P\bar{1}$	Monoclinic, $P2_1/n$
Temperature (K)	150	150	150
<i>a</i> , <i>b</i> , <i>c</i> (Å)	8.2339 (1), 24.4629 (3), 33.5522 (4)	11.8753 (2), 11.8990 (2), 17.3022 (3)	13.4237 (1), 20.7255 (1), 19.2516 (2)
α , β , γ (°)	100.852 (1), 94.324 (1), 93.271 (1)	85.316 (2), 88.851 (2), 66.559 (2)	90, 108.357 (1), 90
<i>V</i> (Å ³)	6600.96 (14)	2235.40 (7)	5083.49 (7)
<i>Z</i>	2	2	4
Radiation type	Cu $K\alpha$	Cu $K\alpha$	Cu $K\alpha$
μ (mm ⁻¹)	8.20	8.06	7.16
Crystal size (mm)	0.17 × 0.07 × 0.05	0.27 × 0.18 × 0.08	0.24 × 0.15 × 0.12
Data Collection			
Diffractometer	SuperNova, Dual, Cu at zero, Atlas Gaussian: <i>CrysAlis PRO</i> 1.171.39.46 (Rigaku Oxford Diffraction, 2018)	SuperNova, Dual, Cu at zero, Atlas Gaussian: <i>CrysAlis PRO</i> 1.171.39.46 (Rigaku Oxford Diffraction, 2018)	SuperNova, Dual, Cu at zero, Atlas Gaussian: <i>CrysAlis PRO</i> 1.171.39.46 (Rigaku Oxford Diffraction, 2018) Numerical absorption correction based on Gaussian integration over a multifaceted crystal model. Empirical absorption correction using spherical harmonics, implemented in SCALE3 ABSPACK.
Absorption correction	Numerical absorption correction based on Gaussian integration over a multifaceted crystal model. Empirical absorption correction using spherical harmonics, implemented in SCALE3 ABSPACK.	Numerical absorption correction based on Gaussian integration over a multifaceted crystal model. Empirical absorption correction using spherical harmonics, implemented in SCALE3 ABSPACK.	Numerical absorption correction based on Gaussian integration over a multifaceted crystal model. Empirical absorption correction using spherical harmonics, implemented in SCALE3 ABSPACK.
<i>T</i> _{min} , <i>T</i> _{max}	0.754, 1.000	0.395, 1.000	0.555, 1.000
No. of measured, independent and observed [<i>I</i> > 2σ(<i>I</i>)] reflections	134884, 26983, 25276	73396, 9136, 8907	29399, 10364, 9495
<i>R</i> _{int}	0.033	0.026	0.021
Refinement			
<i>R</i> [$F^2 > 2\sigma(F^2)$], <i>wR</i> (F^2), <i>S</i>	0.025, 0.056, 1.07	0.016, 0.040, 1.08	0.021, 0.051, 1.04
No. of reflections	26983	9136	10364
No. of parameters	1674	551	618
No. of restraints	56	0	0
(Δ/σ) _{max}	0.005	0.002	0.001
Δρ _{max} , Δρ _{min} (e Å ⁻³)	1.84, -1.05	0.86, -0.34	1.43, -0.60

Complex	$(^{Mes,Ph}L)Bi(N'')$ (7)	$(^{Mes,Ph}L)Bi(CH_2Ph)$ (8)	$(^{Mes,Ph}L)Bi\{(R)-OC(H)(Me)C(=O)O^tBu\}$ (9)
Crystal data			
Chemical formula	$C_{49}H_{55}BiN_4Si_2$	$C_{50}H_{44}BiN_3$	$2(C_{50}H_{50}BiN_3O_3), C_4H_{10}O$
M_r	965.13	895.86	986.97
Crystal system, space group	Triclinic, $P\bar{1}$	Triclinic, $P\bar{1}$	Triclinic, $P1$
Temperature (K)	150	150	150
a, b, c (Å)	11.7809 (2), 13.0248 (3), 15.5509 (3)	10.4648 (1), 15.9209 (4), 16.6460 (5)	14.0468 (3), 15.2097 (3), 24.2383 (5)
α, β, γ (°)	79.571 (2), 77.942 (2), 70.326 (2)	114.196 (3), 94.541 (2), 97.365 (2)	76.010 (2), 77.167 (2), 72.303 (2)
V (Å ³)	2181.39 (8)	2482.12 (11)	4724.79 (18)
Z	2	2	2
Radiation type	$Cu K\alpha$	$Cu K\alpha$	$Cu K\alpha$
μ (mm ⁻¹)	8.74	7.20	7.67
Crystal size (mm)	0.17 × 0.11 × 0.08	0.27 × 0.12 × 0.06	0.60 × 0.22 × 0.11
Data Collection			
Diffractometer	SuperNova, Dual, Cu at zero, Atlas	SuperNova, Dual, Cu at zero, Atlas	SuperNova, Dual, Cu at zero, Atlas
Absorption correction	Multi-scan: <i>CrysAlis PRO</i> 1.171.39.46 (Rigaku Oxford Diffraction, 2018) Empirical absorption correction using spherical harmonics, implemented in SCALE3 ABSPACK.	Gaussian : <i>CrysAlis PRO</i> 1.171.39.46 (Rigaku Oxford Diffraction, 2018) Numerical absorption correction based on Gaussian integration over a multifaceted crystal model. Empirical absorption correction using spherical harmonics, implemented in SCALE3 ABSPACK.	Gaussian: <i>CrysAlis PRO</i> 1.171.39.46 (Rigaku Oxford Diffraction, 2018) Numerical absorption correction based on Gaussian integration over a multifaceted crystal model. Empirical absorption correction using spherical harmonics, implemented in SCALE3 ABSPACK.
T_{min}, T_{max}	0.534, 1.000	0.552, 1.000	0.096, 0.733
No. of measured, independent and observed [$I > 2\sigma(I)$] reflections	44251, 8915, 8354	47983, 10132, 9501	86221, 36580, 31219
R_{int}	0.036	0.092	0.055
Refinement			
$R[F^2 > 2\sigma(F^2)], wR(F^2), S$	0.023, 0.059, 1.04	0.086, 0.221, 1.04	0.065, 0.182, 1.05
No. of reflections	8915	10132	36580
No. of parameters	559	487	2133
No. of restraints	105	0	21
$(\Delta/\sigma)_{max}$	0.001	0.001	0.004
$\Delta\rho_{max}, \Delta\rho_{min}$ (e Å ⁻³)	1.29, -0.96	14.72, -3.07	2.09, -2.13
Absolute structure parameter	-	-	-0.044 (12)

Complex	$(^{Mes,Ph}L)Bi\{OC(H)(Me)C(=O)O^iPr\}$ (11)
Crystal data	
Chemical formula	C ₄₉ H ₄₈ BiN ₃ O ₃
M_r	935.88
Crystal system, space group	Triclinic, $P\bar{1}$
Temperature (K)	150
a, b, c (Å)	15.1641 (4), 17.9448 (4), 17.9851 (4)
α, β, γ (°)	101.318 (2), 113.562 (2), 97.502 (2)
V (Å ³)	4278.19 (19)
Z	4
Radiation type	Cu $K\alpha$
μ (mm ⁻¹)	8.43
Crystal size (mm)	0.24 × 0.11 × 0.04
Data Collection	
Diffractometer	SuperNova, Dual, Cu at zero, Atlas diffractometer
Absorption correction	Gaussian <i>CrysAlis PRO</i> 1.171.39.46 (Rigaku Oxford Diffraction, 2018) Numerical absorption correction based on Gaussian integration over a multifaceted crystal model Empirical absorption correction using spherical harmonics, implemented in SCALE3 ABSPACK scaling algorithm.
T_{min}, T_{max}	0.236, 1.000
No. of measured, independent and observed [$I > 2\sigma(I)$] reflections	68712, 17478, 14409
R_{int}	0.071
Refinement	
$R[F^2 > 2\sigma(F^2)], wR(F^2), S$	0.039, 0.099, 1.01
No. of reflections	17478
No. of parameters	1027
No. of restraints	0
$(\Delta/\sigma)_{max}$	0.002
$\Delta\rho_{max}, \Delta\rho_{min}$ (e Å ⁻³)	1.81, -1.76
Absolute structure parameter	-

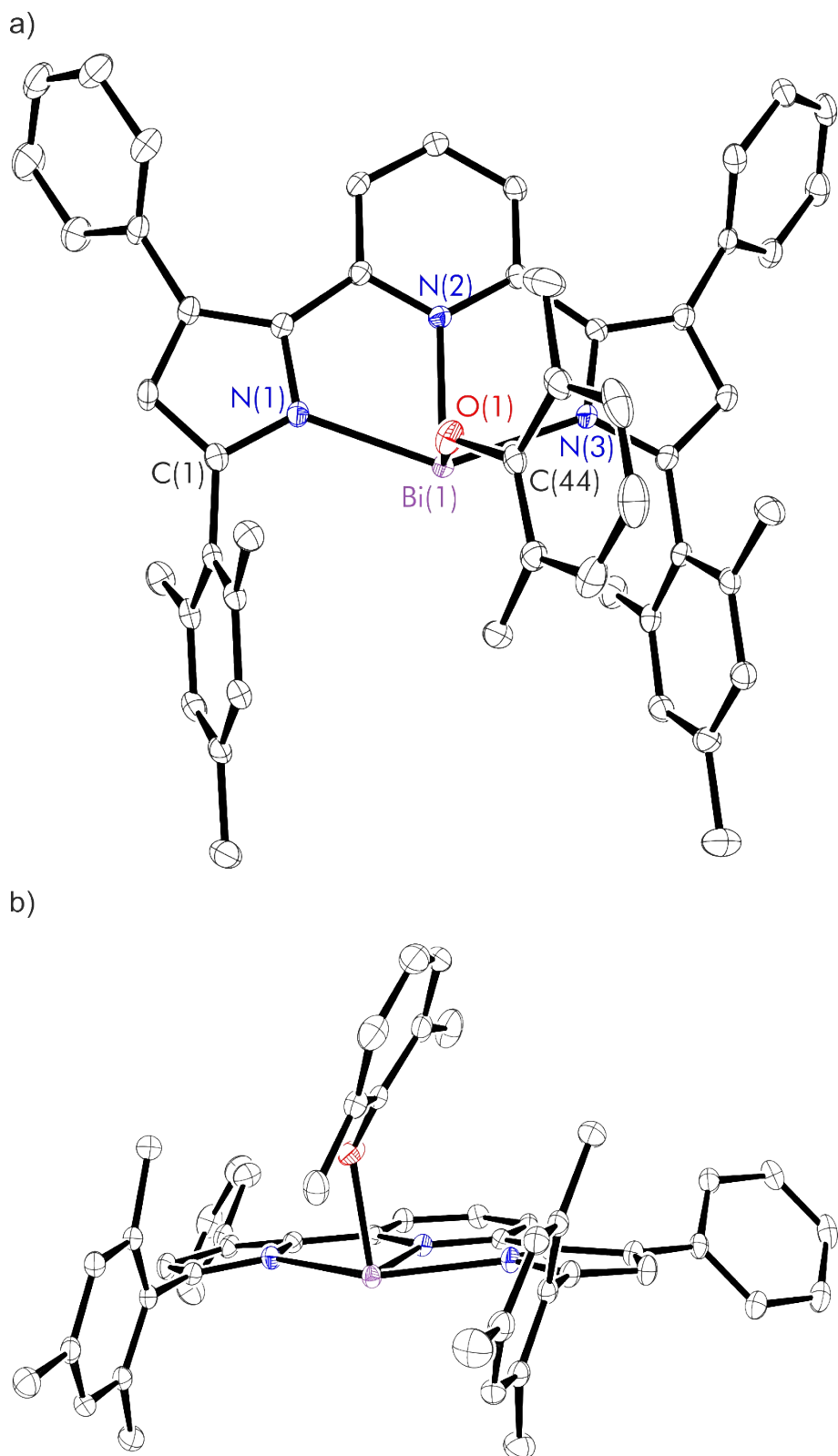


Fig. S25. Thermal displacement ellipsoid drawing (30% probability) of (^{Mes,Ph}L)Bi(OXyl) (**1**); a) top and b) side view. All hydrogen atoms have been omitted for clarity.

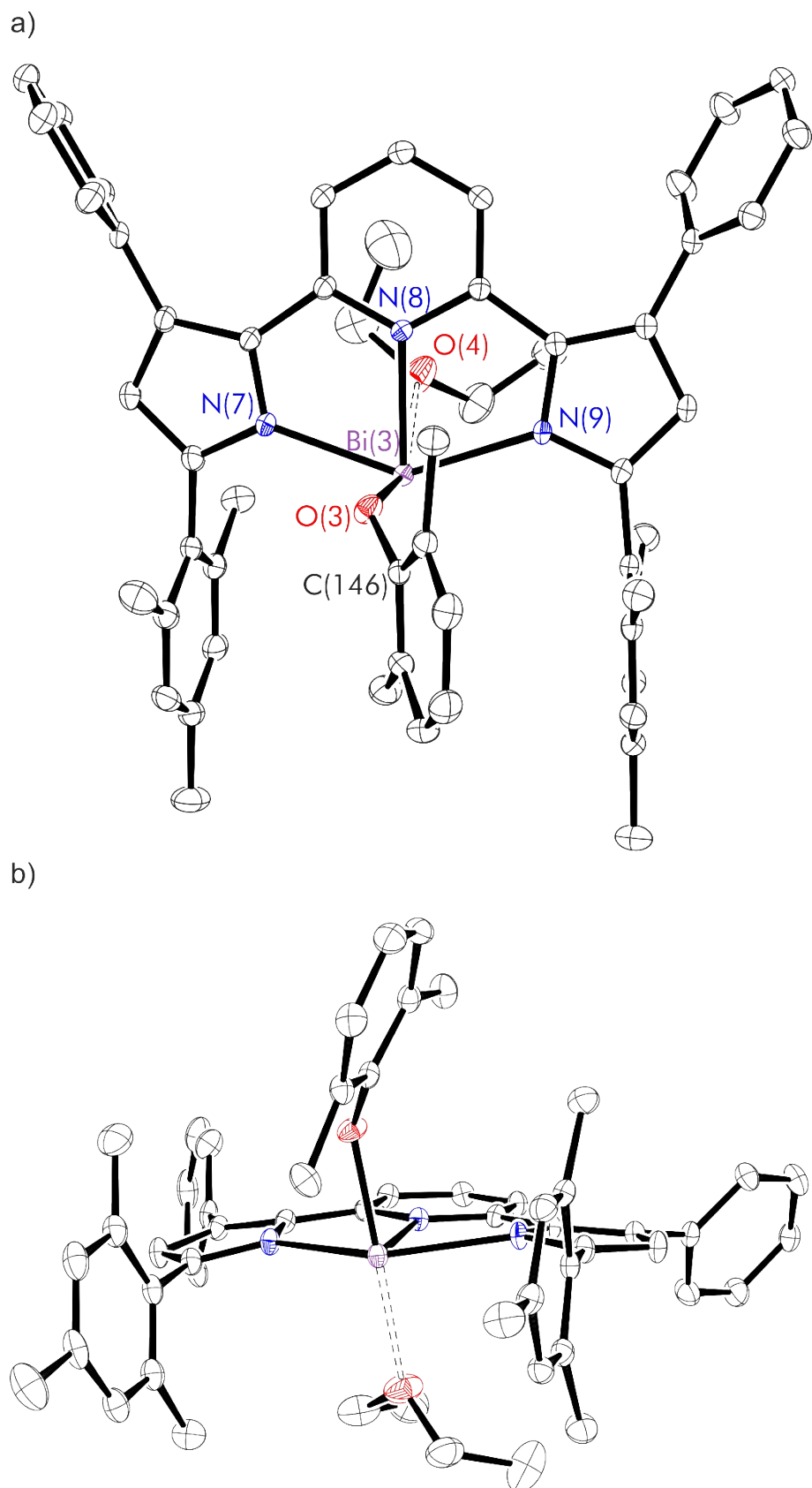


Fig. S26. Thermal displacement ellipsoid drawing (30% probability) of (^{Mes,Ph}L)Bi(OXyl)(Et₂O) (1·Et₂O); a) top and b) side view. All hydrogen atoms have been omitted for clarity.

Table S2. Experimental metrical parameters (bond lengths in Å and angles in °) in **1**.

Bi(1)-O(1)	2.077(2)
Bi(1)-N(1)	2.262(2)
Bi(1)-N(2)	2.301(2)
Bi(1)-N(3)	2.305(2)
C(5)-N(2)	1.366(3)
C(5)-C(6)	1.403(4)
C(6)-C(7)	1.382(4)
C(7)-C(8)	1.381(4)
C(8)-C(9)	1.395(4)
C(9)-N(2)	1.362(3)
Bi(1)-O(1)-C(44)	133.49(19)
N(1)-Bi(1)-N(3)	139.71(8)
N(1)-Bi(1)-N(2)	69.86(8)
N(2)-Bi(1)-N(3)	70.58(8)
N(1)-Bi(1)-O(1)	81.73(8)
N(2)-Bi(1)-O(1)	93.09(9)
N(3)-Bi(1)-O(1)	93.05(8)

Table S3. Experimental metrical parameters (bond lengths in Å and angles in °) in **1·Et₂O**.

Bi(3)-O(3)	2.1064(19)
Bi(3)-O(4)	2.7638(1)
Bi(3)-N(7)	2.277(2)
Bi(3)-N(8)	2.298(2)
Bi(3)-N(9)	2.315(2)
C(107)-N(8)	1.359(3)
C(107)-C(108)	1.401(4)
C(108)-C(109)	1.382(4)
C(109)-C(110)	1.381(4)
C(110)-C(111)	1.402(4)
C(111)-N(8)	1.362(3)
Bi(3)-O(3)-C(146)	133.41(17)
O(3)-Bi(3)-O(4)	157.39(1)
N(7)-Bi(3)-N(9)	140.76(8)
N(7)-Bi(3)-N(8)	70.36(8)
N(8)-Bi(3)-N(9)	70.58(8)
N(7)-Bi(3)-O(3)	82.52(8)
N(8)-Bi(3)-O(3)	89.15(8)
N(9)-Bi(3)-O(3)	93.33(8)

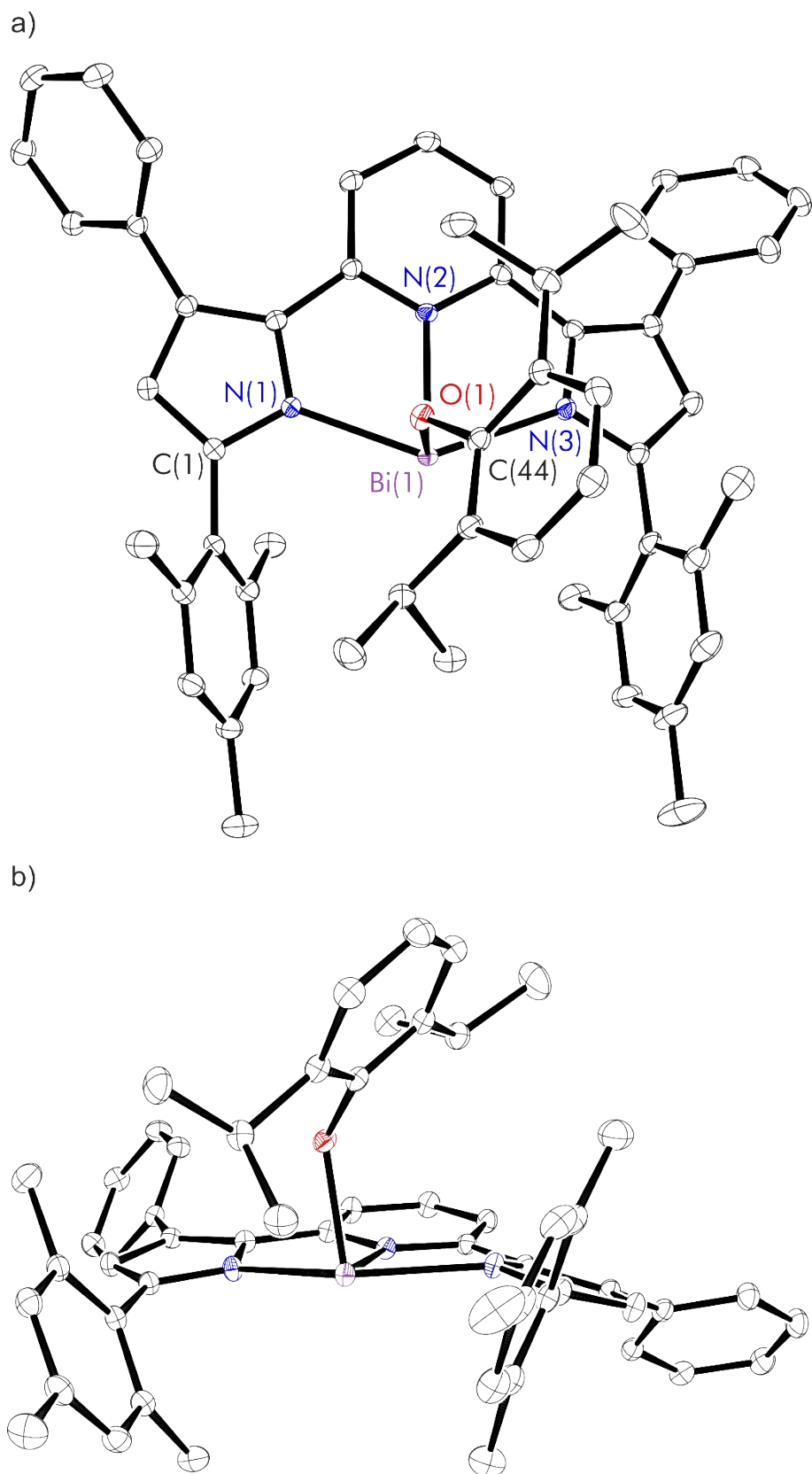
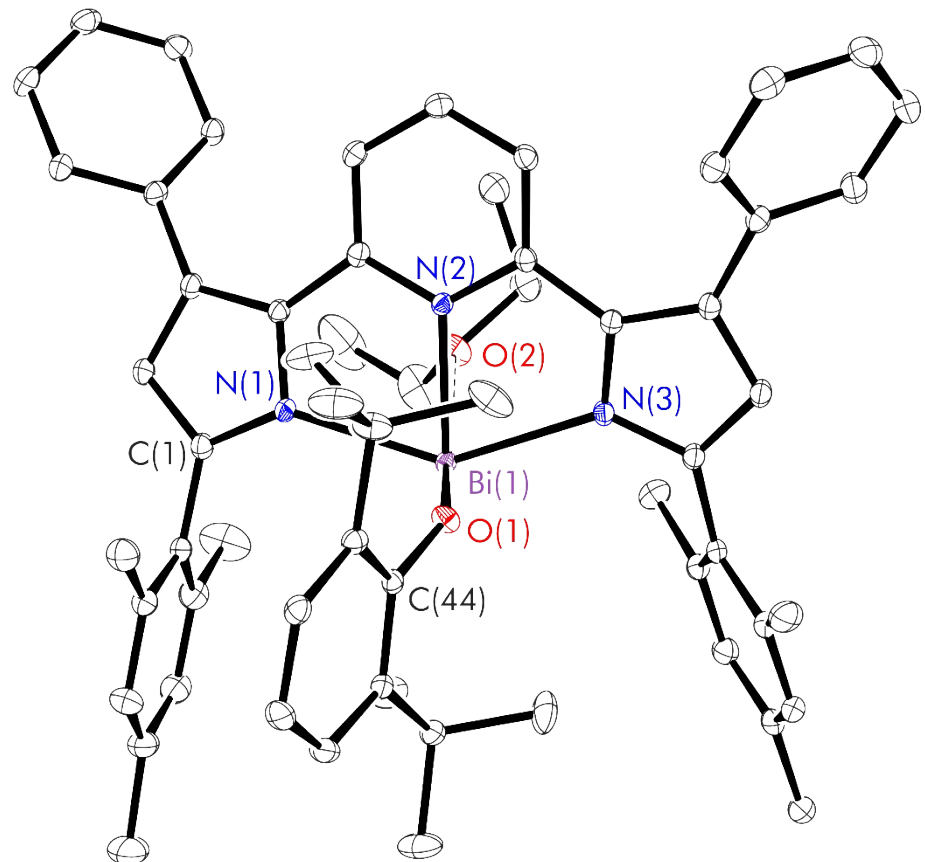


Fig. S27. Thermal displacement ellipsoid drawings (30% probability) of (^{Mes,Ph}L)Bi(ODipp) (**3**); a) top and b) side view. All hydrogen atoms have been omitted for clarity.

Table S4. Experimental metrical parameters (bond lengths in Å and angles in °) in **3**.

Bi(1)-O(1)	2.0801(12)
Bi(1)-N(1)	2.2526(14)
Bi(1)-N(2)	2.3047(14)
Bi(1)-N(3)	2.3031(14)
C(5)-N(2)	1.367(2)
C(5)-C(6)	1.397(2)
C(6)-C(7)	1.383(3)
C(7)-C(8)	1.386(3)
C(8)-C(9)	1.396(2)
C(9)-N(2)	1.362(2)
Bi(1)-O(1)-C(44)	129.10(10)
N(1)-Bi(1)-N(3)	139.95(5)
N(1)-Bi(1)-N(2)	69.89(5)
N(2)-Bi(1)-N(3)	70.09(5)
N(1)-Bi(1)-O(1)	83.91(5)
N(2)-Bi(1)-O(1)	86.85(5)
N(3)-Bi(1)-O(1)	95.44(5)

a)



b)

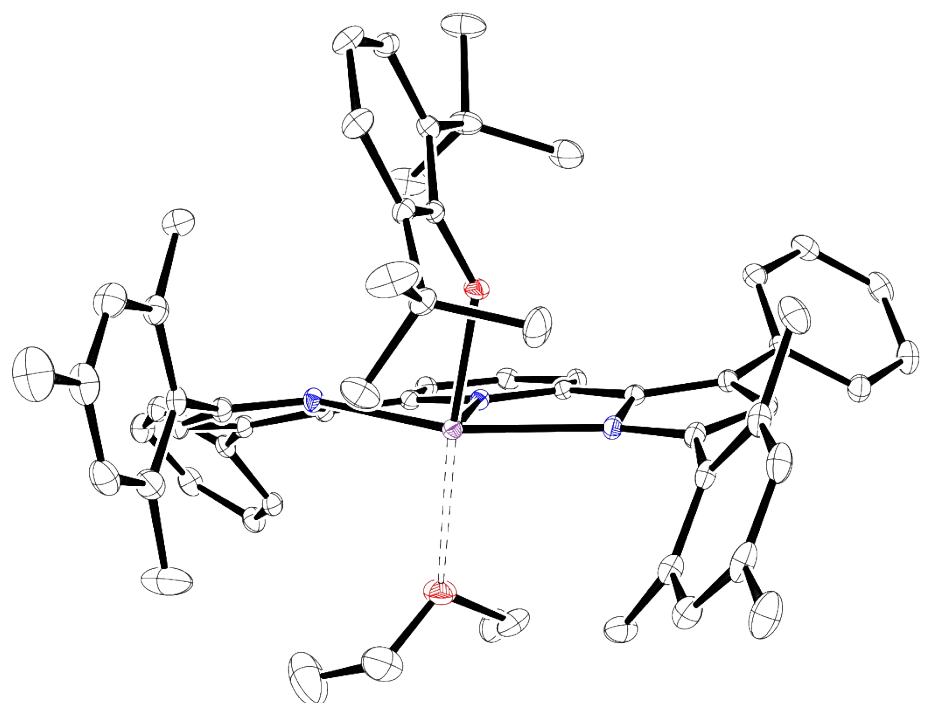


Fig. S28. Thermal displacement ellipsoid drawing (30% probability) of $(^{\text{Mes},\text{Ph}}\text{L})\text{Bi}(\text{OAr}^{\text{tBu}})(\text{Et}_2\text{O})$ (4· Et_2O); a) top and b) side view. All hydrogen atoms have been omitted for clarity.

Table S5. Experimental metrical parameters (bond lengths in Å and angles in °) in **4·Et₂O**.

Bi(1)-O(1)	2.1137(15)
Bi(1)-O(2)	2.8419(1)
Bi(1)-N(1)	2.3482(18)
Bi(1)-N(2)	2.2659(18)
Bi(1)-N(3)	2.3443(17)
C(5)-N(2)	1.365(3)
C(5)-C(6)	1.398(3)
C(6)-C(7)	1.383(3)
C(7)-C(8)	1.387(3)
C(8)-C(9)	1.393(3)
C(9)-N(2)	1.362(3)
Bi(1)-O(1)-C(44)	142.51(13)
N(1)-Bi(1)-N(3)	142.18(7)
N(1)-Bi(1)-N(2)	71.48(6)
N(2)-Bi(1)-N(3)	70.93(6)
N(1)-Bi(1)-O(1)	96.25(6)
N(2)-Bi(1)-O(1)	94.66(6)
N(3)-Bi(1)-O(1)	82.87(6)

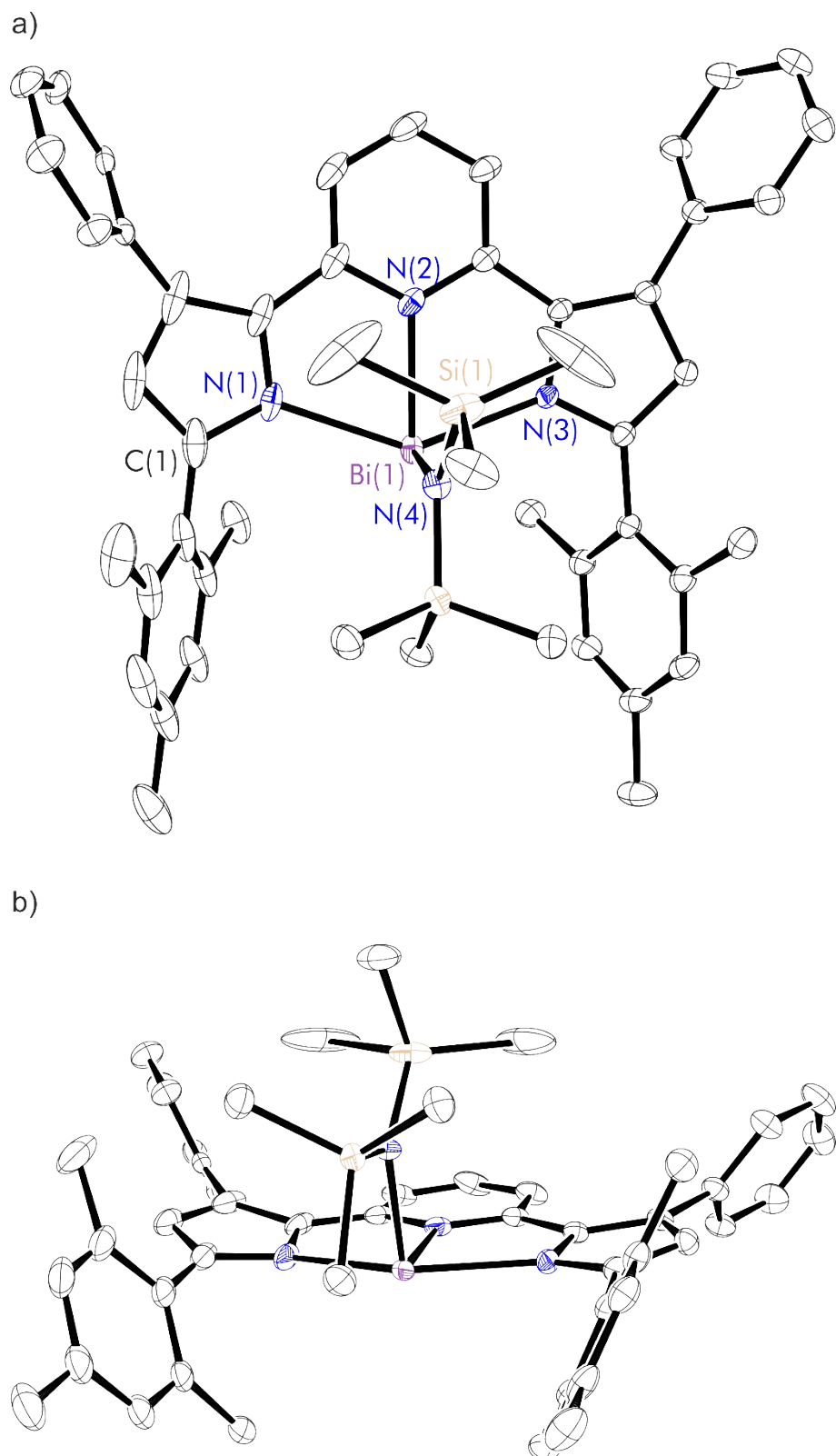
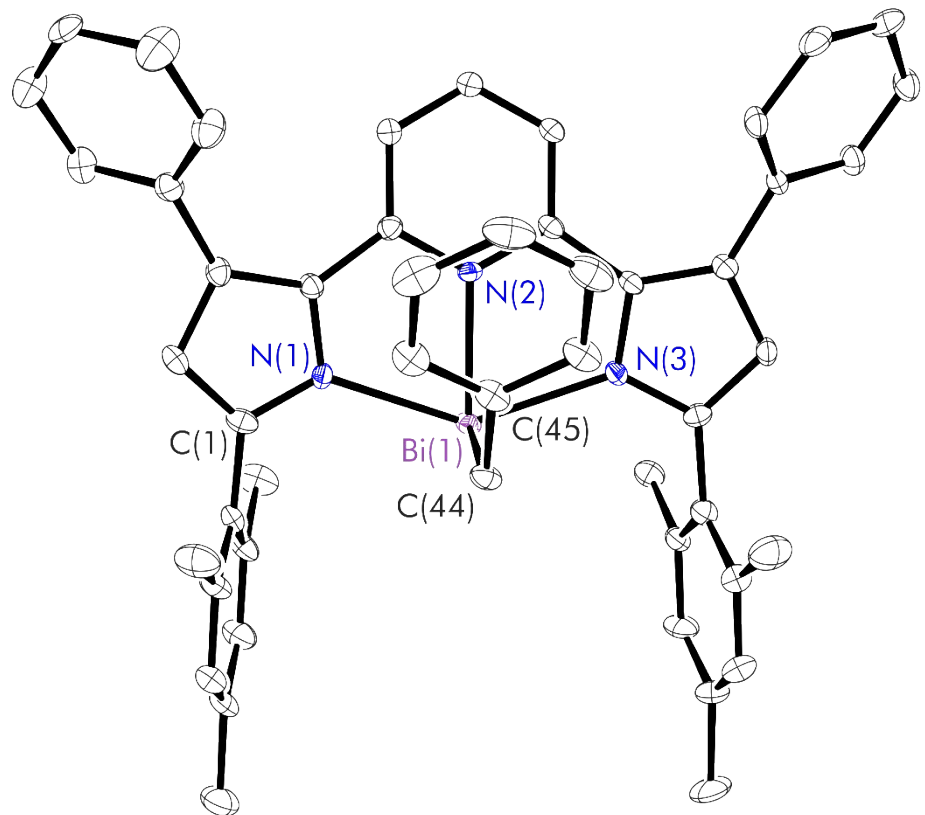


Fig. S29. Thermal displacement ellipsoid drawing (30% probability) of (^{Mes,Ph}L)Bi(N'') (7); a) top and b) side view. All hydrogen atoms have been omitted for clarity.

Table S6. Experimental metrical parameters (bond lengths in Å and angles in °) in 7.

Bi(1)-N(1)	2.339(2)
Bi(1)-N(2)	2.302(2)
Bi(1)-N(3)	2.327(2)
Bi(1)-N(4)	2.143(2)
C(5)-N(2)	1.371(4)
C(5)-C(6)	1.394(5)
C(6)-C(7)	1.377(6)
C(7)-C(8)	1.384(5)
C(8)-C(9)	1.397(4)
C(9)-N(2)	1.367(4)
Bi(1)-N(4)-Si(1)	125.63(13)
Bi(1)-N(4)-Si(2)	112.18(12)
N(1)-Bi(1)-N(3)	140.61(9)
N(1)-Bi(1)-N(2)	70.85(10)
N(2)-Bi(1)-N(3)	69.94(8)
N(1)-Bi(1)-N(4)	94.77(9)
N(2)-Bi(1)-N(4)	100.27(9)
N(3)-Bi(1)-N(4)	95.69(9)

a)



b)

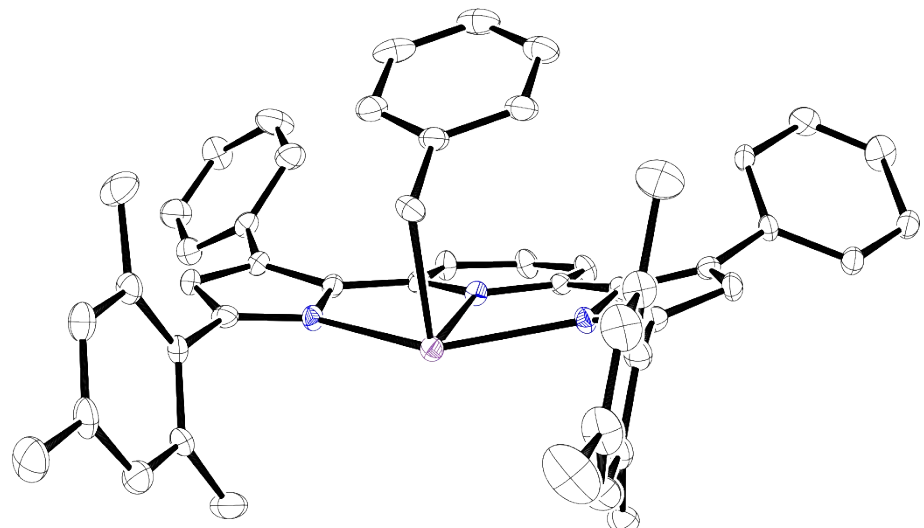


Fig. S30. Thermal displacement ellipsoid drawing (30% probability) of $(\text{Mes},\text{PhL})\text{Bi}(\text{CH}_2\text{Ph})$ (8); a) top and b) side view. All hydrogen atoms have been omitted for clarity.

Table S7. Experimental metrical parameters (bond lengths in Å and angles in °) in **8**.

Bi(1)-C(44)	2.281(8)
Bi(1)-N(1)	2.329(6)
Bi(1)-N(2)	2.303(6)
Bi(1)-N(3)	2.321(6)
C(5)-N(2)	1.352(10)
C(5)-C(6)	1.401(11)
C(6)-C(7)	1.382(12)
C(7)-C(8)	1.384(12)
C(8)-C(9)	1.413(11)
C(9)-N(2)	1.367(10)
Bi(1)-C(44)-C(45)	110.2(5)
N(1)-Bi(1)-N(3)	139.4(2)
N(1)-Bi(1)-N(2)	69.9(2)
N(2)-Bi(1)-N(3)	70.4(2)
N(1)-Bi(1)-C(44)	87.9(3)
N(2)-Bi(1)-C(44)	94.9(3)
N(3)-Bi(1)-C(44)	87.4(3)

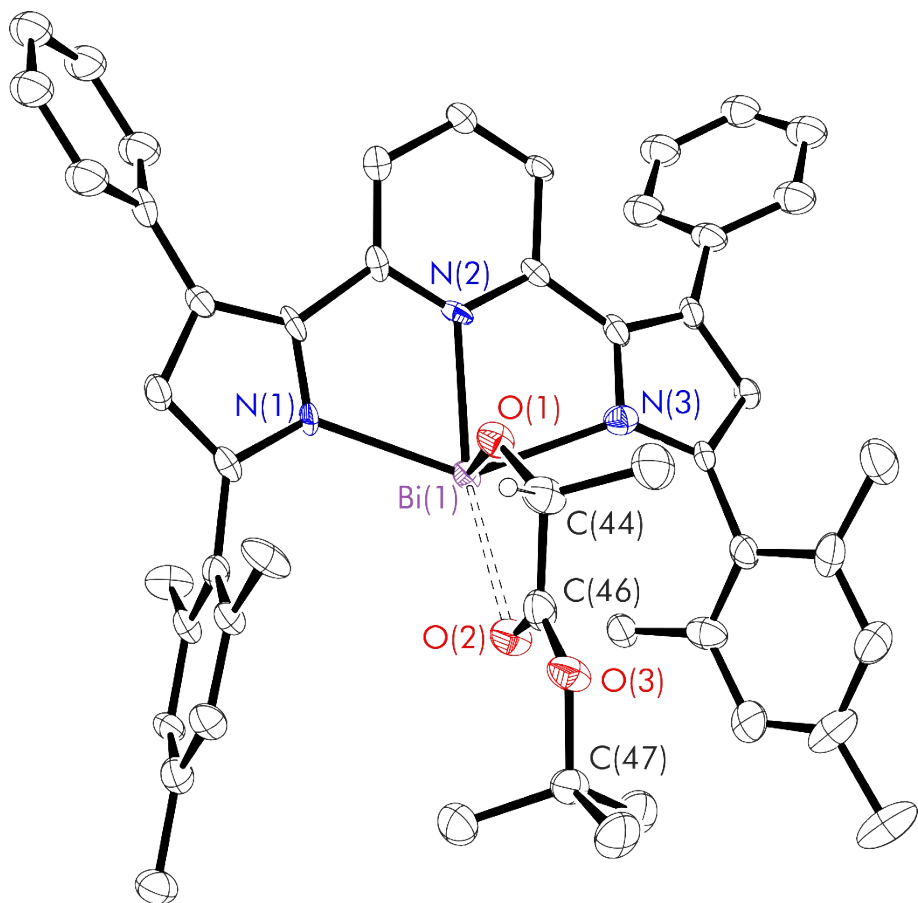


Fig. S31. Thermal displacement ellipsoid drawing (30% probability) of $(^{Mes,Ph}L)\text{Bi}\{(R)\text{-OC(H)(Me)C(=O)O}'\text{Bu}\}$ (**9**) All hydrogen atoms have been omitted for clarity except that attached to the chiral centre C(44).

Table S8. Experimental metrical parameters (bond lengths in Å and angles in °) in **9**.

Bi(1)-N(1)	2.350(12)
Bi(1)-N(2)	2.305(13)
Bi(1)-N(3)	2.392(15)
Bi(1)-O(1)	2.063(13)
Bi(1)-O(2)	2.660(15)
C(44)-O(1)	1.35(2)
C(46)-O(2)	1.24(3)
C(46)-O(3)	1.31(3)
C(47)-O(3)	1.48(3)
C(5)-N(2)	1.35(2)
C(5)-C(6)	1.39(3)
C(6)-C(7)	1.41(2)
C(7)-C(8)	1.35(2)
C(8)-C(9)	1.47(2)
C(9)-N(2)	1.344(19)
N(1)-Bi(1)-N(3)	141.4(5)
N(1)-Bi(1)-N(2)	69.5(5)
N(2)-Bi(1)-N(3)	72.0(5)
N(1)-Bi(1)-O(1)	84.1(5)
N(2)-Bi(1)-O(1)	85.8(5)
N(3)-Bi(1)-O(1)	90.5(5)
N(1)-Bi(1)-O(2)	111.7(5)
N(2)-Bi(1)-O(2)	154.4(5)
N(3)-Bi(1)-O(2)	101.8(5)
O(1)-Bi(1)-O(2)	69.2(5)
Bi(1)-O(1)-C(44)	128.7(12)

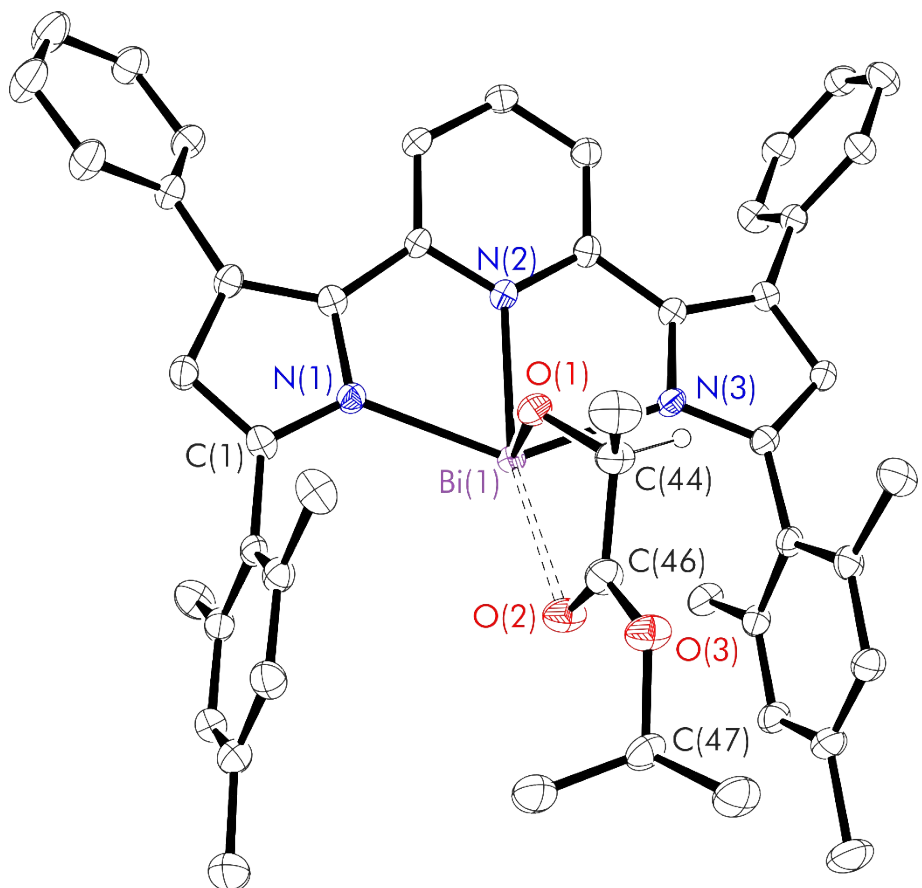


Fig. S32. Thermal displacement ellipsoid drawing (30% probability) of (^{Mes,Ph}L)Bi{OC(H)(Me)C(=O)O*i*Pr} (**11**). All hydrogen atoms have been omitted for clarity except that attached to the chiral centre C(44).

Table S8. Experimental metrical parameters (bond lengths in Å and angles in °) in **11**.

Bi(1)-N(1)	2.279(4)
Bi(1)-N(2)	2.323(4)
Bi(1)-N(3)	2.352(4)
Bi(1)-O(1)	2.070(3)
Bi(1)-O(2)	2.658(4)
C(44)-O(1)	1.275(7)
C(46)-O(2)	1.203(7)
C(46)-O(3)	1.337(7)
C(47)-O(3)	1.504(8)
C(5)-N(2)	1.377(5)
C(5)-C(6)	1.396(6)
C(6)-C(7)	1.384(6)
C(7)-C(8)	1.396(6)
C(8)-C(9)	1.378(7)
C(9)-N(2)	1.369(5)
N(1)-Bi(1)-N(3)	138.75(15)
N(1)-Bi(1)-N(2)	69.66(13)
N(2)-Bi(1)-N(3)	70.15(13)
N(1)-Bi(1)-O(1)	81.69(15)
N(2)-Bi(1)-O(1)	88.05(13)
N(3)-Bi(1)-O(1)	88.07(15)
N(1)-Bi(1)-O(2)	117.67(14)
N(2)-Bi(1)-O(2)	152.37(12)
N(3)-Bi(1)-O(2)	94.53(14)
O(1)-Bi(1)-O(2)	68.02(13)

Table S9. Comparison of experimental metrical parameters (bond lengths in Å and angles in °) in (^{Mes,Ph}L)Bi(OXyl) (**1**), (^{Mes,Ph}L)Bi(ODipp) (**3**), (^{Mes,Ph}L)Bi(OAr^tBu)(Et₂O) (**4·Et₂O**), (^{Mes,Ph}L)Bi(N") (**7**), (^{Mes,Ph}L)Bi(CH₂Ph) (**8**), (^{Mes,Ph}L)Bi{OC(H)(Me)C(=O)O^tBu} (**9**).

(^{Mes,Ph} L)Bi(X)	OXyl (1)	ODipp (3)	OAr ^t Bu (4·Et₂O)	N" (7)	CH ₂ Ph (8)	OC(H)(Me)C(=O)O ^t Bu (9)
Bi(1)-N(1)	2.262(2)	2.2526(14)	2.3482(18)	2.339(2)	2.329(6)	2.350(12)
Bi(1)-N(2)	2.301(2)	2.3047(14)	2.2659(18)	2.302(2)	2.303(6)	2.305(13)
Bi(1)-N(3)	2.305(2)	2.3031(14)	2.3443(17)	2.327(2)	2.321(6)	2.392(15)
Bi(1)-X(1)	2.077(2)	2.0801(12)	2.1137(15)	2.143(2)	2.281(8)	2.063(13)
Bi(1)-O(2)	-	-	2.8419(1)	-	-	2.660(15)
C(5)-N(2)	1.366(3)	1.367(2)	1.365(3)	1.371(4)	1.352(10)	1.35(2)
C(5)-C(6)	1.403(4)	1.397(2)	1.398(3)	1.394(5)	1.401(11)	1.39(3)
C(6)-C(7)	1.382(4)	1.383(3)	1.383(3)	1.377(6)	1.382(12)	1.41(2)
C(7)-C(8)	1.381(4)	1.386(3)	1.387(3)	1.384(5)	1.384(12)	1.35(2)
C(8)-C(9)	1.395(4)	1.396(2)	1.393(3)	1.397(4)	1.413(11)	1.47(2)
C(9)-N(2)	1.362(3)	1.362(2)	1.362(3)	1.367(4)	1.367(10)	1.344(19)
N(1)-Bi(1)-N(3)	139.71(8)	139.95(5)	142.18(7)	140.61(9)	139.4(2)	141.4(5)
N(1)-Bi(1)-N(2)	69.86(8)	69.89(5)	71.48(6)	70.85(10)	69.9(2)	69.5(5)
N(2)-Bi(1)-N(3)	70.58(8)	70.09(5)	70.93(6)	69.94(8)	70.4(2)	72.0(5)
N(1)-Bi(1)-X(1)	81.73(8)	83.91(5)	96.25(6)	94.77(9)	87.9(3)	84.1(5)
N(2)-Bi(1)-X(1)	93.09(9)	86.85(5)	94.66(6)	100.27(9)	94.9(3)	85.8(5)
N(3)-Bi(1)-X(1)	93.05(8)	95.44(5)	82.87(6)	95.69(9)	87.4(3)	90.5(5)
Bi(1)-X(1)-E	133.49(19)	129.10(10)	142.51(13)	125.63(13)	110.2(5)	128.7(12)
				112.18(12)		

IV. Polymerisation data

L-, *D*-, *meso*- or *rac*-lactide (40 mg, 0.278 mmol) was weighed into a Young's tap NMR spectroscopy tube. Stock solutions of complex in an amount of deuterated solvent corresponding to an initial lactide concentration ($[LA]_0$) of 0.5 M were prepared and the desired quantity added to the NMR tube. Polymerisations were run at 70–90 °C and the conversion was monitored by ^1H NMR spectroscopy. On completion, the reaction mixture was decanted into –5 °C pentane (10 mL), the solution allowed to settle and the solvent removed. The polymer was then washed with diethyl ether (2×10 mL) and dried under vacuum at 30 °C for 18 hours.

The tacticity of PLA was analysed by $^1\text{H}\{^1\text{H}\}$ NMR spectroscopy performed with a Bruker Avance III 400 spectrometer at ambient temperature. P_S values were calculated from integration obtained from $^1\text{H}\{^1\text{H}\}$ NMR spectra. Alternatively, peak deconvolution, using the Mnova software package, was used to improve accuracy in the determination.^[11] The probability of a particular tetrad can be calculated using Bernoullian statistics.^[12] Samples were prepared by dissolving PLA (10 mg) in chloroform-*d* (0.6 mL) and transferring the solution to an NMR tube.

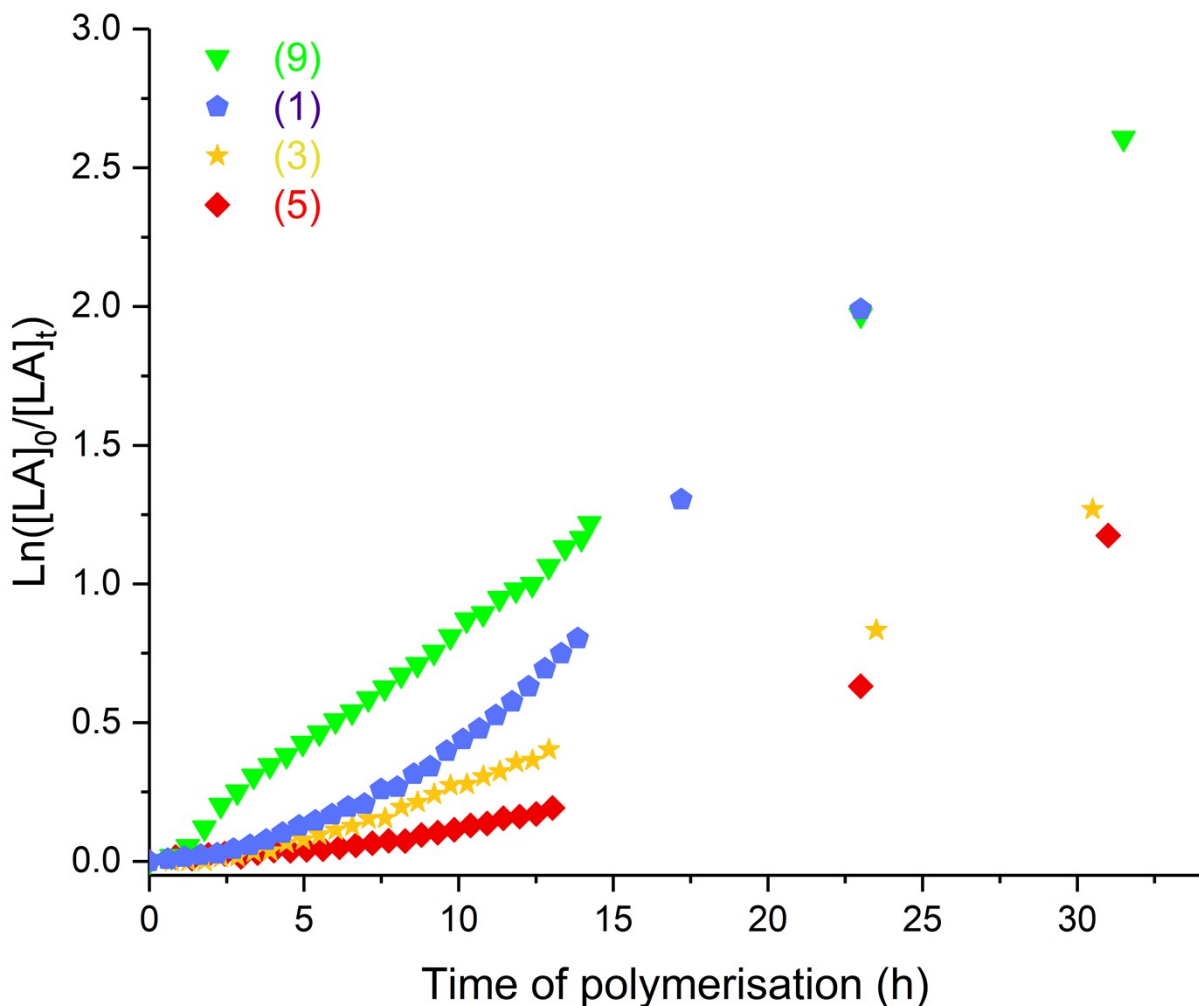


Fig. S33. *L*-Lactide polymerisation using $(^{Mes,Ph}L)Bi(OXyl)$ (1) (violet pentagon, $k_{obs} = 0.097 \pm 0.005 \text{ h}^{-1}$), $(^{Mes,Ph}L)Bi(ODipp)$ (3) (orange star, $k_{obs} = 0.045 \pm 0.001 \text{ h}^{-1}$), $(^{Mes,Ph}L)Bi(O^tBu)$ (5) (red diamond, $k_{obs} = 0.065 \pm 0.004 \text{ h}^{-1}$) and $(^{Mes,Ph}L)Bi\{OC(H)(Me)C(=O)O^tBu\}$ (9) (green down triangle, $k_{obs} = 0.083 \pm 0.001 \text{ h}^{-1}$). Polymerisation conditions: C_6D_6 , 80°C , $[LA]_0/[Bi]_0 = 50$ and $[LA]_0 = 0.5 \text{ M}$.

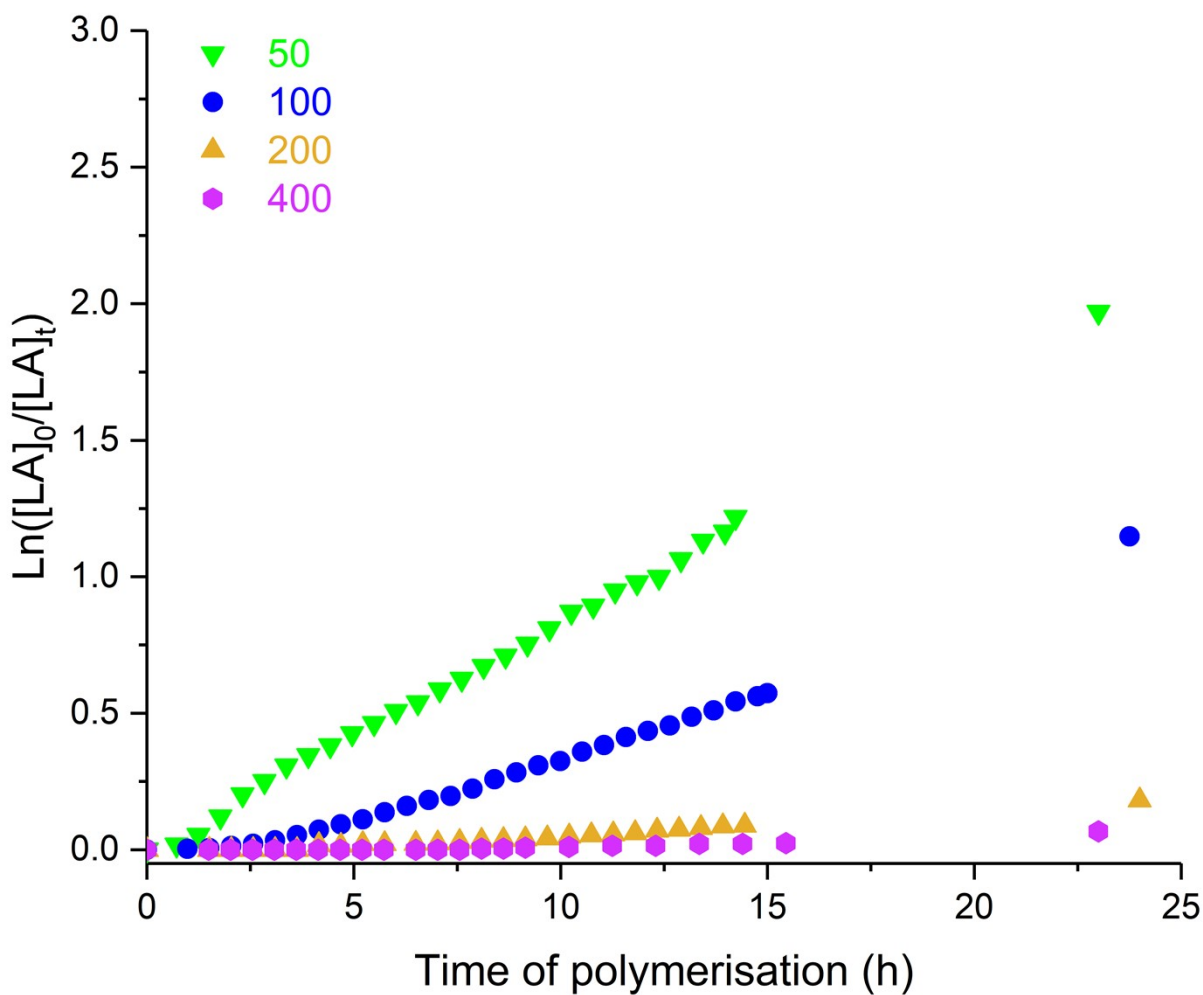


Fig. S34. *L*-Lactide polymerisation using $(^{Mes,Ph}L)Bi\{OC(H)(Me)C(=O)O^tBu\}$ (**9**) with $[LA]_0/[Bi]_0 = 50$ (green down triangle, $k_{obs} = 0.083 \pm 0.001 \text{ h}^{-1}$), $[LA]_0/[Bi]_0 = 100$ (blue circle, $k_{obs} = 0.053 \pm 0.001 \text{ h}^{-1}$), $[LA]_0/[Bi]_0 = 200$ (orange up triangle, $k_{obs} = 0.018 \pm 0.001 \text{ h}^{-1}$) and $[LA]_0/[Bi]_0 = 400$ (purple hexagon, $k_{obs} = 0.009 \pm 0.001 \text{ h}^{-1}$). Polymerisation conditions: C_6D_6 , 80°C and $[LA]_0 = 0.5 \text{ M}$.

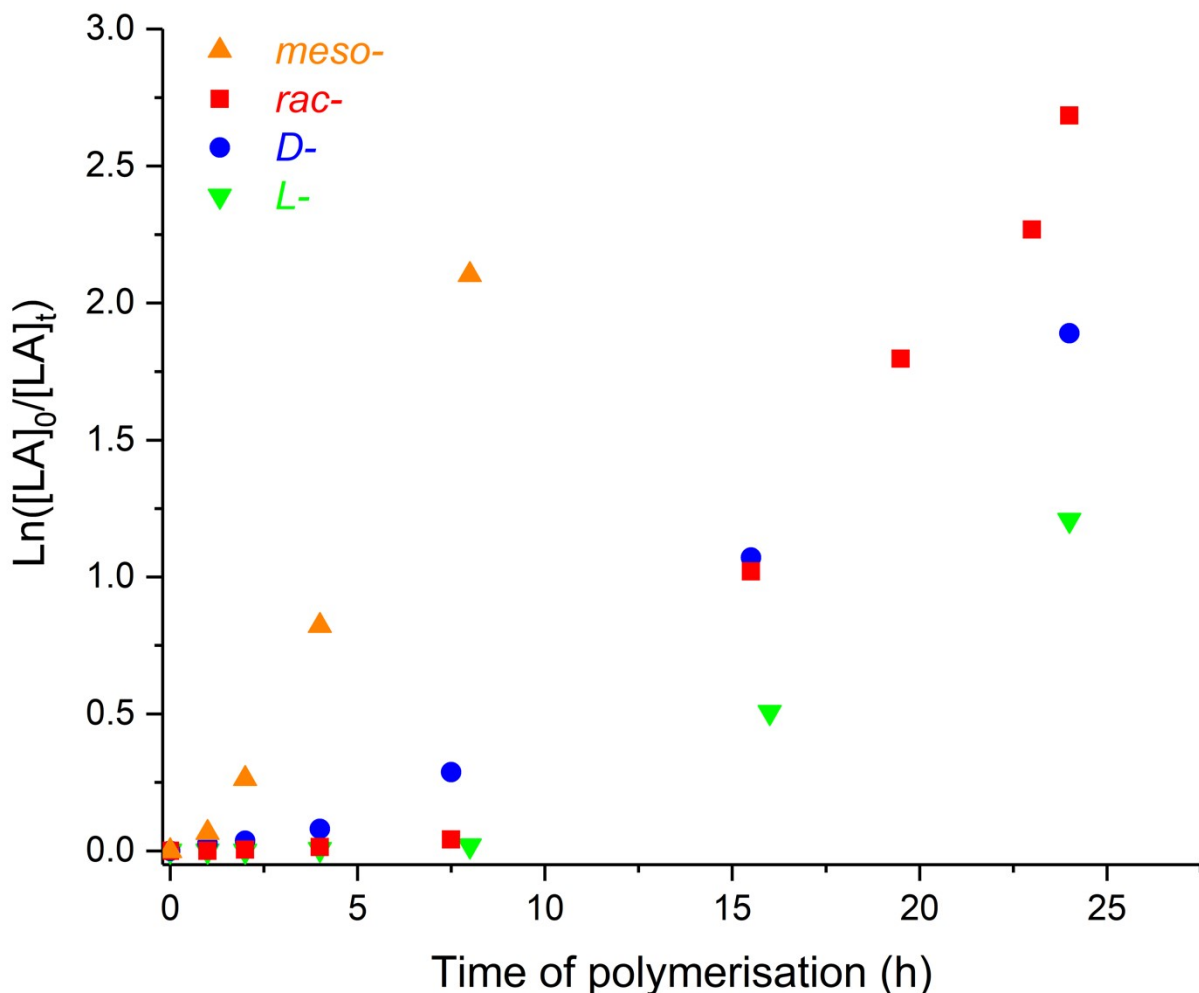


Fig. S35. Lactide polymerisation using $(^{Mes,Ph}L)Bi(OXyl)$ (1) with *meso*- (orange up triangle, $k_{obs} = 0.296 \pm 0.014 \text{ h}^{-1}$), *rac*- (red square, $k_{obs} = 0.146 \pm 0.010 \text{ h}^{-1}$), *D*- (blue circle, $k_{obs} = 0.097 \pm 0.000 \text{ h}^{-1}$) and *L*- (green down triangle, $k_{obs} = 0.071 \pm 0.006 \text{ h}^{-1}$). Polymerisation conditions: $CDCl_3$, 80°C , $[LA]_0/[Bi]_0 = 50$ and $[LA]_0 = 0.5 \text{ M}$.

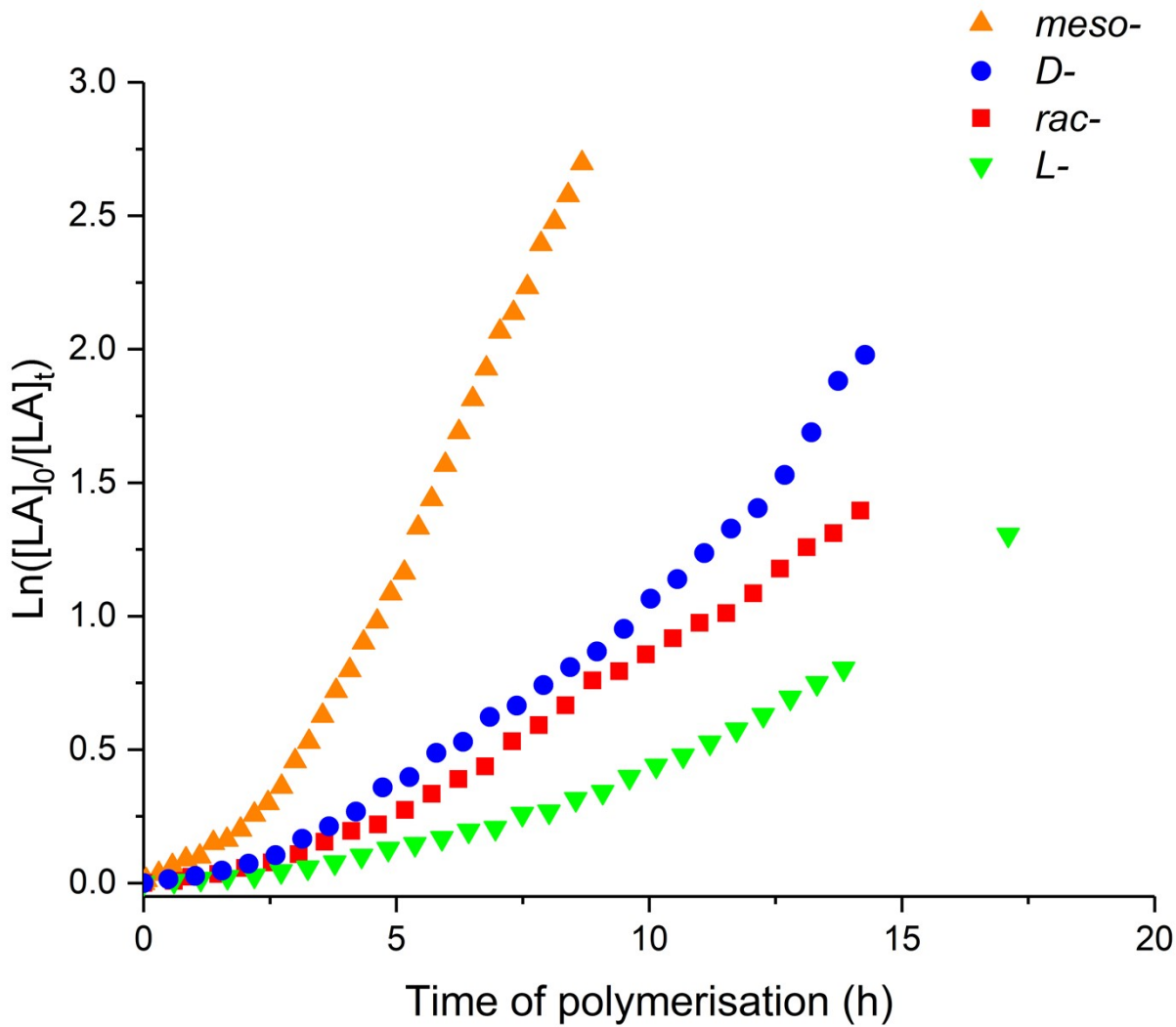


Fig. S36. Lactide polymerisation using $(^{Mes,Ph}L)Bi(OXyl)$ (**1**) with *meso*- (orange up triangle, $k_{obs} = 0.412 \pm 0.005 \text{ h}^{-1}$), *rac*- (red square, $k_{obs} = 0.104 \pm 0.004 \text{ h}^{-1}$), *D*- (blue circle, $k_{obs} = 0.145 \pm 0.005 \text{ h}^{-1}$) and *L*- (green down triangle, $k_{obs} = 0.097 \pm 0.005 \text{ h}^{-1}$). Polymerisation conditions: C_6D_6 , 80°C , $[LA]_0/[Bi]_0 = 50$ and $[LA]_0 = 0.5 \text{ M}$.

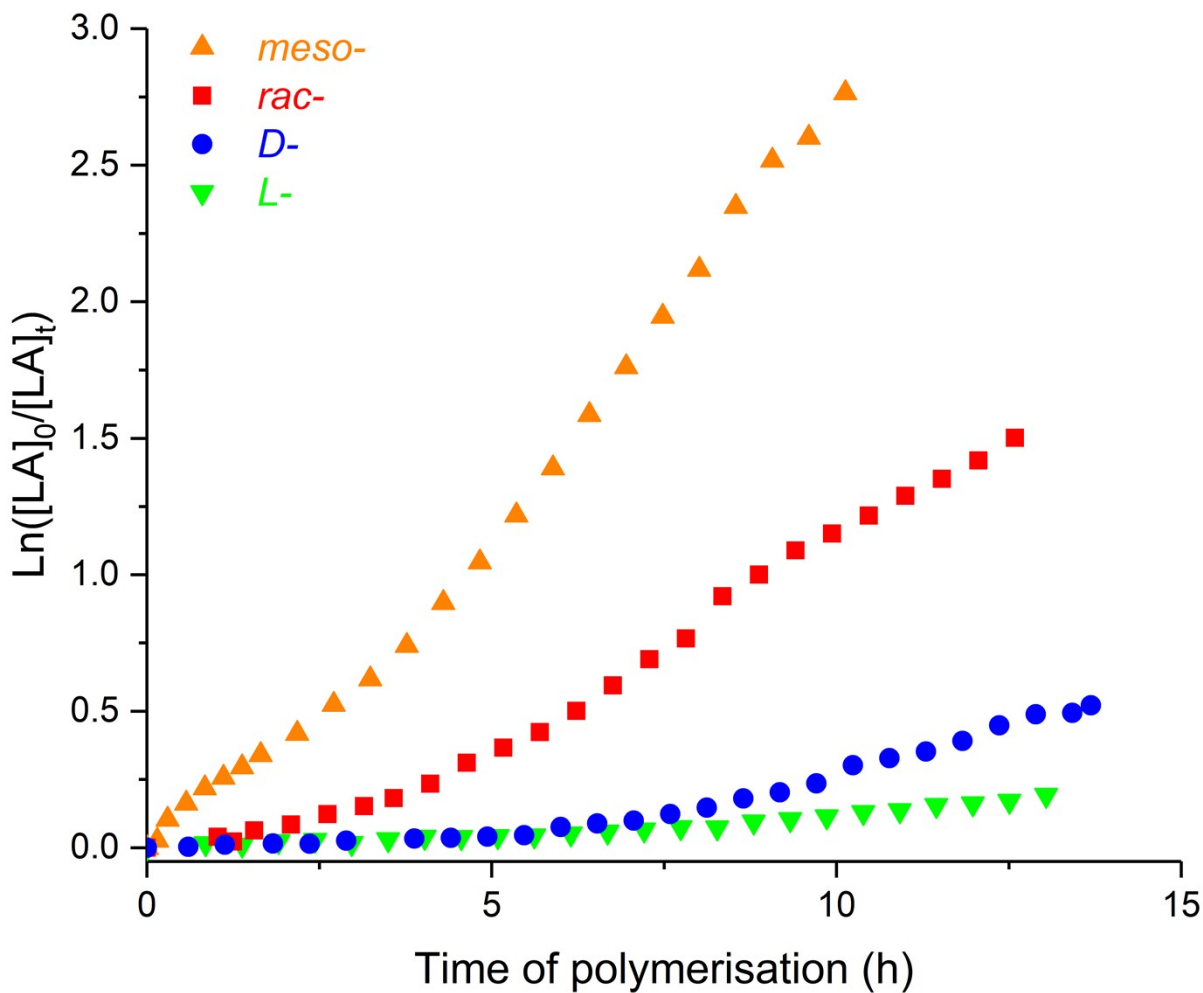


Fig. S37. Lactide polymerisation using $(^{Mes,Ph}L)Bi(O^tBu)_2$ (**5**) with *meso*- (orange up triangle, $k_{obs} = 0.276 \pm 0.006 \text{ h}^{-1}$), *rac*- (red square, $k_{obs} = 0.158 \pm 0.004 \text{ h}^{-1}$), *D*- (blue circle, $k_{obs} = 0.093 \pm 0.003 \text{ h}^{-1}$) and *L*- (green down triangle, $k_{obs} = 0.065 \pm 0.004 \text{ h}^{-1}$). Polymerisation conditions: C_6D_6 , 80°C , $[LA]_0/[Bi]_0 = 50$ and $[LA]_0 = 0.5 \text{ M}$.

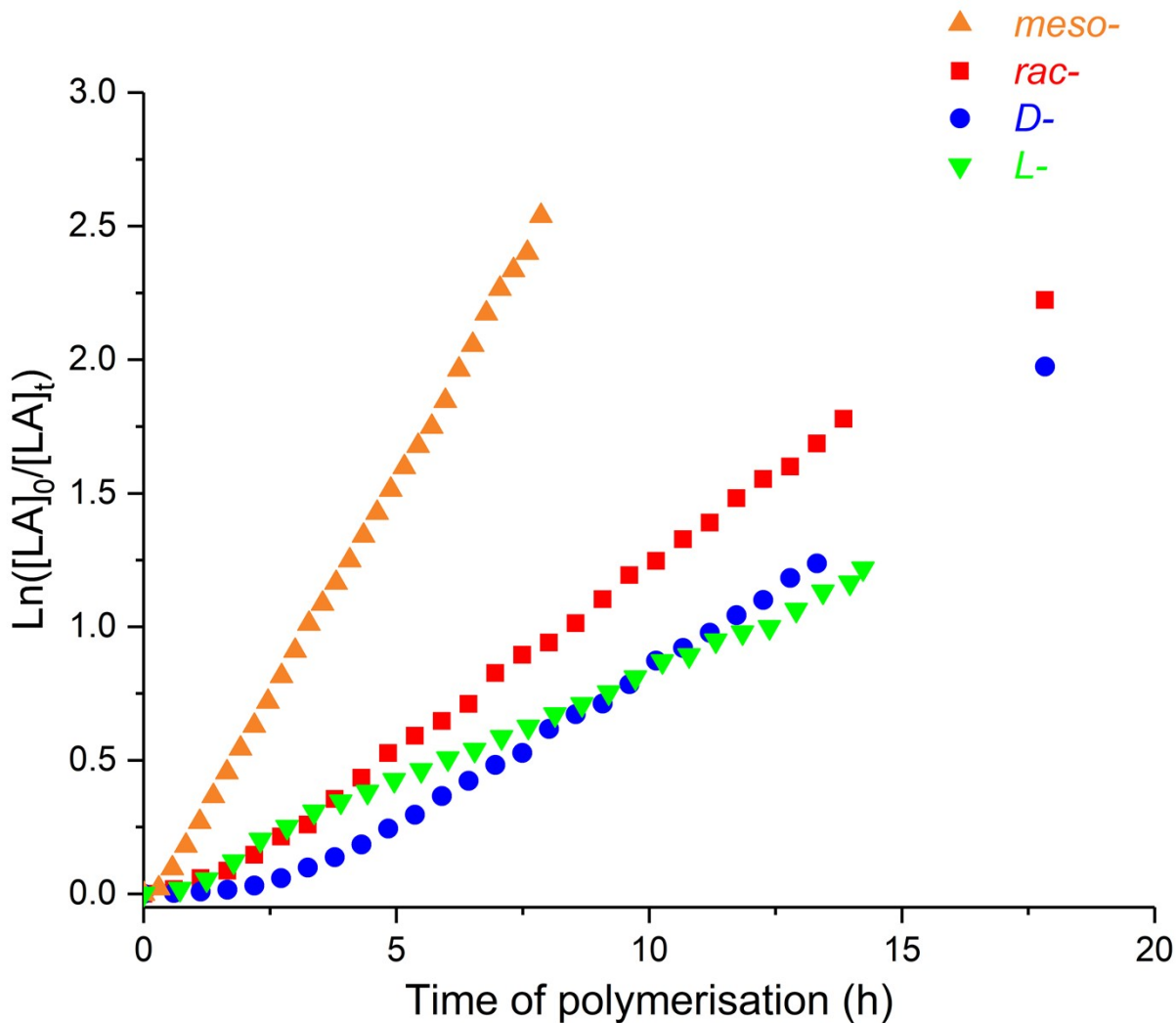


Fig. S38. Lactide polymerisation using $(^{Mes,Ph}L)Bi\{OC(H)(Me)C(=O)O^tBu\}$ (**9**) with *meso*- (orange up triangle, $k_{obs} = 0.329 \pm 0.002 \text{ h}^{-1}$), *rac*- (red square, $k_{obs} = 0.140 \pm 0.001 \text{ h}^{-1}$), *D*- (blue circle, $k_{obs} = 0.116 \pm 0.001 \text{ h}^{-1}$) and *L*- (green down triangle, $k_{obs} = 0.083 \pm 0.001 \text{ h}^{-1}$). Polymerisation conditions: C_6D_6 , $80^\circ C$, $[LA]_0/[Bi]_0 = 50$ and $[LA]_0 = 0.5 \text{ M}$.

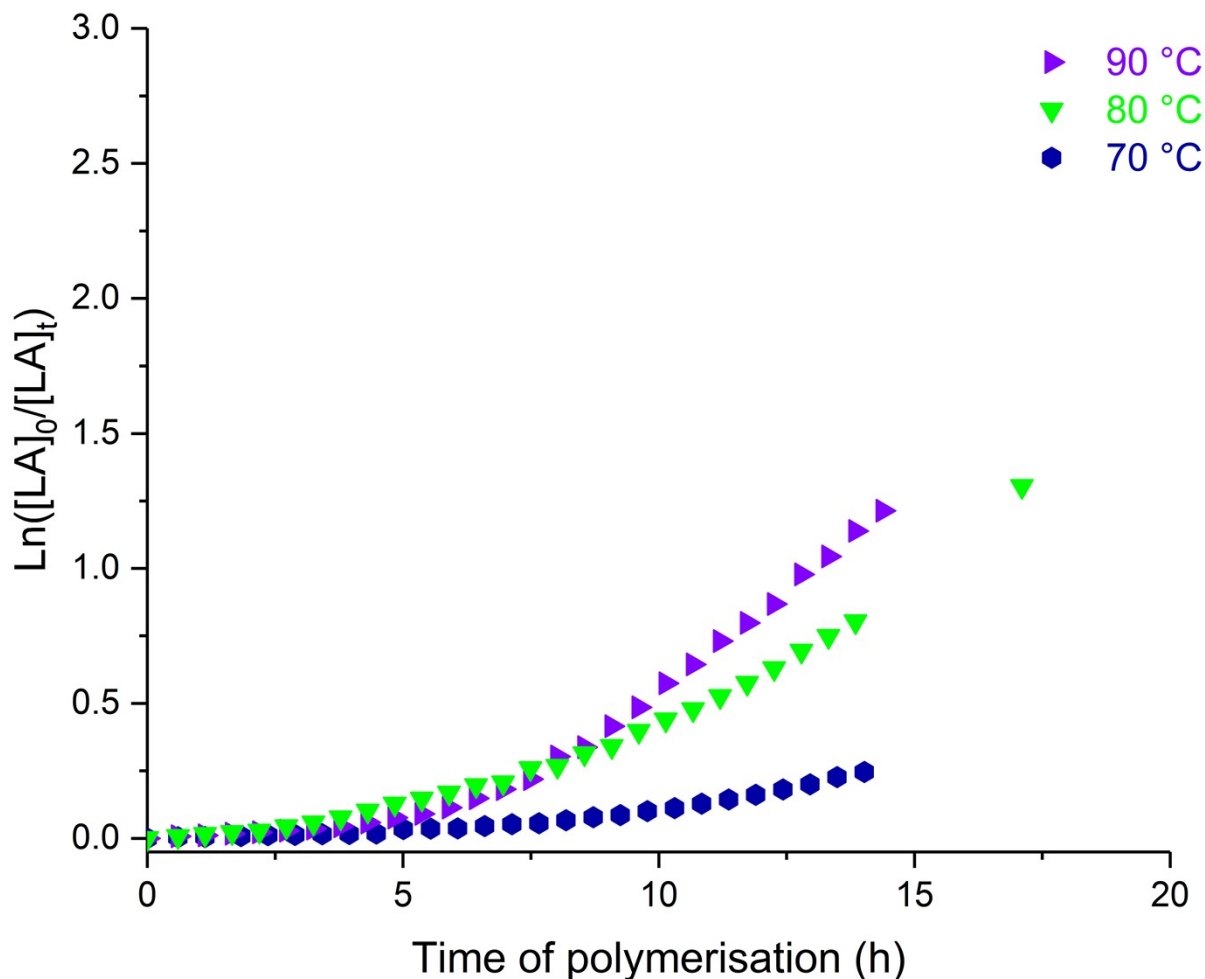


Fig. S39. *L*-Lactide polymerisation using (^{Mes,Ph}L)Bi(OXyl) (**1**) at 70 °C (navy hexagon, $k_{\text{obs}} = 0.064 \pm 0.002 \text{ h}^{-1}$), 80 °C (green down triangle, $k_{\text{obs}} = 0.097 \pm 0.005 \text{ h}^{-1}$) and 90 °C (purple right triangle, $k_{\text{obs}} = 0.132 \pm 0.002 \text{ h}^{-1}$). Polymerisation conditions: C₆D₆, [LA]₀/[Bi]₀ = 50 and [LA]₀ = 0.5 M.

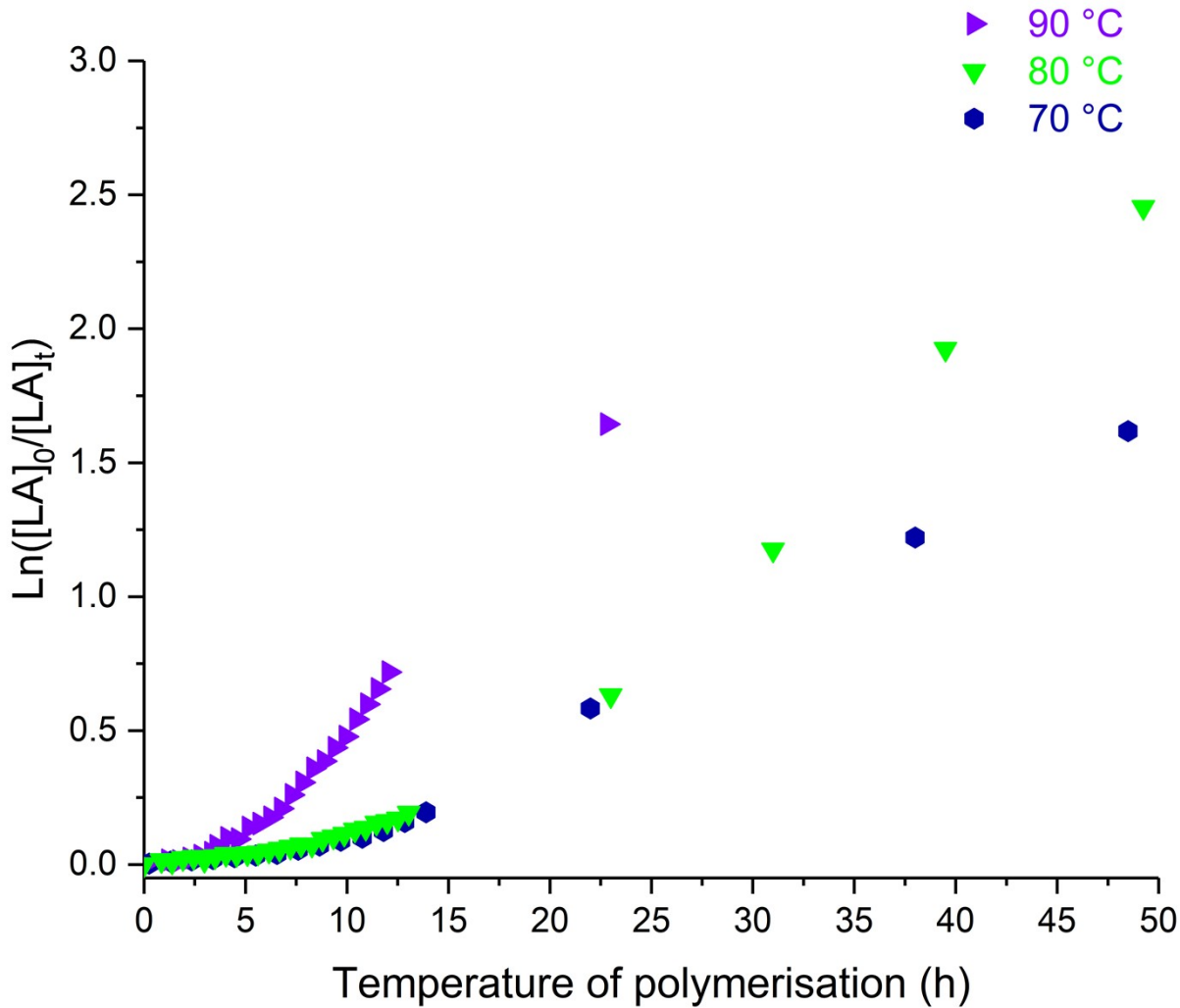


Fig. S40. *L*-Lactide polymerisation using $(^{Mes,Ph}L)Bi(O^tBu)_2$ (**5**) at 70 °C (navy hexagon, $k_{obs} = 0.041 \pm 0.001 \text{ h}^{-1}$), 80 °C (green down triangle, $k_{obs} = 0.065 \pm 0.004 \text{ h}^{-1}$) and 90 °C (purple right triangle, $k_{obs} = 0.090 \pm 0.001 \text{ h}^{-1}$). Polymerisation conditions: C₆D₆, [LA]₀/[Bi]₀ = 50 and [LA]₀ = 0.5 M.

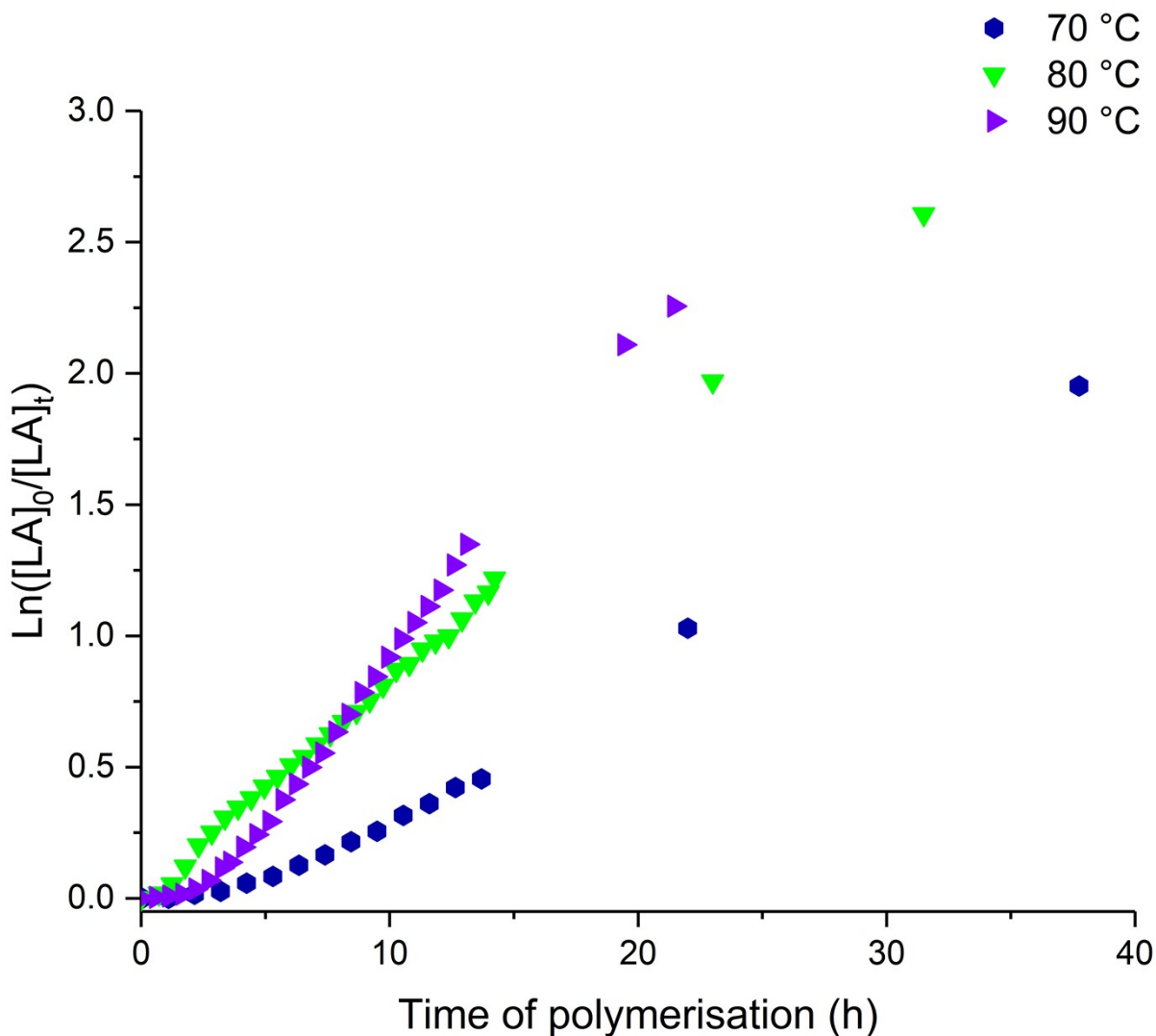


Fig. S41. *L*-Lactide polymerisation using $(^{Mes,Ph}L)Bi\{OC(H)(Me)C(=O)O^tBu\}$ (**9**) at 70 °C (navy hexagon, $k_{obs} = 0.057 \pm 0.001 \text{ h}^{-1}$), 80 °C (green down triangle, $k_{obs} = 0.083 \pm 0.001 \text{ h}^{-1}$) and 90 °C (purple right triangle, $k_{obs} = 0.123 \pm 0.002 \text{ h}^{-1}$). Polymerisation conditions: C₆D₆, [LA]₀/[Bi]₀ = 50 and [LA]₀ = 0.5 M.

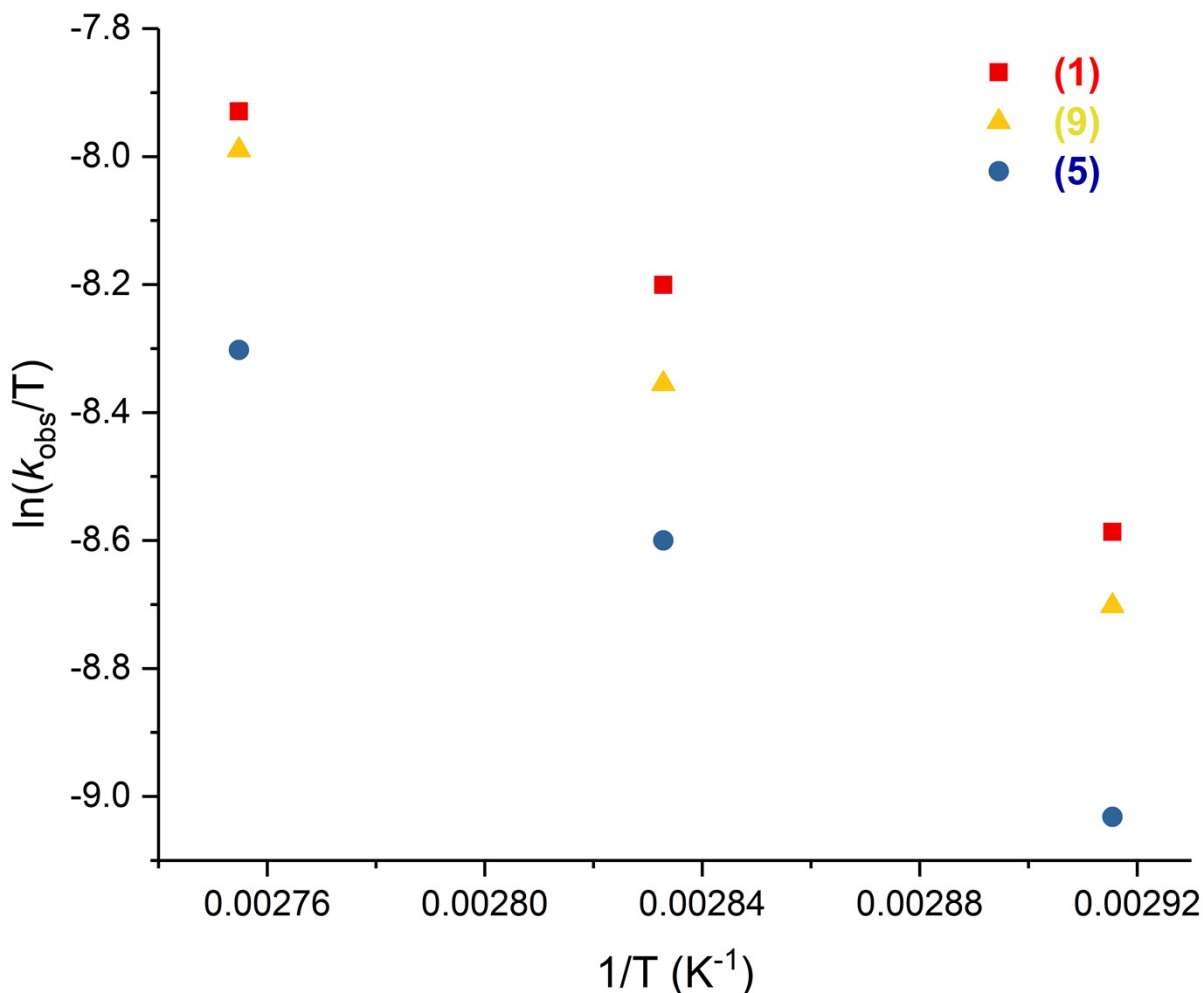


Fig. S42. Semi-logarithmic Eyring plot of the rate of propagation as a function of the inverse of the temperature polymerisation of *L*-lactide using $(^{\text{Mes},\text{Ph}}\text{L})\text{Bi(OXyl)}$ (1) (red square, $\Delta H = 34 \pm 3 \text{ kJ mol}^{-1}$ and $\Delta S = -169 \pm 8 \text{ J mol}^{-1} \text{ K}^{-1}$), $(^{\text{Mes},\text{Ph}}\text{L})\text{Bi(O}^t\text{Bu)}$ (5) (blue circle, $\Delta H = 37 \pm 1 \text{ kJ mol}^{-1}$ and $\Delta S = -163 \pm 4 \text{ J mol}^{-1} \text{ K}^{-1}$) and $(^{\text{Mes},\text{Ph}}\text{L})\text{Bi}\{\text{OC(H)(Me)C(=O)O}^t\text{Bu}\}$ (9) (orange triangle, $\Delta H = 38 \pm 3 \text{ kJ mol}^{-1}$ and $\Delta S = -162 \pm 10 \text{ J mol}^{-1} \text{ K}^{-1}$). Polymerisation conditions: C_6D_6 , $[\text{LA}]_0/[\text{Bi}]_0 = 50$ and $[\text{LA}]_0 = 0.5 \text{ M}$.

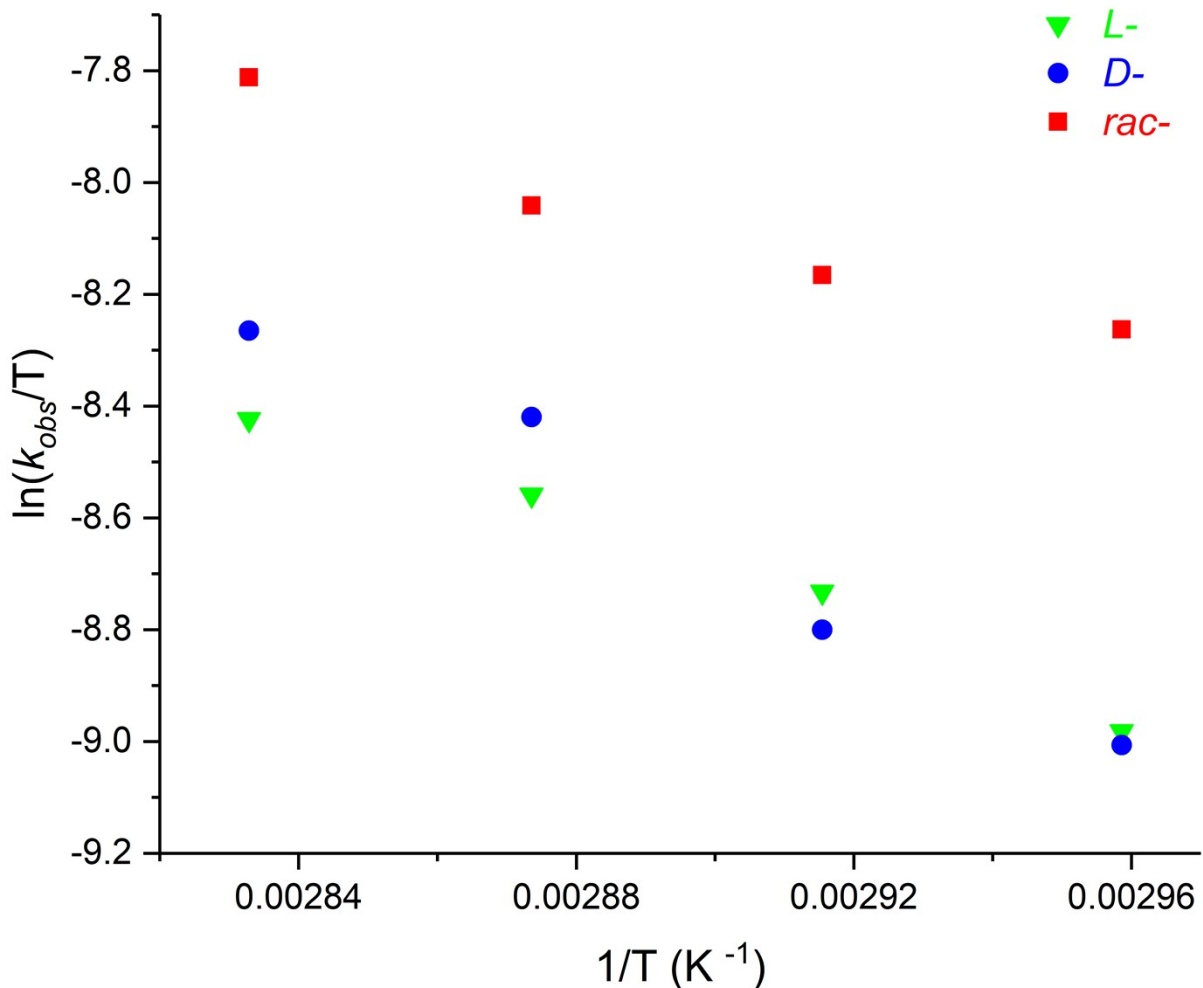


Fig. S43. Semi-logarithmic Eyring plot of the rate of propagation as a function of the inverse of the temperature polymerisation using $(^{\text{Mes},\text{Ph}}\text{L})\text{Bi(OXyl)} \textbf{(1)}$: L -lactide (green down triangle, $\Delta H = 38 \pm 3 \text{ kJ mol}^{-1}$ and $\Delta S = -163 \pm 10 \text{ J mol}^{-1} \text{ K}^{-1}$), D -lactide (blue circle, $\Delta H = 51 \pm 6 \text{ kJ mol}^{-1}$ and $\Delta S = 120 \pm 1 \text{ J mol}^{-1} \text{ K}^{-1}$) and rac -lactide (red square, $\Delta H = 29 \pm 5 \text{ kJ mol}^{-1}$ and $\Delta S = -180 \pm 13 \text{ J mol}^{-1} \text{ K}^{-1}$). Polymerisation conditions: CDCl_3 , $[\text{LA}]_0/[\text{Bi}]_0 = 50$ and $[\text{LA}]_0 = 0.5 \text{ M}$.

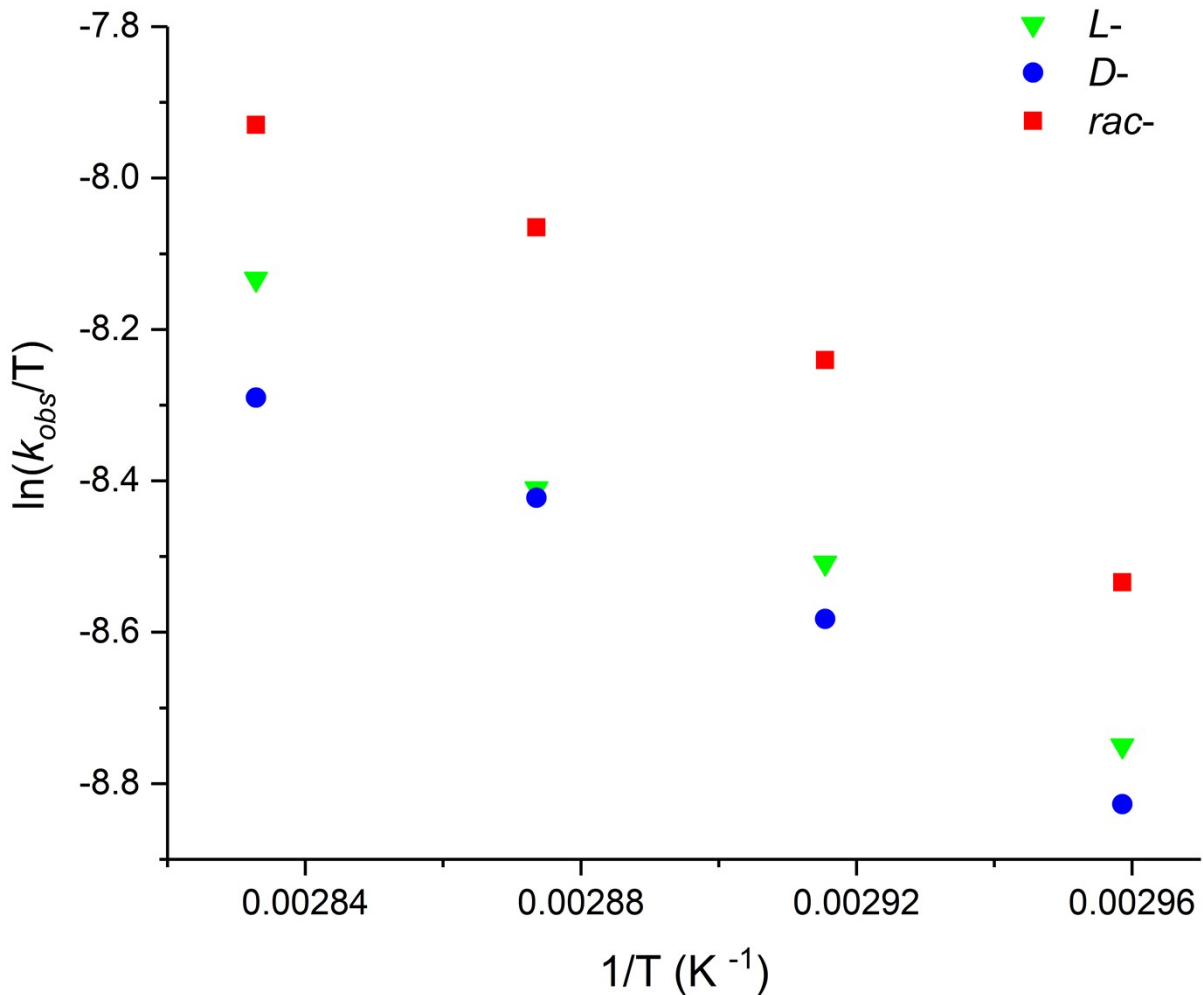


Fig. S44. Semi-logarithmic Eyring plot of the rate of propagation as a function of the inverse of the temperature polymerisation using $(^{Mes,Ph}L)Bi(OAr'^{Bu})$ (4): L -lactide (green down triangle, $\Delta H = 39 \pm 5 \text{ kJ mol}^{-1}$ and $\Delta S = -156 \pm 14 \text{ J mol}^{-1} \text{ K}^{-1}$), D -lactide (blue circle, $\Delta H = 35 \pm 3 \text{ kJ mol}^{-1}$ and $\Delta S = -167 \pm 10 \text{ J mol}^{-1} \text{ K}^{-1}$) and rac -lactide (red square, $\Delta H = 40 \pm 5 \text{ kJ mol}^{-1}$ and $\Delta S = -151 \pm 14 \text{ J mol}^{-1} \text{ K}^{-1}$). Polymerisation conditions: $CDCl_3$, $[LA]_0/[Bi]_0 = 50$ and $[LA]_0 = 0.5 \text{ M}$.

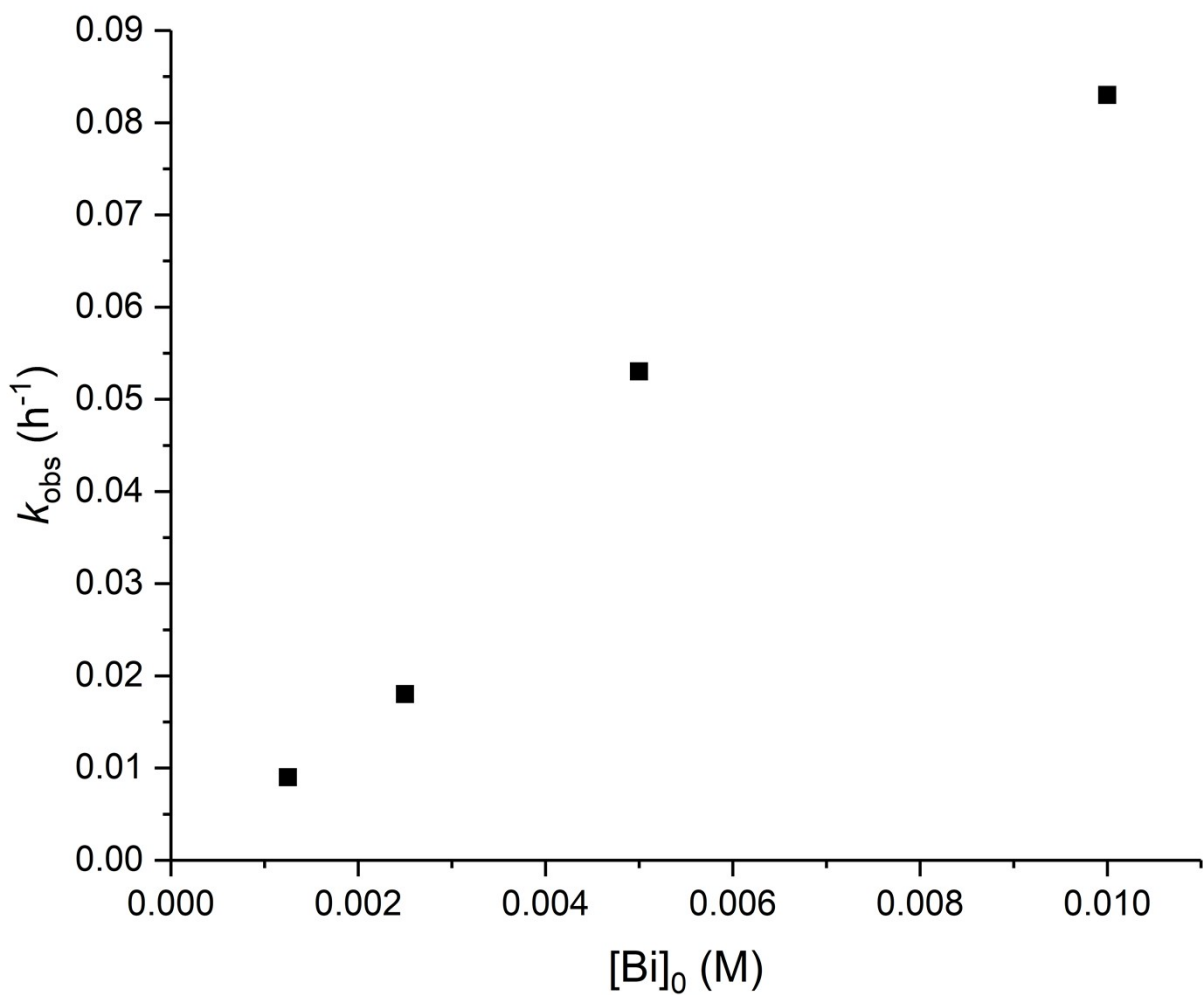


Fig. S45. k_{obs} as a function of $[\text{Bi}]_0$: polymerisation of *L*-lactide using $(^{\text{Mes,Ph}}\text{L})\text{Bi}\{\text{OC(H)(Me)C(=O)O}^{\text{i}}\text{Bu}\}$ (**9**) ($k_p = 8.6 \pm 1.2 \text{ M}^{-1} \text{ h}^{-1}$ with $R^2 = 0.964$). Polymerisation conditions: C_6D_6 , 80°C and $[\text{LA}]_0 = 0.5 \text{ M}$.

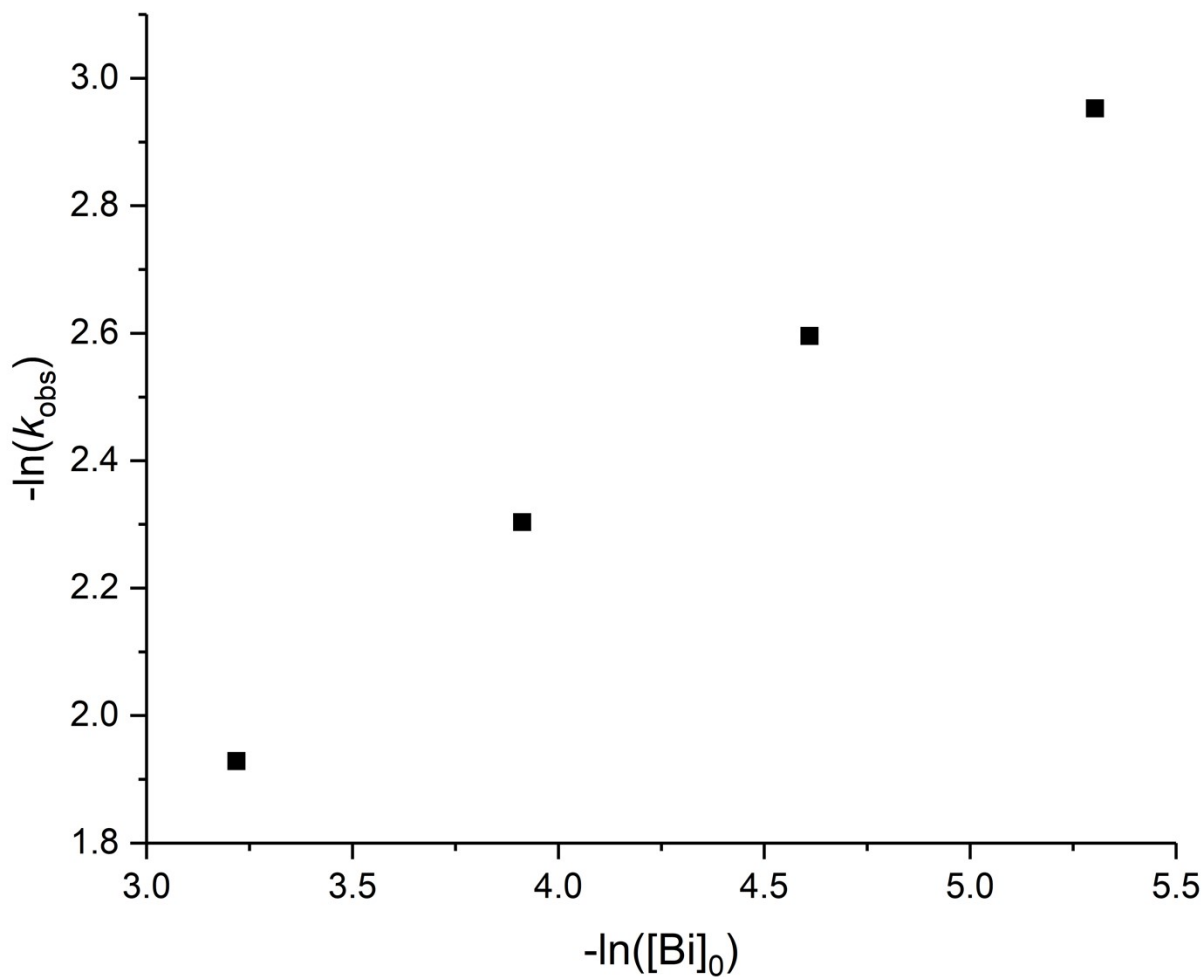


Fig. S46. $-\ln(k_{\text{obs}})$ as a function of $-\ln([\text{Bi}]_0)$: polymerisation of *L*-lactide using $(^{\text{Mes},\text{Ph}}\text{L})\text{Bi(OXyl)}\text{ (1)}$ (slope = 0.48 ± 0.02 with $R^2 = 0.998$). Polymerisation conditions: CDCl_3 , 80°C and $[\text{LA}]_0 = 0.5 \text{ M}$.

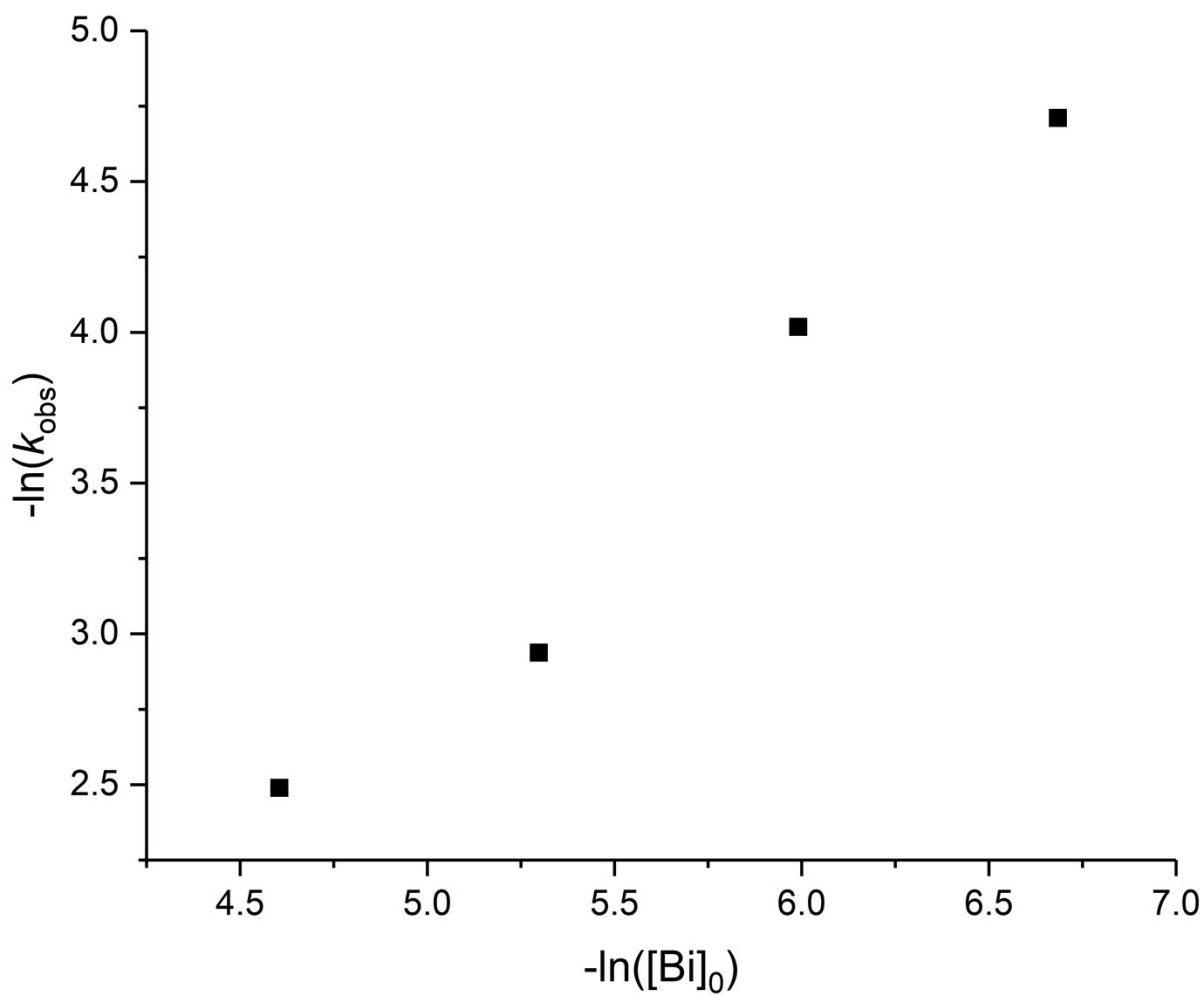


Fig. S47. $-\ln(k_{\text{obs}})$ as a function of $-\ln([\text{Bi}]_0)$: polymerisation of *L*-lactide using $(^{\text{Mes}, \text{Ph}}\text{L})\text{Bi}\{\text{OC}(\text{H})(\text{Me})\text{C}(=\text{O})\text{O}^t\text{Bu}\}$ (**9**) (slope = 1.12 ± 0.12 with $R^2 = 0.967$). Polymerisation conditions: C_6D_6 , 80°C and $[\text{LA}]_0 = 0.5 \text{ M}$.

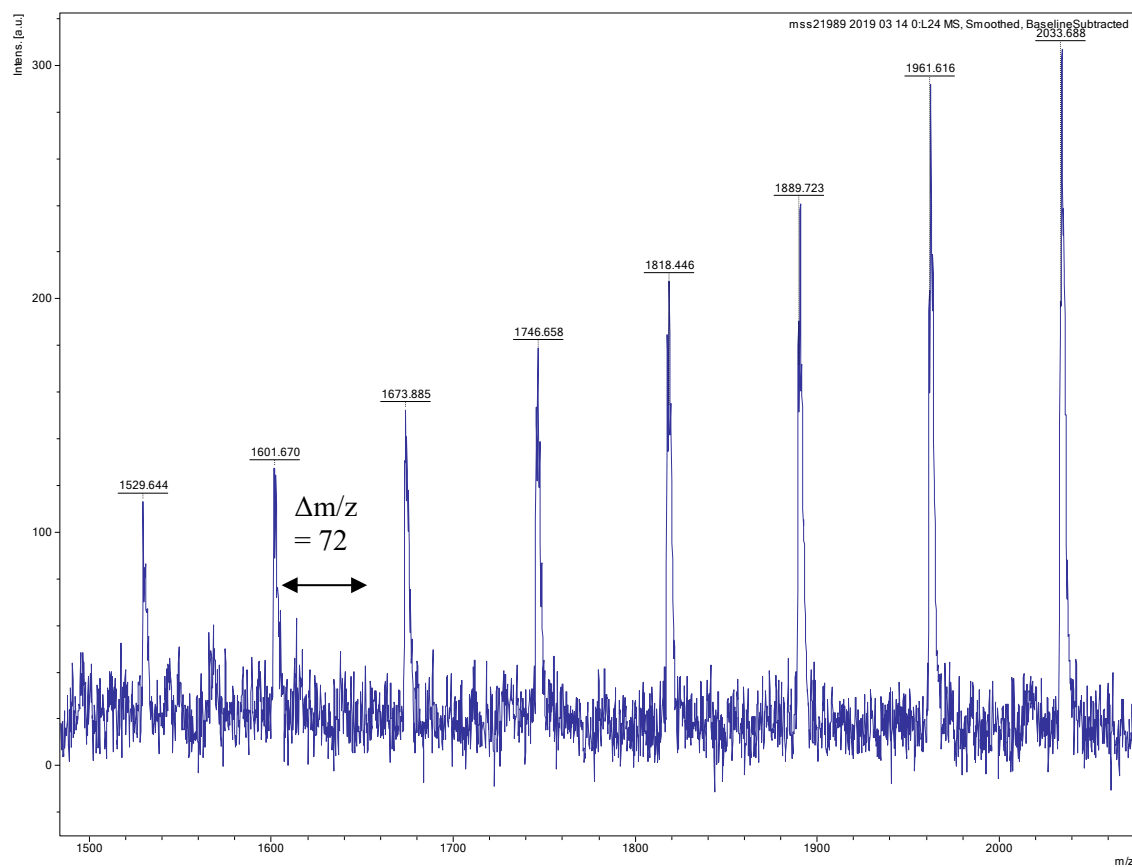


Fig. S48. MALDI-TOF mass spectrum for poly-*L*-lactide synthesised using (^{Mes,Ph}L)Bi(OXyl) (**1**). Polymerisation conditions: CDCl₃, 80 °C, [LA]₀ = 0.5 M and [LA]₀/[Bi]₀ = 10.

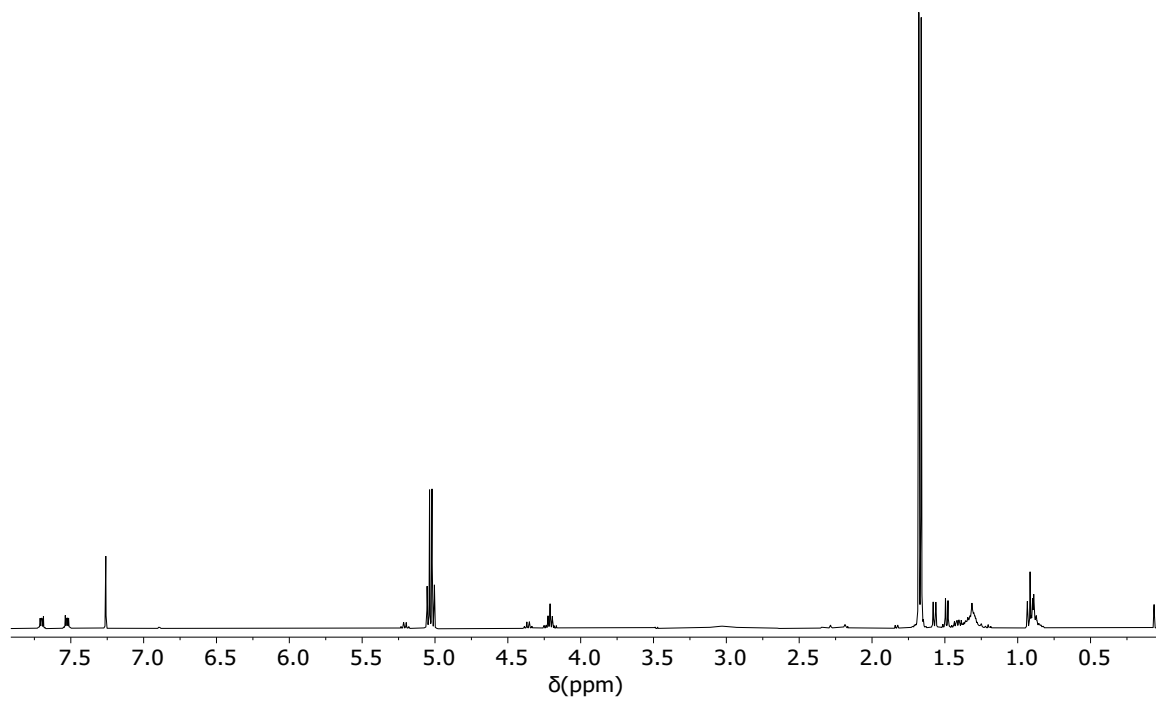


Fig. S49. ¹H NMR spectrum for poly-*L*-lactide synthesised using (^{Mes,Ph}L)Bi(ODipp) (3). Polymerisation conditions: CDCl₃, 80 °C, [LA]₀ = 0.5 M and [LA]₀/[Bi]₀ = 10.

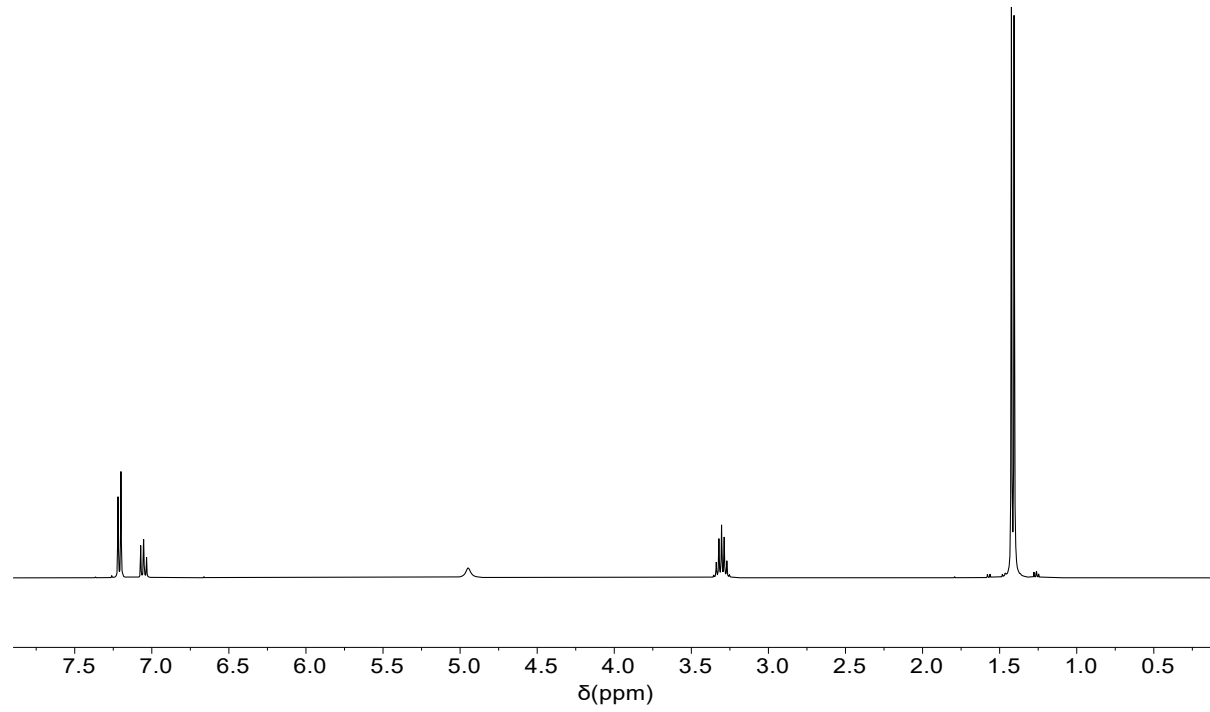


Fig. S50. ¹H NMR spectrum (CDCl₃, 400 MHz, 298 K) of HO-2,6-ⁱPr-C₆H₃.

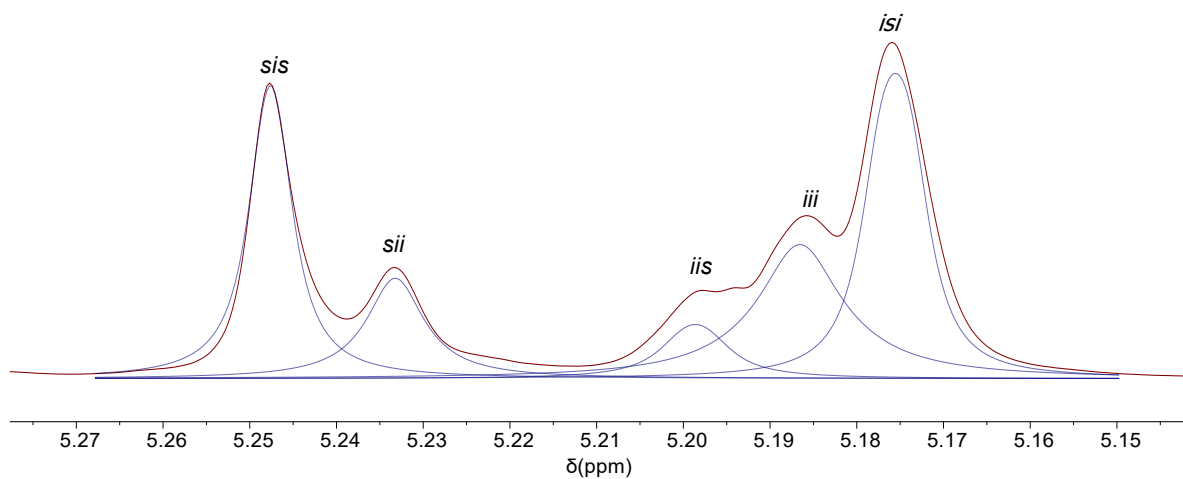


Fig. S51. Methine proton region of ${}^1\text{H}\{{}^1\text{H}\}$ NMR spectrum of poly-*rac*-lactide synthesised using $({}^{\text{Mes},\text{Ph}}\text{L})\text{Bi(OXyl)}$ (**1**). Polymerisation conditions: CDCl_3 , 80°C , $[\text{LA}]_0 = 0.5 \text{ M}$ and $[\text{LA}]_0/[\text{Bi}]_0 = 50$. Red line denotes original spectrum and blue lines the deconvoluted spectrum; *i* indicates an isotactic linkage and *s* a syndiotactic linkage.

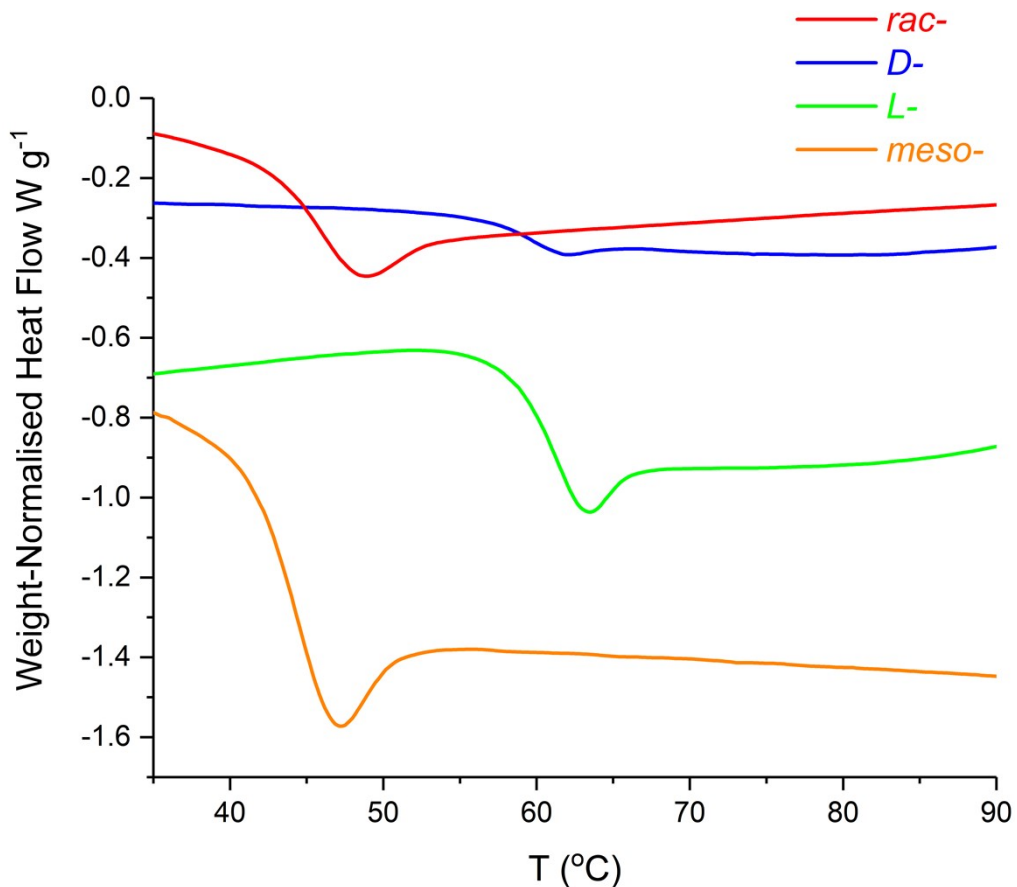


Fig. S52. Glass-transition region DSC traces for the 2nd heating cycle of poly(lactides synthesised using $(^{\text{Mes},\text{Ph}}\text{L})\text{Bi(OXyl)}$ (**1**). Polymerisation conditions: CDCl_3 , 80 $^{\circ}\text{C}$, $[\text{LA}]_0 = 0.5 \text{ M}$ and $[\text{LA}]_0/[\text{Bi}]_0 = 50$.

Table S10. Lactide polymerisation using (^{Mes,Ph}L)Bi(OXyl) (1).^a

Monomer	T	<i>k</i>_{obs}^b	Time	Conv.^c	[LA]₀/[Bi]₀	<i>M</i>_{n, theo}^d	<i>M</i>_{n, exp}^e	<i>M</i>_w/<i>M</i>_n^e	<i>P</i>_s^f	<i>T</i>_g^g
	(°C)	(h ⁻¹)	(h)	(%)		(g mol ⁻¹)	(g mol ⁻¹)			(°C)
<i>meso</i> -	80	0.296 ± 0.014	16	95	50	6989	14407	1.06	0.54	46.2
<i>rac</i> -	80	0.146 ± 0.010	24	93	50	6830	9979	1.26	0.71	48.3
<i>D</i> -	80	0.097 ± 0.000	32	92	50	6830	9484	1.23	-	65.8
<i>L</i> -	80	0.145 ± 0.000	40	94	10	1484	2093	1.28	-	
<i>L</i> -	80	0.100 ± 0.005	56	93	25	3512	5458	1.27	-	63.2
<i>L</i> -	80	0.071 ± 0.006	64	93	50	6818	10364	1.37	-	
<i>L</i> -	80	0.047 ± 0.003	64	86	100	13370	17206	1.22	-	

^aPolymerisation conditions: [L-LA]₀ = 0.5 M, 0.56 mL CDCl₃. ^bFirst order rate constant (*k*_{obs}) with standard error and *R*² were obtained from plots of ln([LA]₀/[LA]_t) vs. time.

^cMeasured by ¹H NMR spectroscopic analyses. ^dCalculated *M*_n for PLA = conv. (%) × [LA]₀/[Bi]₀ × 144.1 + 136.1. ^eDetermined by GPC in THF against PS standards using the appropriate Mark-Houwink corrections.^{11,12} ^fDetermined by ¹H{¹H}NMR spectroscopy. ^gDetermined by Differential Scanning Calorimetry.

Table S11. Lactide polymerisation using (^{Mes,Ph}L)Bi(OXyl) (1).^a

Monomer	T (°C)	<i>k</i> _{obs} ^b (h ⁻¹)	Time (h)	Conv. ^c (%)	[LA] ₀ /[Bi] ₀	<i>M</i> _{n, theo} ^d (g mol ⁻¹)	<i>M</i> _{n, exp} ^e (g mol ⁻¹)	<i>M</i> _w / <i>M</i> _n ^e
<i>meso</i> -	80	0.412 ± 0.005	8.7	93	50	6959	5700	1.58
<i>rac</i> -	80	0.104 ± 0.004	23.3	87	50	6527	12875	1.73
<i>D</i> -	80	0.145 ± 0.005	20.5	91	50	6807	8082	2.42
<i>L</i> -	80	0.097 ± 0.005	24	86	50	6455	8254	2.52
<i>L</i> -	70	0.064 ± 0.002	39	86	50	6455	9294	1.37
<i>L</i> -	90	0.132 ± 0.002	23	89	50	6671	9440	1.43

^aPolymerisation conditions: [LA]₀ = 0.5 M, 0.56 mL C₆D₆. ^bFirst order rate constant (*k*_{obs}) with standard error and *R*² were obtained from plots of ln([LA]₀/[LA]_t) vs. time.

^cMeasured by ¹H NMR spectroscopic analyses. ^dCalculated *M*_n for PLA = conv. (%) × [LA]₀/[Bi]₀ × 144.1 + 136.1. ^eDetermined by GPC in THF against PS standards using the appropriate Mark-Houwink corrections.^{11,12}

Table S12. Lactide polymerisation using (^{Mes,Ph}L)Bi(ODipp) (3).^a

Monomer	T (°C)	<i>k</i> _{obs} ^b (h ⁻¹)	Time (h)	Conv. ^c (%)	[LA] ₀ /[Bi] ₀	<i>M</i> _{n, theo} ^d (g mol ⁻¹)	<i>M</i> _{n, exp} ^e (g mol ⁻¹)	<i>M</i> _w / <i>M</i> _n ^e	<i>P</i> _s ^f
<i>meso</i> -	80	0.358	8	93	50	6884	7635	1.42	0.56
<i>rac</i> -	80	0.127	32	97	50	7160	13070	1.35	0.77
<i>D</i> -	80	0.109	48	94	50	6909	16443	1.30	-
<i>L</i> -	80	0.104	72	87	50	6347	37322	1.45	-

^aPolymerisation conditions: [LA]₀ = 0.5 M, 0.56 mL CDCl₃. ^bFirst order rate constant (*k*_{obs}) with standard error and *R*² were obtained from plots of ln([LA]₀/[LA]_t) vs. time.

^cMeasured by ¹H NMR spectroscopic analyses. ^dCalculated *M*_n for PLA = conv. (%) × [LA]₀/[Bi]₀ × 144.1 + 192.3. ^eDetermined by GPC in THF against PS standards using the appropriate Mark-Houwink corrections.^{11,12} ^fDetermined by ¹H{¹H}NMR spectroscopy.

Table S13. Lactide polymerisation using (^{Mes,Ph}L)Bi(OAr^{tBu}) (4).^a

Monomer	T	<i>k</i> _{obs} ^b	Time	Conv. ^c	[LA] ₀ /[Bi] ₀	<i>M</i> _{n, theo} ^d	<i>M</i> _{n, exp} ^e	<i>M</i> _w / <i>M</i> _n ^e	<i>P</i> _s ^f
	(°C)	(h ⁻¹)	(h)	(%)		(g mol ⁻¹)	(g mol ⁻¹)		
<i>meso</i> -	80	0.176	20	96	50	7123	18465	1.27	0.55
<i>rac</i> -	80	0.096	40	91	50	6718	16789	1.27	0.79
<i>D</i> -	80	0.043	64	88	50	6529	-	-	-
<i>L</i> -	80	0.043	72	91	50	6764	-	-	-

^aPolymerisation conditions: [LA]₀ = 0.5 M, 0.56 mL CDCl₃. ^bFirst order rate constant (*k*_{obs}) with standard error and *R*² were obtained from plots of ln([LA]₀/[LA]_t) vs. time.^cMeasured by ¹H NMR spectroscopic analyses. ^dCalculated *M*_n for PLA = conv. (%) × [LA]₀/[Bi]₀ × 144.1 + 220.4. ^eDetermined by GPC in THF against PS standards using the appropriate Mark-Houwink corrections.^{11,12} ^fDetermined by ¹H{¹H}NMR spectroscopy.**Table S14.** Lactide polymerisation using (^{Mes,Ph}L)Bi(O^tBu) (5).^a

Monomer	T	<i>k</i> _{obs} ^b	Time	Conv. ^c	[LA] ₀ /[Bi] ₀	<i>M</i> _{n, theo} ^d	<i>M</i> _{n, exp} ^e	<i>M</i> _w / <i>M</i> _n ^e
	(°C)	(h ⁻¹)	(h)	(%)		(g mol ⁻¹)	(g mol ⁻¹)	
<i>meso</i> -	80	0.276 ± 0.006	11.5	95	50	6992	6206	1.76
<i>rac</i> -	80	0.158 ± 0.004	32	92	50	6776	-	-
<i>D</i> -	80	0.093 ± 0.003	32	91	50	6705	8804	2.59
<i>L</i> -	80	0.065 ± 0.004	49.3	91	50	6705	-	-
<i>L</i> -	70	0.041 ± 0.001	48.5	80	50	5911	-	-
<i>L</i> -	90	0.090 ± 0.001	22.8	81	50	5983	8892	2.05

^aPolymerisation conditions: [LA]₀ = 0.5 M, 0.56 mL C₆D₆. ^bFirst order rate constant (*k*_{obs}) with standard error and *R*² were obtained from plots of ln([LA]₀/[LA]_t) vs. time.^cMeasured by ¹H NMR spectroscopic analyses. ^dCalculated *M*_n for PLA = conv. (%) × [LA]₀/[Bi]₀ × 144.1 + 73.1. ^eDetermined by GPC in THF against PS standards using the appropriate Mark-Houwink corrections.^{11,12}

Table S15. Lactide polymerisation using $(^{Mes,Ph}L)Bi\{OC(H)(Me)C(=O)O^tBu\}$ (**9**).^a

Monomer	T (°C)	k_{obs}^b (h ⁻¹)	Time (h)	Conv. ^c (%)	[LA] ₀ /[Bi] ₀	$M_n, theo^d$ (g mol ⁻¹)	M_n, exp^e (g mol ⁻¹)	M_w/M_n^e
<i>meso</i> -	80	0.329 ± 0.002	7.9	92	50	6934	-	-
<i>rac</i> -	80	0.140 ± 0.001	23.4	92	50	6934	9690	2.54
<i>D</i> -	80	0.116 ± 0.001	23.3	90	50	6790	7752	1.82
<i>L</i> -	80	0.083 ± 0.001	31.5	93	50	7006	7980	2.79
<i>L</i> -	70	0.057 ± 0.001	43	88	50	6646	9031	2.29
<i>L</i> -	90	0.123 ± 0.002	21.5	90	50	6790	8853	2.60
<i>L</i> -	80	0.053 ± 0.001	46.5	89	100	13132	18024	1.23
<i>L</i> -	80	0.018 ± 0.001	144	92	200	26824	13316	1.89
<i>L</i> -	80	0.009 ± 0.001	143	67	400	38930	6092	1.69

^aPolymerisation conditions: [LA]₀ = 0.5 M, 0.56 mL C₆D₆. ^bFirst order rate constant (k_{obs}) with standard error and R^2 were obtained from plots of ln([LA]₀/[LA]_t) vs. time.

^cMeasured by ¹H NMR spectroscopic analyses. ^dCalculated M_n for PLA = conv. (%) × [LA]₀/[Bi]₀ × 144.1 + 159.2. ^eDetermined by GPC in THF against PS standards using the appropriate Mark-Houwink corrections.^{11,12}

Table S16. *L*-Lactide polymerisation using (^{Mes,Ph}**L**)**Bi(OXyl)** (**1**) at 70 °C with [LA]₀/[Bi]₀ = 50 and C₆D₆.

Time (h)	Conversion	
		(%)
0		0
0.6		0
1.13		1
1.83		1
2.36		1
2.89		1
3.42		2
3.95		2
4.48		2
5.01	3	
5.54	4	
6.07	4	
6.6	4	
7.13	5	
7.66	5	
8.19	7	
8.72	8	
	9.25	8
9.78	10	
10.31	11	
10.84	12	
11.37	13	
11.9	15	
12.43	17	
12.96	18	
13.49	20	
	14.02	22

Table S17. *L*-Lactide polymerisation using (^{Mes,Ph}**L**)**Bi(OXyl)** (**1**) at 80 °C with [LA]₀/[Bi]₀ = 50 and CDCl₃.

Time (h)	Conversion (%)
0	0
1	0
2	0
4	6
8	19
16	40
24	70

Table S18. *L*-Lactide polymerisation using (^{Mes,Ph}L)Bi(OXyl) (**1**) at 80 °C with [LA]₀/[Bi]₀ = 50 and C₆D₆

Time (h)	Conversion	
		(%)
0		0
0.6		1
1.13		2
1.66		2
2.19		3
2.72		4
3.25		6
3.78		7
4.31		10
4.84	12	
5.37	14	
5.9	15	
6.43	18	
6.96	19	
7.49	23	
8.02	24	
8.55	27	
	9.08	29
	9.61	33
	10.14	36
	10.67	38
	11.2	41
	11.73	44
	12.26	47
	12.79	50
	13.32	53
	13.85	55
	17.1	73

Table S19. *L*-Lactide polymerisation using (^{Mes,Ph}L)Bi(OXyl) (**1**) at 90 °C with [LA]₀/[Bi]₀ = 50 and C₆D₆

Time (h)	Conversion	
		(%)
0		0
0.6		1
1.13		1
1.66		2
2.19		2
2.72		3
3.25		4
3.78		4
4.31		6
4.84	7	
5.37	9	
5.9	11	
6.43	14	
6.96	17	
7.49	20	
8.02	26	
8.55	29	
	9.08	34
	9.61	38
	10.14	44
	10.67	47
	11.2	52
	11.73	55
	12.26	58
	12.79	62
	13.32	65
	13.85	68
	14.38	70

Table S20. *meso*-Lactide polymerisation using (^{Mes,Ph}L)Bi(OXyl) (**1**) at 80 °C with [LA]₀/[Bi]₀ = 50 and CDCl₃.

Time (h)	Conversion (%)
0	0
1	6
2	23
4	56
8	88

Table S21. *meso*-Lactide polymerisation using (^{Mes,Ph}L)Bi(OXyl) (**1**) at 80 °C with [LA]₀/[Bi]₀ = 50 and C₆D₆.

	Time (h)	Conversion (%)
	0	0
	0.05	1
	0.3	3
	0.57	6
	0.84	9
	1.11	9
	1.38	14
	1.65	15
	1.92	18
2.19	23	
2.46	26	
2.73	30	
3	37	
3.27	41	
3.54	47	
3.81	51	
4.08	55	
	4.35	59
	4.62	63
	4.89	66
	5.16	69
	5.43	74
	5.7	76
	5.97	79
	6.24	82
6.51	84	
6.78	86	
7.05	87	
7.32	88	
7.59	89	
7.86	91	
8.13	92	
8.4	92	

Table S22. *rac*-Lactide polymerisation using (^{Mes,Ph}L)Bi(OXyl) (**1**) at 80 °C with [LA]₀/[Bi]₀ = 50 and CDCl₃.

Time (h)	Conversion (%)
0	0
1	0
2	4
4	14
7.5	40
15.5	64
19.5	83
23	90
24	93

Table S23. *rac*-Lactide polymerisation using (^{Mes,Ph}L)Bi(OXyl) (**1**) at 80 °C with [LA]₀/[Bi]₀ = 50 and C₆D₆.

Time (h)	Conversion	
		(%)
0		0
0.6		1
0.95		2
1.48		3
2.01		6
2.54		7
3.07		10
3.58		14
4.11		18
4.64	20	
5.17	24	
5.7	28	
6.23	32	
6.76	35	
7.29	41	
7.82	45	
8.35	49	
	8.88	53
	9.41	55
	9.94	58
	10.47	60
	11	62
	11.53	64
	12.06	66
	12.59	69
13.12	72	
13.65	73	
14.18	75	

Table S24. *D*-Lactide polymerisation using (^{Mes,Ph}L)Bi(OXyl) (**1**) at 80 °C with [LA]₀/[Bi]₀ = 50 and CDCl₃.

Time (h)	Conversion (%)
0	0
1	3
2	4
4	8
7.5	25
15.5	66
24	85

Table S25. *D*-Lactide polymerisation using (^{Mes,Ph}L)Bi(OXyl) (**1**) at 80 °C with [LA]₀/[Bi]₀ = 50 and C₆D₆.

	Time	Conversion
	(h)	(%)
	0	0
	0.49	1
	1.02	3
	1.55	5
	2.08	7
	2.61	10
	3.14	15
	3.67	19
	4.2	24
4.73	30	
5.26	33	
5.79	39	
6.32	41	
6.85	46	
7.38	49	
7.91	52	
8.44	55	
	8.97	58
	9.5	61
	10.03	66
	10.56	68
	11.09	71
	11.62	74
	12.15	75
	12.68	78
13.21	82	
13.74	85	
14.27	86	

Table S26. *L*-Lactide polymerisation using (^{Mes,Ph}L)Bi(O*t*Bu) (**5**) at 70 °C with [LA]₀/[Bi]₀ = 50 and C₆D₆.

Time (h)	Conversion	
		(%)
0		0
0.25		0
1.3		1
2.35		2
3.4		2
4.45		3
5.5		3
6.55		4
7.6		5
8.65	7	
9.7	9	
10.75	10	
11.8	12	
12.85	15	
13.9	18	
22	44	
38	71	
	48.5	80

Table S27. *L*-Lactide polymerisation using (^{Mes,Ph}L)Bi(O*t*Bu) (**5**) at 80 °C with [LA]₀/[Bi]₀ = 50 and C₆D₆.

Time (h)	Conversion	
		(%)
0		0
0.85		1
1.38		1
1.91		2
2.44		3
2.97		2
3.5		3
4.03		4
4.56		4
5.09	4	
5.62	4	
6.15	5	
6.68	6	
7.21	6	
7.74	7	
8.27	7	
8.8	9	
	9.33	10
	9.86	11
	10.39	12
	10.92	12
	11.45	14
	11.98	15
	12.51	16
	13.04	18
	23	47
	31	69
	39.5	85
	49.25	91

Table S28. *L*-Lactide polymerisation using (^{Mes,Ph}L)Bi(O*t*Bu) (**5**) at 90 °C with [LA]₀/[Bi]₀ = 50 and C₆D₆.

Time (h)	Conversion	
		(%)
0		0
1.2		1
1.73		1
2.26		2
2.79		3
3.32		4
3.85		5
3.58		7
4.11		9
4.64	9	
5.17	13	
5.7	14	
6.23	16	
6.76	19	
7.29	23	
7.82	26	
8.35	30	
	8.88	32
	9.41	35
	9.94	38
	10.47	42
	11	45
	11.53	48
	12.06	51
	22.83	81

Table S29. *meso*-Lactide polymerisation using (^{Mes,Ph}L)Bi(O^tBu) (**5**) at 80 °C with [LA]₀/[Bi]₀ = 50 and C₆D₆.

Time (h)	Conversion	
		(%)
0		0
0.15		3
0.3		10
0.57		15
0.84		20
1.11		23
1.38		26
1.65		29
2.18		34
2.71	41	
3.24	46	
3.77	52	
4.3	59	
4.83	65	
5.36	70	
5.89	75	
6.42	80	
	6.95	81
	7.48	86
	8.01	88
	8.54	90
	9.07	92
	9.6	93
	10.13	94

Table S30. *rac*-Lactide polymerisation using (^{Mes,Ph}L)Bi(O^tBu) (**5**) at 80 °C with [LA]₀/[Bi]₀ = 50 and C₆D₆.

Time (h)	Conversion	
		(%)
0		0
1.25		2
1.03		4
1.56		6
2.09		8
2.62		11
3.15		14
3.58		17
4.11		21
4.64	27	
5.17	31	
5.7	36	
6.23	39	
6.76	45	
7.29	50	
7.82	54	
8.35	60	
	8.88	63
	9.41	66
	9.94	68
	10.47	70
	11	72
	11.53	74
	12.06	76
	12.59	78

Table S31. *D*-Lactide polymerisation using (^{Mes,Ph}L)Bi(O^tBu) (**5**) at 80 °C with [LA]₀/[Bi]₀ = 50 and C₆D₆.

	Time	Conversion
	(h)	(%)
	0	0
	0.6	0
	1.13	1
	1.83	2
	2.36	2
	2.89	3
	3.88	3
	4.41	4
	4.94	4
5.47	5	
6	7	
6.53	9	
7.06	10	
7.59	12	
8.12	14	
8.65	17	
9.18	18	
	9.71	21
	10.24	26
	10.77	28
	11.3	30
	11.83	32
	12.36	36
	12.89	39
	13.42	39
13.69	41	

Table S32. *L*-Lactide polymerisation using (^{Mes,Ph}L)Bi{OC(H)(Me)C(=O)O^tBu} (9) at 70 °C with [LA]₀/[Bi]₀ = 50 and C₆D₆.

Time (h)	Conversion	
		(%)
0		0
0.05		0
1.1		0
2.15		2
3.2		3
4.25		6
5.3		8
6.35		12
7.4		15
8.45	19	
9.5	23	
10.55	27	
11.6	30	
12.65	35	
13.7	37	

Table S33. *L*-Lactide polymerisation using (^{Mes,Ph}L)Bi{OC(H)(Me)C(=O)O^tBu} (9) at 80 °C with [LA]₀/[Bi]₀ = 50 and C₆D₆.

Time (h)	Conversion	
		(%)
0		0.
0.72		2
1.25		4
1.78		11
2.31		18
2.84		22
3.37		27
3.9		29
4.43		32
4.96	35	
5.49	37	
6.02	40	
6.55	42	
7.08	44	
7.61	47	
8.14	49	
8.67	51	
	9.2	53
	9.73	56
	10.26	58
	10.79	59
	11.32	61
	11.85	62
	12.38	63
	12.91	66
	13.44	68
	13.97	69
	14.23	70
	23	86
31.5	93	

Table S34. *L*-Lactide polymerisation using (^{Mes,Ph}L)Bi{OC(H)(Me)C(=O)O^tBu} (9) at 90 °C with [LA]₀/[Bi]₀ = 50 and C₆D₆.

Time (h)	Conversion	
		(%)
0		0
0.6		0
1.13		1
1.66		2
2.19		3
2.72		7
3.25		11
3.58		13
4.11		18
4.64	22	
5.17	25	
5.7	31	
6.23	35	
6.76	39	
7.29	43	
7.82	47	
8.35	50	
	8.88	54
	9.41	57
	9.94	60
	10.47	63
	11	65
	11.53	67
	12.06	69
	12.59	72
	13.12	74
	19.45	88
	21.45	90

Table S35. *L*-Lactide polymerisation using (^{Mes,Ph}L)Bi{OC(H)(Me)C(=O)O^tBu} (9) at 80 °C with [LA]₀/[Bi]₀ = 100 and C₆D₆.

Time (h)	Conversion	
		(%)
0		0
0.98		0
1.51		1
2.04		1
2.57		2
3.1		3
3.63		5
4.16		7
4.69		9
5.22	11	
5.75	13	
6.28	15	
6.81	17	
7.34	18	
7.87	20	
8.4	23	
8.93	25	
	9.46	27
	9.99	28
	10.52	30
	11.05	32
	11.58	34
	12.11	35
	12.64	37
	13.17	39
13.7	40	
14.23	42	
14.76	43	
15	44	
23.75	68	

Table S36. *L*-Lactide polymerisation using (^{Mes,Ph}L)Bi{OC(H)(Me)C(=O)O^tBu} (9) at 80 °C with [LA]₀/[Bi]₀ = 200 and C₆D₆.

Time (h)	Conversion	
		(%)
0		0
1.51		0
2.04		0
2.57		0
3.1		0
3.63		0
4.16		2
4.69		2
5.22		2
5.75	2	
6.5	2	
7.03	2	
7.56	2	
8.09	3	
8.62	4	
9.15	4	
9.68	4	
	10.21	5
	10.74	5
	11.27	6
	11.8	6
	12.33	7
	12.86	7
	13.39	8
	13.92	8
14.45	9	
24	17	

Table S37. *L*-Lactide polymerisation using (^{Mes,Ph}L)Bi{OC(H)(Me)C(=O)O^tBu} (9) at 80 °C with [LA]₀/[Bi]₀ = 400 and C₆D₆.

Time (h)	Conversion	
		(%)
0	0	0
1.49	0	0
2.02	0	0
2.55	0	0
3.08	0	0
3.61	0	0
4.14	0	0
4.67	0	0
5.2	0	0
5.73	0	0
6.5	0	0
7.03	0	0
7.56	0	0
8.09	0	0
8.62	0	0
9.15	1	0
10.2	1	0
	11.25	2
	12.3	2
	13.35	2
	14.4	2
	15.45	2
	23	7

Table S38. *meso*-Lactide polymerisation using (^{Mes,Ph}L)Bi{OC(H)(Me)C(=O)O*t*Bu} (9) at 80 °C with [LA]₀/[Bi]₀ = 50 and C₆D₆.

Time (h)	Conversion	
		(%)
0		0
0.3		2
0.57		9
0.84		17
1.11		24
1.38		31
1.65		37
1.92		42
2.19		47
2.46	51	
2.73	56	
3	60	
3.27	64	
3.54	66	
3.81	69	
4.08	71	
4.35	74	
	4.62	76
	4.89	78
	5.16	80
	5.43	81
	5.7	83
	5.97	84
	6.24	86
	6.51	87
6.78	89	
7.05	90	
7.32	90	
7.59	91	
7.86	92	

Table S39. *rac*-Lactide polymerisation using (^{Mes,Ph}L)Bi{OC(H)(Me)C(=O)O^tBu} (9) at 80 °C with [LA]₀/[Bi]₀ = 50 and C₆D₆.

Time (h)	Conversion	
		(%)
0		0
0.6		2
1.13		6
1.66		8
2.19		14
2.72		19
3.25		23
3.78		30
4.31		35
4.84	41	
5.37	45	
5.9	48	
6.43	52	
6.96	56	
7.49	59	
8.02	61	
8.55	64	
	9.08	67
	9.61	70
	10.14	71
	10.67	73
	11.2	75
	11.73	77
	12.26	79
	12.79	80
13.32	82	
13.85	83	

Table S40. *D*-Lactide polymerisation using (^{Mes,Ph}L)Bi{OC(H)(Me)C(=O)O^tBu} (9) at 80 °C with [LA]₀/[Bi]₀ = 50 and C₆D₆.

Time (h)	Conversion	
		(%)
0		0
0.6		0
1.13		1
1.66		2
2.19		3
2.72		6
3.25		9
3.78		13
4.31		17
4.84	22	
5.37	26	
5.9	31	
6.43	35	
6.96	38	
7.49	41	
8.02	46	
8.55	49	
	9.08	51
	9.61	54
	10.14	58
	10.67	60
	11.2	62
	11.73	65
	12.26	67
	12.79	69
13.32	71	
18	86	

Table S41. Enthalpy and entropy of activation values for polymerisation of lactide monomers using complexes **1**, **3**, **5** and **9**.

Lactide	Complex	Solvent	ΔH^\ddagger	ΔS^\ddagger
			(kJ mol ⁻¹)	(J mol ⁻¹ K ⁻¹)
<i>L</i> -	1	CDCl ₃	38 ± 3	-163 ± 10
<i>L</i> -	1	C ₆ D ₆	34 ± 3	-169 ± 8
<i>D</i> -	1	CDCl ₃	51 ± 6	-120 ± 1
<i>rac</i> -	1	CDCl ₃	29 ± 5	-180 ± 13
<i>L</i> -	3	CDCl ₃	39 ± 5	-156 ± 14
<i>D</i> -	3	CDCl ₃	35 ± 3	-167 ± 10
<i>rac</i> -	3	CDCl ₃	40 ± 5	-151 ± 14
<i>L</i> -	5	C ₆ D ₆	38 ± 3	-162 ± 10
<i>L</i> -	9	C ₆ D ₆	37 ± 1	-163 ± 4

V. References

- [1] Z. R. Turner, *Inorg. Chem.* **2019**, *58*, 14212-14227.
- [2] M. J. Monreal, R. K. Thomson, T. Cantat, N. E. Travia, B. L. Scott, J. L. Kiplinger, *Organometallics* **2011**, *30*, 2031-2038.
- [3] Y. Sarazin, D. Roșca, V. Poirier, T. Roisnel, A. Silvestru, L. Maron, J.-F. o. Carpentier, *Organometallics* **2010**, *29*, 6569-6577.
- [4] P. J. Bailey, R. A. Coxall, C. M. Dick, S. Fabre, L. C. Henderson, C. Herber, S. T. Liddle, D. Loroño-González, A. Parkin, S. Parsons, **2003**, *9*, 4820-4828.
- [5] V. S. Cherepakhin, K. V. Zaitsev, *Catal. Commun.* **2018**, *106*, 36-39.
- [6] J. Cosier, A. M. Glazer, *J. Appl. Crystallogr.* **1986**, *19*, 105-107.
- [7] CrysAlisPRO, Oxford Diffraction /Agilent Technologies UK Ltd, Yarnton, England.
- [8] A. Altomare, G. Cascarano, C. Giacovazzo, A. Guagliardi, *J. Appl. Crystallogr.* **1993**, *26*, 343-350.
- [9] L. Palatinus, G. Chapuis, *J. Appl. Crystallogr.* **2007**, *40*, 786-790.
- [10] L. Farrugia, *J. Appl. Crystallogr.* **1999**, *32*, 837-838.
- [11] P. McKeown, M. G. Davidson, G. Kociok-Köhn, M. D. Jones, *Chem. Commun.* **2016**, *52*, 10431-10434.
- [12] J. Coudane, C. Ustariz-Peyret, G. Schwach, M. Vert, **1997**, *35*, 1651-1658.